UNIVERSITÀ
DEGLI STUDI
DI PADOVA

Sede Amministrativa: Università degli Studi di Padova

Dipartimento di Ingegneria Civile, Edile e Ambientale (ICEA)

SCUOLA DI DOTTORATO DI RICERCA IN:
SCIENZE DELL'INGEGNERIA CIVILE ED AMBIENTALE
XXXI CICLO

Unravelling the impact of anthropogenic regulation on river flow regimes

Direttore della Scuola: Ch.mo Prof. Marco Marani

Supervisore: Ch.mo Prof. Gianluca Botter

Dottorando: Marta Ferrazzi

Anno Accademico 2017/2018

Acknowledgements

I first wish to express my gratitude to my advisor, Prof. Gianluca Botter, for his valuable teachings and guidance during the past three years. In addition, I would like to thank Ross Woods for the collaboration during my visiting period at the Bristol University. A special thank goes also to the support and affection of my parents, Dario and Nicoletta. Last but most importantly, thank you to my boyfriend Andrea for his unconditional encouragement, help, patience and love.

UNIVERSITY OF PADOVA

Abstract

Department of Civil, Architectural and Environmental Engineering

Doctor of Philosophy

Unravelling the impact of anthropogenic regulation on river flow regimes

Marta Ferrazzi

In the last century, more than 45,000 large dams have been constructed all around the world to sustain population growth and economic development, so that unregulated rivers are now rare in most regions of the Earth. Damming of rivers has produced global-scale alterations of the hydrologic cycle, inducing severe consequences on the ecological and morphological equilibrium of streams. Nevertheless, the construction of new dams has been also proposed to mitigate the risks related to natural and human induced changes in climate drivers, which threaten the sustainability of anthropogenic water uses. The existing literature has documented that hydrological regimes of regulated reaches are typically characterized by a reduced temporal variability and spatial heterogeneity of streamflows. However, whether specific types of anthropogenic uses of reservoirs could generate distinctive, contrasting impacts on flow regimes has not been disclosed yet. Additionally, very little is known about the combined contribution of river regulation and hydroclimatic variability to flow regime alterations in engineered rivers. In this thesis, extensive hydrologic data and theoretical analyses are used to investigate hydrological alterations downstream of 47 dams in the Central Eastern US, spanning a wide range of climatic conditions and water uses. Results reveal a strong connection between the anthropogenic use and the hydrological impact of dams. Whereas flood control smooths the temporal and spatial heterogeneity of river flows, water supply is able to increase the relative variability and regional heterogeneity of streamflows. Accordingly, the magnitude of hydrological alteration downstream of flood control dams is reduced when these structures are also operated for water supply, because of the compensation

effect generated by overlapping uses. Despite the significant and distinct impacts of dams on the frequency distribution of downstream flows, clustering of catchment based on climatic signatures leads to hydrologically coherent classes in term of both regulated and unregulated river flows, thus revealing that climate signatures are typically visible also downstream of dams. Furthermore, the analysis shows that temporal patterns of regulated flow regimes are controlled by the inter-annual variability of natural discharges upstream of dams, as long as reservoirs obey to time-invariant operating schemes driven by the underlying specific water uses. These findings represent a critical step forward for scientists and water managers. In view of the increasing trend of global freshwater demand and the uncertain impact of climate change on human freshwater exploitation, especially reservoirs will help promoting the anthropogenic exploitation of freshwater. Nevertheless, the current patterns of water consumption could generate a shift in the cumulative effects of dams at global scale, reshaping the trajectories of regulated streamflows and of eco-morphological alterations of dammed rivers. Moreover, reservoirs as they are currently operated are not helpful in enhancing the long-term stability of flow regimes in downstream reaches, unless new self-adapting dynamic regulation strategies are implemented.

UNIVERSITÀ DEGLI STUDI DI PADOVA

Sommario

Dipartimento di Ingegneria Civile, Edile ed Ambientale

Dottorato di Ricerca

Analisi dell'impatto della regolazione antropica sul regime dei deflussi

Marta Ferrazzi

Nel corso del XX secolo, più di 45000 grandi dighe sono state costruite in tutto il mondo per supportare l'aumento demografico e lo sviluppo economico. In tal modo i corsi d'acqua naturali sono diventati rari nella maggior parte delle regioni del mondo. La costruzione di dighe ha comportato l'alterazione del ciclo idrologico a scala globale, con significative conseguenze sull'equilibrio ecologico e geomorfologico dei fiumi. Tuttavia, la messa in opera di nuove infrastrutture idrauliche è stata anche proposta per mitigare i rischi collegati al cambiamento climatico, il quale rappresenta una seria minaccia per la sostenibilità dello sfruttamento antropico della risorsa idrica. La letteratura esistente ha evidenziato come il regime idrologico in corsi d'acqua regolati sia tipicamente caratterizzato da una ridotta variabilità temporale e eterogeneità spaziale dei deflussi. Ciononostante, ad oggi, non è noto se esista una relazione tra l'utilizzo antropico dei serbatoi e l'impatto che essi generano sui regimi idrologici. Inoltre, non si conosce come la regolazione antropica e le fluttuazioni idroclimatiche interagiscano nel modellare il regime dei deflussi a valle delle dighe. In questo studio, l'analisi delle serie temporali di portata è stata combinata ad analisi modellistiche e teoriche al fine di investigare le alterazioni idrologiche a valle di 47 dighe situate nella parte centro-orientale degli Stati Uniti. Tali strutture abbracciano diverse zone climatiche e diversi utilizzi della risorsa idrica. I risultati rivelano che esiste un'importante connessione tra le funzioni per cui è utilizzato un serbatoio e l'impatto che esso genera sul regime idrologico. La laminazione delle piene determina una riduzione della variabilità temporale e spaziale dei deflussi; al contrario, l'approvvigionamento idrico favorisce l'aumento della variabilità temporale

dei regimi idrologici, generando un processo di diversificazione del grado di variabilità delle portate in alveo. A causa dell'effetto distinto e compensatore della laminazione delle piene e dell'approvvigionamento idrico, l'entità delle alterazioni dovute a strutture per la laminazione delle piene si riduce quando tra gli utilizzi è presente anche l'approvvigionamento idrico. Nonostante l'impatto delle dighe sui regimi idrologici sia tutt'altro che trascurabile, la classificazione sulla base di caratteristiche climatiche dei siti oggetto di studio permette di ottenere gruppi idrologicamente omogenei considerando sia i regimi naturali sia a valle dei serbatoi, sottolineando dunque come l'impronta climatica sia visibile anche a valle delle dighe. Inoltre, l'analisi mostra che le dinamiche temporali dei regimi regolati vengono controllate dalla variabilità inter-annuale tipica dei deflussi naturali a monte delle dighe. Questo è dovuto agli schemi statici a cui è soggetta la regolazione antropica, che dipendono unicamente dall'utilizzo del serbatoio. I risultati ottenuti in questa tesi assumono particolare rilievo nell'ambito di una corretta gestione della risorsa idrica. A fronte del costante aumento del fabbisogno mondiale d'acqua e dell'incontrollabile impatto dei cambiamenti climatici sullo sfruttamento della risorsa idrica, le dighe acquisiranno un ruolo strategico. Tuttavia, la crescente domanda d'acqua potrebbe rimodellare l'impatto antropico sui regimi idrologici, favorendo un potenziale cambiamento dell'effetto cumulativo delle dighe a scala globale. Inoltre, l'attuale gestione dei serbatoi sembra essere inadatta al fine di mitigare le fluttuazioni dei regimi idrologici, al cui scopo sarebbe necessario attuare delle strategie di regolazione dinamica.

Contents

List of Figures

List of Tables

Chapter 1

Introduction

Dams and impoundments have long been designed to reconcile the systematic conflict between patterns of anthropogenic water uses and the temporal variability of river flows. Over the course of the 20th century, population and economic growth caused a significant increase in the construction and operation of massive engineering projects capable of helping communities by storing water for flood control, urban water supply, hydropower production, irrigation or a combination of such purposes [Lehener et al., 2011; Jaramillo and Destouni, 2015]. Overall, by the end of the century, more than 45000 large dams were constructed around the world, so that unregulated rivers are now rare in most regions of the Earth and global-scale modifications of the hydrologic cycle are no longer negligible [WCD, 2000]. Damming of rivers for anthropogenic freshwater exploitation not only affect stream hydrology, but also ecology and geomorphology. Flow regime alterations through dams and reservoirs, coupled with their tendency to detain a large part of the sediment load, profoundly disrupt the dynamic equilibrium between river flows and erosion/sedimentation phenomena, inducing a complete readjustment of channel and floodplain morphology throughout entire river networks [Dunne and Leopold, 1978; Petts, 1979]. Additionally, as a result of profound hydrological alterations, river regulation affects aquatic ecosystems and riverine biodiversity, often creating new thermochemical regimes and habitat conditions to which native species are poorly adapted [Poff et al., 1997, 2007]. Accordingly, the perception of socio-economic benefits provided by dams has grown along with an increased awareness of the harmful effects connected to flow regime alterations, bringing to light the need to conceive new strategies for a sustainable management of water resources [Ziv et al., 2012]. These strategies can only arise from a deeper understanding of the nature of anthropogenic modifications of flow

regimes and shall aim at satisfying human needs with reduced resources and fewer ecological and geomorphological disruptions [Gleick, 2000]. Nowadays, the large majority of existing studies describes the hydrological impacts of individual dams and only a small number broadens out by investigating the spectrum of downstream alterations at the regional and global scale. Previous large scale investigations have revealed that river impoundments affect the magnitude, frequency and timing of both high and low flows, with an intensity that is controlled by the storage capacity of reservoirs properly scaled to the mean annual inflow [Graff, 1999; Magilligan et al., 2003; Magilligan and Nislow, 2005; Graff, 2006]. These alterations are believed to smooth the temporal variability of flow regimes in regulated reaches, thereby reducing the heterogeneity of regional river dynamics [Poff et al., 2007; Destouni et al., 2013; Jaramillo and Destouni, 2015]. However, a broad understanding of the correlation between regulation impacts and specific reservoir functions, encompassing multiple time scales and heterogeneous patterns of water uses, is lacking. Information on the connection between reservoir functions and the features of downstream flow regimes modifications by dams would represent a critical step forward for scientists and water managers, espacially in the light of the current increase of global freshwater demand [USGS, 1950–2010], which is triggered by population growth and will potentially reshape the impact of damming on rivers.

Compounding matter, nowadays, the rapidly increasing demand of water is growing along with climate change, exacerbating conflicts over freshwater resources and potentially leading to an escalation of water-engineering solutions [Field et al., 2014]. Owing to the pronounced sensitivity of the saturation vapour pressure of water to air temperature, natural and human induced climate patterns are producing significant alterations of the hydrologic cycle at global scale [Lettenmaier et al., 1994; Groisman et al., 2001; Milly et al., 2005]. These accelerating modifications of the hydrologic cycle are seriously endangering riverine ecosystems and anthropogenic water uses, and challenge the paradigm of stationary flow regimes, based on which hydraulic infrastructures have long been designed and operated [Barnett et al., 2008; Kundzewicz et al., 2008; Milly et al., 2008; NRC, 2011; Van Vliet et al., 2012]. On account of dams ability to regulate water fluxes, allowing anthropogenic freshwater exploitation, the revamping of old engineering structures and the construction of new dams has been proposed to mitigate the risks

induced by fluctuations in climate drivers [ICOLD, 2014; Zarfl et al., 2014; Poff et al., 2015]. Nevertheless, damming of river is known to induce severe consequences on the ecological and morphological equilibrium of stream [Dunne and Leopold, 1978; Petts, 1979; Poff et al., 1997, 2007]. Moreover, a broad understanding on the combined contribution of river regulation through dams and hydroclimatic variability to flow regime alterations is lacking and would represent a significant step forward for the exploitation of running water in regulated reaches. This issue is made particularly urgent by the indiscriminate growth of engineered rivers, where infrastructures for the exploitation of running water are often built in cascade also downstream of existing dams [Lebel et al., 2005; Lazzaro et al., 2013]. These infrastructures play a fundamental role in energy production, irrigation and urban water supply, and their functioning, design and operation can be significantly affected by river regulation of upstream dams and climate variability [Ashley and Cashman, 2006; Asnar et al., 2014]. Therefore, there is an urgent need to quantify and accommodate projected variability in river runoff upstream and downstream of dams [Milly et al., 2008; Müller et al., 2014; Majone et al., 2016]. The large majority of the existing studies has focused on climate-induced hydrological variations in pristine rivers and almost nothing is known about the sensitivity of regulated flow regimes to climate drivers [Dai, 2013; MacDonald, 2010; Chezik et al., 2010]. A notable exception is represented by a recent study by Ficklin et al. [2018], that highlights the similarity of the response of natural and anthropogenic flow regimes to climate change. In this context, a clear understanding on the possible presence of climate signatures downstream of dams and on the characterization of the impact of these structures on the response of regulated regimes to inter-annual fluctuations of climate and hydrologic properties would be of particular relevance. These pieces of information would help hydrologists, water managers and environmental scientists, allowing an enhanced understanding of the future sustainability of anthropogenic water uses, as well as of ecological and geomorphological evolution of engineered rivers.

In summary, the thesis investigates the following research questions:

- Are there distinctive patterns of river regime alterations associated to specific water uses?

- May possible shifts in anthropogenic water uses alter observed trends of flow regime modifications in the future?
- Are climate signatures still visible in regulated flow regimes? Is this dependent on the type of regulation?
- Are hydroclimatic fluctuations responsible for controlling the inter-annual variability of flow regimes in regulated rivers?

These questions are addressed by investigating statistically the differences between unregulated and regulated flow regimes, upstream and downstream of a representative selection of isolated dams distributed throughout the Central-Eastern United States. In particular, Chapter 2 presents an analysis on the hidden connection between reservoir functions and the features of downstream flow regimes modifications by dams. Conversely, Chapter 3 presents an analysis that uncovers the relation between regulated regimes and climatic conditions, with particular emphasis on the combined contribution of river regulation through dams and hydroclimatic variability to flow regime alterations. Finally, Chapter 4 concludes the thesis by describing the major findings of the presented study and possible future developments. This arrangement derives by three papers currently under review, in which the aforementioned issues are treated separately.

Chapter 2

Distinct signatures of human water uses in regulated flow regimes

2.1 Introduction

Damming of river for anthropogenic freshwater exploitation is a massive phenomenon. Nowadays, more than 45000 large dams are operated all around the world to mitigate floods, supply freshwater, produce hydropower or a combination of such purposes [WCD, 2000; Lehener et al., 2011; Jaramillo and Destouni, 2015]. Dam building has produced global-scale alterations of the hydrologic cycle, inducing severe consequences on stream ecology and geomorphology. Above all, reservoirs disrupt the dynamic equilibrium between the movement of water and patterns of erosion and sedimentation, and create downstream habitat conditions to which the native biota may be poorly adapted [Dunne and Leopold, 1978; Petts, 1979; Poff et al., 1997, 2007]. Previous studies have emphasized that flow regimes of regulated rivers are typically characterized by a smoothed temporal variability and spatial heterogeneity [Poff et al., 2007; Destouni et al., 2013; Jaramillo and Destouni, 2015]. However, a recognizable link between specific uses of reservoirs and their impact on flow regimes has not been disclosed yet, and would represent a significant step forward to conceive new strategies for a sustainable management of water resources. Here, an innovative framework for investigating the

relationship between key characteristics of reservoirs, including their functions, and regional alterations of river regimes is developed. The study analyzes statistically the differences between flow regimes upstream and downstream of several isolated dams in the US, grounding on both extensive hydrologic data and a physically-based model designed to predict natural flow regimes in ungauged settings [Botter et al., 2009]. The approach eliminates the confounding effect of climate change, which is typically superimposed to that of regulation in pre-impact versus post-impact comparisons and might be of particular importance in catchments that underwent significant climate gradients [Botter et al., 2010]. Moreover, the method uses model simulations to overcome the lack of synchronous discharge records upstream and downstream of reservoirs, which are seldom available. Overall, the approach is applied to 47 isolated dams distributed throughout the Central-Eastern United States, spanning a wide range of hydro-climatic settings and three different water uses (namely flood control, urban water supply and hydropower production).

2.2 Theoretical Framework

In this study, the impact of river regulation is investigated seasonally and annually, by analyzing the long-term differences between synchronous discharge records, upstream and downstream of reservoirs, through different statistical data analyses. The analysis of streamflow time series is combined to a physically-based method capable of predicting natural flow regimes on the basis of geomorphic and climate features typical of the catchment.

The downstream impact of regulation is primarily investigated by comparing the mean and the coefficient of variation of flows upstream and downstream of a representative selection of dams. In fact, the significance of mean water availability and hydrological variability to both stream ecology and geomorphology has been widely proven, leading to the recognition of their key role in managed rivers [Olden and Poff, 2003; Doyle et al., 2005]. Mean discharge, $\overline{Q}$, is a complex function of catchment area, climatic conditions, vegetation and soil properties, the last two being responsible for the partitioning of precipitation into evapotranspiration and drainage [Budiko, 1974; Milly, 1994; Porporato

et al., 2004; Doulatyari et al., 2015]. The coefficient of variation of daily flows, CV_Q, depends on the sequence of stochastic flow pulses and recessions experienced by the considered stream and allows an objective classification of flow regimes as highly variable "erratic" regimes ($CV_Q > 1$) or stable "persistent" regimes ($CV_Q < 1$) [Botter et al., 2013; Lazzaro et al., 2013]. Both the magnitude and temporal trajectories of discharge variability affect riverine ecosystems, playing a fundamental role in population dynamics and persistence [Sabo and Post, 2008; Petchey et al., 1997]. Accordingly, in this study, the temporal autocorrelation and frequency stability analysis are also implemented to investigate seasonal and inter-annual patterns of variation in natural and regulated river flows.

Mean discharge, $\overline{Q}$, and the coefficient of variation of daily flows, CV_Q, are evaluated considering both the data-driven approach and the model-based framework. Conversely, autocorrelation and frequency stability analysis are only estimated based on streamflow time series. To ensure a proper comparison between natural (upstream) and regulated (downstream) river flow, each statistic is evaluated based on discharge records properly scaled to the drainage area (i.e., area of the contributing catchment at the stream gauge location).

2.2.1 Analytical Characterization of Flow Regimes

Natural flow regimes are embodied by the seasonal probability density function (PDF) of daily flows, here described through a mechanistic stochastic method [Botter et al., 2009]. The approach mimic the hydrological response of the basin by describing the underlying evolution of the catchment water storage [Laio et al., 2001]. The dynamics of the catchment storage are assumed to result from the superposition of evapotranspiration losses and stochastic increments triggered by precipitation, here assimilated to a marked Poisson process with frequency λ_P and exponentially distributed depths with mean α [Botter et al., 2007; Porporato et al., 2004]. When the soil water deficit created by evapotranspiration is filled by precipitation, the catchment water storage exceeds the field capacity and the excess of water is drained from the catchment according to a non-linear storage-discharge relationship, ultimately contributing to streamflow. Not all rainfall events are able to bring enough water to drive the catchment water storage above

the field capacity. Accordingly, the sequence of rainfall events that actively contributes to the hydrological response is a suitable subset of the overall rainfall and is approximated by a Poisson process similar to the main rainfall, though characterized by a reduced frequency $\lambda < \lambda_P$ [Botter et al., 2007]. Overall, daily streamflow dynamics result from the combination of sudden discharge increments during streamflow-producing rainfall events and non-linear recessions in between events (as implied by the assumption of a non-linear storage-discharge) [Kirchner, 2009; Porporato and Ridolfi, 2003]. The relation describing the temporal dynamics of specific streamflow, Q, is the following:

$$\frac{dQ(t)}{dt} = -KQ(t)^a + \xi_Q(t) \tag{2.1}$$

In Eq. (2.1) recessions are modeled as power-law decays with coefficient K and exponent a, while the sequence of random jumps induced on Q by streamflow-producing rainfall events is represented by ξ_Q. The steady-state PDF of streamflows, $p(Q)$, can be derived from the solution of the master equation associated to eq. (2.1) as [Botter et al., 2009]:

$$p(Q) \propto Q^{-a} \exp\left(-\frac{Q^{2-a}}{\alpha K(2-a)} + \frac{\lambda Q^{1-a}}{K(1-a)}\right) \tag{2.2}$$

Eq. (2.2) relies on four physically-based parameters (i.e., α, λ, K and a) and is valid only for $a > 1$, a restriction that is typically fulfilled in real world catchments. These parameters incorporate various climatic and geomorphologic features typical of the contributing catchment and should be estimated on a seasonal basis to account for the strong seasonality of flow regimes and possible regime shifts between seasons [Botter et al., 2013]. In this way, eq. (2.2) allows for the characterization of seasonal flow regimes.

Finally, the flow duration curve results from the integration of eq. (2.2) and is, thus, expressed as a cumulative distribution function (CDF):

$$D(Q) = \int_Q^\infty p(Q)dQ \tag{2.3}$$

It should be noted that the above model not only account for subsurface/groundwater contributions to river flows, but also for surface contributions generally triggered by

intense storms. This is fundamental in order not to underestimate the probability associated to the largest streamflows while predicting the nature of flow regimes and is done by implicitly incorporating the fast components of the hydrologic response in the non-linear storage-discharge relationship that drives the soil drainage. Conversely, the model does not account for precipitation falling as snow, disregarding possible carryover flows across seasons due to accumulation and melting processes. However, this is done implicitly by suitably adjusting the frequency of streamflow-producing events, λ, while estimating model parameters.

Figure 2.1 represents an example of the aforementioned model (figure 2.1, *B*) for one of the catchments considered in this study (figure 2.1, *A*).

2.2.2 Model Parameters Estimation

For the prediction of $p(Q)$ in the absence of discharge data, the four parameters of eq. (2.2) need to be set on a seasonal basis exploiting geomorphic and climate data. The beginning and ending dates of each season are identified based on calendar dates: (i) winter from 12/01 to 02/28; (ii) spring from 03/01 to 05/31; (iii) summer from 06/01 to 08/31; (iv) autumn from 09/01 to 11/30.

Mean rainfall depth, α, is evaluated as the mean precipitation during wet days of a given season. Calculations rely on spatially-averaged daily rainfall time series, which are estimated from synchronous rainfall records measured in one or more meteorological stations located within the boundaries of the considered catchment. The number of stations is preferably greater in large basins.

The frequency of streamflow-producing events, λ, is equal to the product between the frequency of rainfall events, λ_P, and the average seasonal runoff coefficient, ϕ, expressing the ratio between mean seasonal precipitation and mean seasonal discharge [Doulatyari et al., 2015; Porporato et al., 2004]:

$$\lambda = \phi \lambda_P \tag{2.4}$$

The frequency of rainfall events, λ_P, can be computed from rainfall records as the relative number of days, in a certain season, with a rainfall depth equal to or higher

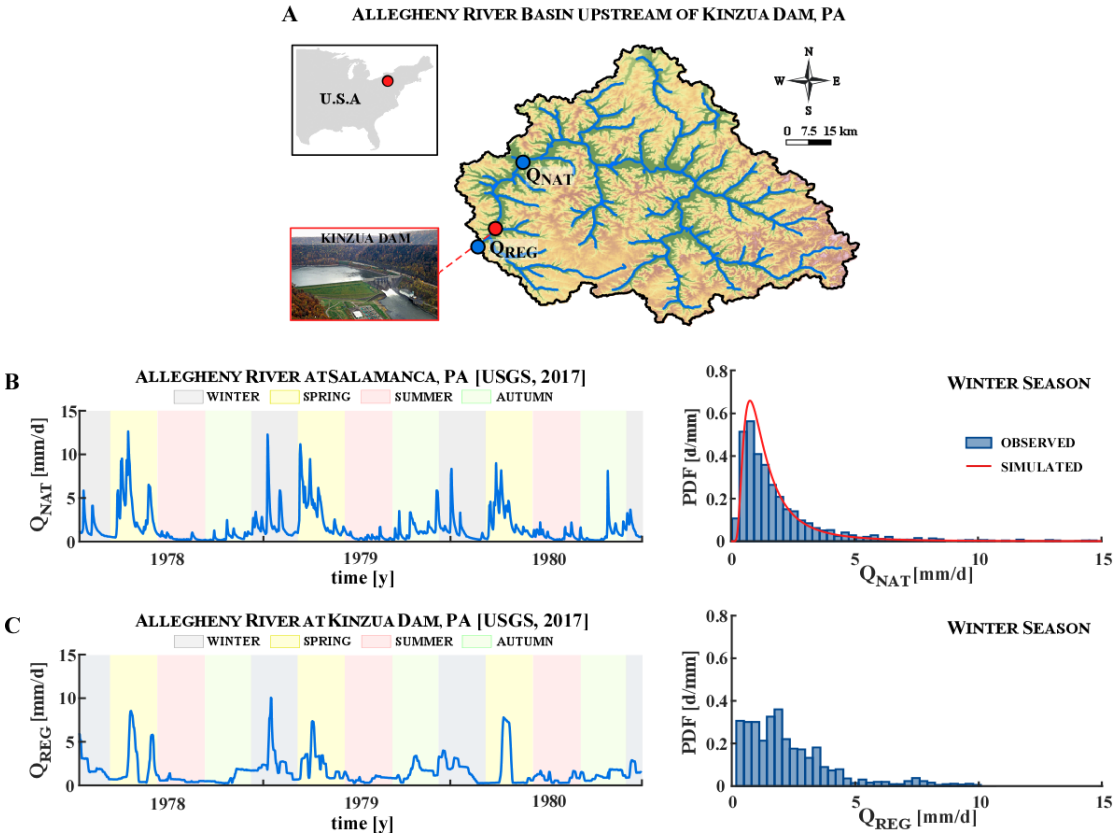

FIGURE 2.1: Mechanistic stochastic method used to predict natural regimes in catchments where undisturbed flow time series are lacking. (*A*) Allegheny River Basin upstream of the Kinzua Dam, one of the most important water infrastructures in northwestern Pennsylvania (USA). Blue circles represent the USGS stations providing discharge time series upstream and downstream of the dam, while the red one indicates the dam itself. (*B*) Temporal dynamics of natural streamflows entering the Allegheny reservoir, and the corresponding observed (blue bars) and simulated (red line) PDFs typical of the winter season. (*C*) Temporal dynamics of regulated streamflows, and the observed PDF for the winter season. The comparison between natural and regulated flow regimes clearly shows the impact of Kinzua dam.

than 1 mm [Doulatyari et al., 2017]. Conversely, the average seasonal runoff coeffcient, ϕ, is estimated by means of the physically-based analytical stochastic model of soil moisture dynamics proposed by Porporato et al. [2004]. This approach investigates the temporal evolution of soil moisture, s, in the root zone at the daily timescale, treating the soil as a reservoir whose capacity depends on the root zone depth, Z_R, and on the root zone porosity, n [Milly, 1993; Settin et al., 2007; Porporato et al., 2004]. Overall, soil moisture dynamics result by the superposition of three different processes: (i) stochastic instantaneous jumps due to rainfall events intermittently filling the soil through infiltration phenomena; (ii) losses due to evapotranspiration, which is assumed to increase linearly from 0, at the wilting point ($s = s_w$), to a maximum value called "potential evapotranspiration", at a suitable soil moisture threshold comprised between field capacity and saturation ($s = s_1$); (iii) instantaneous deep percolation triggered by the excess rainfall, inducing the increase of the soil moisture above the threshold s_1. The resulting mean runoff coeffcient, ϕ, is defined as [Botter et al., 2007]:

$$\phi = \frac{D_I \gamma^{\frac{\gamma}{D_I}} e^{-\gamma}}{\gamma \Gamma\left(\frac{\gamma}{D_I}, \gamma\right)} \tag{2.5}$$

In eq. (2.5), $\Gamma(.,.)$ represents the lower incomplete Gamma function, D_I is the Budyko's dryness index and is defined as the ratio between the average seasonal potential evapotranspiration and precipitation (i.e., $D_I = \overline{PET}/\overline{P}$), and γ is the maximum soil water storage available to plants normalized to the mean rainfall depth (i.e., $\gamma = \zeta/\alpha$, with $\zeta = [(s_1 - s_w)nZ_R])$. Soil and vegetation parameters involved in the evaluation of ζ are assumed to be constant in time during each season, throughout the entire catchment and among different catchments. More specifically, n, s_w and s_1 are time invariant and spatially uniform across sites, and are set by assuming literature values (i.e., $n = 0.35$, $s_w = 0.20$ and $s_1 = 0.50$), whereas Z_R is calibrated seasonally based on observed rainfall and discharge data in fully gauged sites. Note that Z_R is the only calibrated parameter of the entire approach.

The evaluation of the recession exponent, a, is grounded on the widespread idea that streamflow values characterizing recession periods are governed by geomorphologic features typical of the contributing catchment [Biswal and Marani, 2010; Biswal and

Nagesh Kumar, 2013; Biswal and Marani, 2014], and so it is based on the geomorphological recession flow model proposed by Biswal and Marani [2010]. This model states that the active drainage network (i.e., the portion of the hydrographic network actively contributing to the flow at the catchment outlet, hereafter indicated as ADN) expands and contracts following the related streamflow fluctuations, thus increasing and decreasing over time during high flow and recession events, respectively. Accordingly, the model defines the specific streamflow, Q, as the product between the length of the ADN, G, and the discharge per unit length, q, properly scaled to the area of the contributing catchment, A.

$$Q(t) = \frac{qG(t)}{A} \tag{2.6}$$

Within this conceptual framework, the following assumptions are made: (i) the rate at which the ADN recedes, c, and the discharge per unit length, q, are constant; (ii) the temporal derivative of streamflow, dQ/dt, is governed by the rate of change of the ADN; (iii) the distance between a specific channel segment and the farthest upstream source, l, is proportional to the period of time in which the same segment contributes to the recession flow, allowing for the exchange of time for length during recession periods. Consequently, the recession equation $dQ/dt = KQ^a$ is rewritten as follows:

$$\frac{N(l)}{A} \propto \left(\frac{G(l)}{A}\right)^a \tag{2.7}$$

where $N(l)$ is the number of channel sources in the ADN configuration at a distance l from the catchment outlet. Eq. (2.7) provides a valuable interpretation of the recession hydrograph solely based on the morphology of the considered catchment, allowing for the evaluation of the recession exponent, a, through a least square regression relation between $G(l)$ and $N(l)$. Information about catchment morphology are readily available through high resolution digital elevation models (DEMs): via a suitable GIS-based manipulation, they permit a reliable reconstruction of the river network and the consequent estimation of the parameter a at the catchment outlet that, in the present study, is always ideally located in correspondence to a dam.

Finally, the recession coefficient, K, quantifies catchment-scale hydrological and morphological attributes and is estimated by means of the empirical model presented by

Doulatyari et al. [2015]. According to the considered approach, K can be expressed as a function of the mean discharge, $\overline{Q} = \lambda\alpha$, and of the recession exponent, a, by mean of the following equation:

$$K = \theta(\alpha\lambda)^{1-a} \tag{2.8}$$

In eq. (2.8), θ is a parameter dependent on the rate at which the ADN recedes. Empirical studies revealed that the value of θ is approximately constant across different sites and seasons, and set its value equal to $0.23\, d^{-1}$ for catchments in the continental United States [Doulatyari et al., 2015].

2.2.3 Coefficient of Variation

The long-term coefficient of variation of daily flows, CV_Q, is evaluated both seasonally and annually. The need to work at the seasonal time scale derives by the strong seasonality of flow regimes, which is in turn related to the underlying climatic control on river flows. Additionally, long term periods are considered in order to fulfill the ergodicity condition, meaning that the statistical properties of the signal can be reasonably deduced from a single, sufficiently long sample of records. Flow regimes are classified as "persistent" when $CV_Q < 1$. In this case, a persistent supply is guaranteed to the stream from the catchment soil, and river flows are weakly variable around the mean and quite predictable. Conversely, flow regimes are called "erratic" when $CV_Q > 1$. In these circumstances, it is not possible to generate a persistent supply to the stream from the catchment because rainfall has to increase the soil water content significantly before creating a new water pulse; consequently, streamflows can vary significantly and their temporal patterns are quite unpredictable. Finally, $CV_Q \approx 1$ indicates "intermediate" flow regimes [Botter et al., 2013].

When discharge time series are concerned, the seasonal coefficient of variation is estimated as the ratio between the standard deviation and the average of daily river flows recorded in a specific season during the time period of analysis. More specifically, for each three-month season, k, belonging to the period of records, the coefficient of variation is evaluated as:

$$CV_{Q_k} = \sqrt{\frac{s^2(Q_k)}{(\overline{Q_k})^2}} \tag{2.9}$$

where Q_k is the time series of daily streamflows observed during the considered three-month season, k, while $\overline{Q_k}$ and $s^2(Q_k)$ are the average and the variance of sample Q_k, respectively. Accordingly, the overall CV_Q for a period composed by a certain season repeated over different years is expressed as:

$$CV_Q = \sqrt{\frac{1}{M}\sum_{k=1}^{M}\psi_k CV_{Q_k}} \qquad \psi_k = \left(\frac{\overline{Q_k}}{\overline{Q}}\right)^2 \tag{2.10}$$

where M is the total number of three-month seasons belonging to the considered long-term period and ψ_k is the square of the specific weight characterizing each season (i.e., the ratio between the mean daily discharge of the season and that of the entire time window). Figure 2.2 graphically represents the approach used to calculate CV_Q. The evaluation of the annual coefficient of variation is analogous (i.e., eqs. 2.9 and 2.10 with k equal to one year).

In catchments where flow time series upstream of dams are lacking, the evaluation of the seasonal coefficient of variation of natural streamflow is based on the moments of the analytical PDF of daily discharge, estimated through the numerical integration of eq. (2.2).

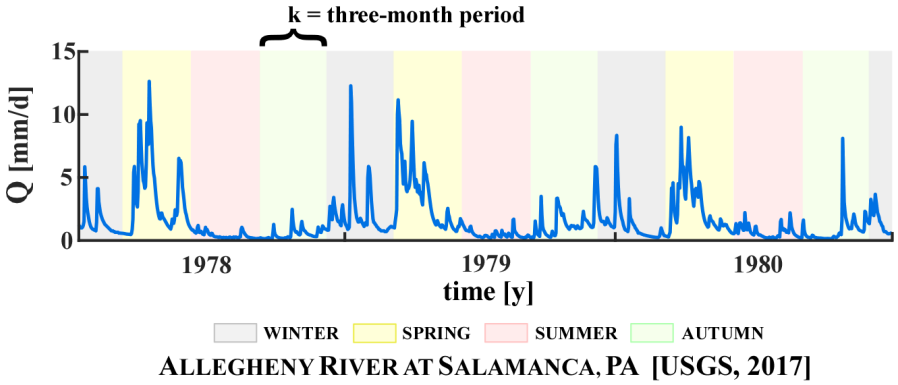

FIGURE 2.2: Estimation of CV_{Q_k} and CV_Q.

In order to identify the distinctive effect of different anthropogenic water uses on natural flow regimes, the comparison between the CV_Q upstream and downstream of reservoirs is carried out stratifying reservoirs on the basis of their use. Moreover, to analyze how flood control and water supply interact in multipurpose structures and identify the extent of the counterbalancing effect of water supply on the overall magnitude of flow

regime alterations due to flood control, the analysis of CV_Q is also performed subdividing multipurpose reservoirs including water supply from those only operated to mitigate floods (see Table 2.1). To ensure a fair comparison, the variation of the CV_Q generated by each structure is properly scaled to the corresponding regulation capacity (see section 2.5.1). Average values obtained for each group of structures are then compared.

2.2.4 Autocorrelation Analysis

The autocorrelation function is a fundamental tool to describe the degree of stability of daily discharges observed in different days. The autocorrelation of the process $Q(t)$ at time-lag τ is evaluated by multiplying $Q(t)$ by a τ-delayed version of itself and is, thus, defined through the following equation [Riley, 2008]:

$$\widehat{\rho}(\tau) = \frac{E[(q_t - \mu_q)(q_{t+\tau} - \mu_q)]}{\sigma_q^2} \tag{2.11}$$

where q_t and $q_{t+\tau}$ are realizations of the process $Q(t)$ at instants t and $t+\tau$, while μ_q and σ_q^2 represent the mean and the variance of $Q(t)$, respectively. A much common and simple way to express the stability of a signal is given by the integral scale, $\widehat{T}$, which represents the area underlying the autocorrelation function and, thus, the time needed for a signal to decorrelate.

$$\widehat{T} = \int_0^{\infty} \rho(\tau) d\tau \tag{2.12}$$

Effectively, only a specific time series of the process $Q(t)$ can be available, therefore the autocorrelation at lag τ and the integral scale are calculated as [Riley, 2008]:

$$\rho(\tau) = \frac{\frac{1}{n}\sum_{t=1}^{n-\tau}(q_t - \overline{q})(q_{t+\tau} - \overline{q})}{\frac{1}{n}\sum_{t=1}^{n}(q_t - \overline{q})^2} \tag{2.13}$$

$$T = \int_0^{T_{max}} \rho(\tau) d\tau \tag{2.14}$$

where $\overline{q}$ is the average of the considered time series of $Q(t)$, including q_t and $q_{t+\tau}$, and n is the number of data characterizing the time series. As the time domain of the empirical autocorrelation function is finite, uncertainties may arise on how best to define the integration domain for the evaluation of the integral scale, T. A good

estimation of T can be obtained when the time domain of the autocorrelation function is large enough that only little changes occur when increasing the upper bond, T_{max} [O'Neill et al., 2004]. However, it is possible to overcome this problem by integrating the autocorrelation function up to the first zero-crossing of $\rho(\tau)$ (i.e., the first instant at which $\rho(\tau)$ passes through zero, crossing the horizontal axis, and changes its sign) [Katul and Parlange, 1995]. This is what is done in this study (i.e., $T_{max} = \tau^*$, where τ^* is the minimal $\tau > 0 \mid \rho(\tau) = 0$).

2.2.5 Frequency Stability Analysis

The time domain stability analysis of river flows adds a quantitative and standardized description of the behaviour of daily discharge time series in regulated and unregulated rivers. This analysis should be based on a second moment measure of the frequency fluctuations typical of a given signal. In most cases, the standard variance, that depends on the variations around the average value, does not provide a simple way to analyze a signal, as it is not convergent for many different noise types; accordingly, other types of variance should be considered [Riley, 2008]. The Allan variance, σ_A^2, which is based on the variation between the averages of consecutive samples spanning a specific time interval τ, provides a measure that avoid the problem of divergence and represents a standard tool for frequency stability analysis in the time domain [Allan, 1966]. In particular, the time domain stability of a signal is expressed by means of a log-log plot of the Allan deviation, σ_A, versus the sample averaging time, τ: by analyzing the slope, α, of the $\sigma_A(\tau)$ curve in a log-log plot different noise types can be identified, as it can be associated to specific spectral power law components. The standard non-overlapped Allan deviation is expressed through the following equation [Allan, 1966; Riley, 2008]:

$$\sigma_A(\tau) = \sqrt{\frac{1}{2(n/m - 1)} \sum_{i=1}^{n/m-1} (\overline{q}_{i+1} - \overline{q}_i)^2} \tag{2.15}$$

where n is the total number of data characterizing a given time series of the signal $Q(t)$, m is the number of data typical of each sample in which the time series is divided (i.e. $m = \tau/t$, with t representing the measurement time), $\overline{q}_i$ is the average of the m values contained in sample $[(i-1)m + 1,\ im]$ and $\overline{q}_{i+1}$ is the average of the m values in the

adjacent sample. The confidence of the resulting stability estimates can be improved by calculating the overlapped Allan deviation as:

$$\begin{aligned}\sigma_A(\tau) &= \sqrt{\frac{1}{2(n-2m+1)}\sum_{i=1}^{n-2m+1}(\overline{q}_{i+1}-\overline{q}_i)^2} = \\ &= \sqrt{\frac{1}{2m^2(n-2m+1)}\sum_{i=1}^{n-2m+1}\left[\sum_{j=i}^{i+m-1}(q_{j+m}-q_j)\right]^2}\end{aligned} \tag{2.16}$$

Differences between the non-overlapped and the overlapped Allan deviation derive by the way in which samples are collected. When the given time series of $Q(t)$ is divided into different samples, each one characterized by m data, and each data q_i belongs to a single sample, the sampling procedure is called non-overlapping and is performed to evaluate the non-overlapped Allan deviation. Differently, when the given time series is divided so as to obtain all possible combinations of the data set and a single data q_i is thus included in more than one sample, the sampling procedure is called overlapping sampling and is performed to evaluate the overlapped Allan deviation. Figure 2.3 reports a graphical representation of the aforementioned sampling procedures.

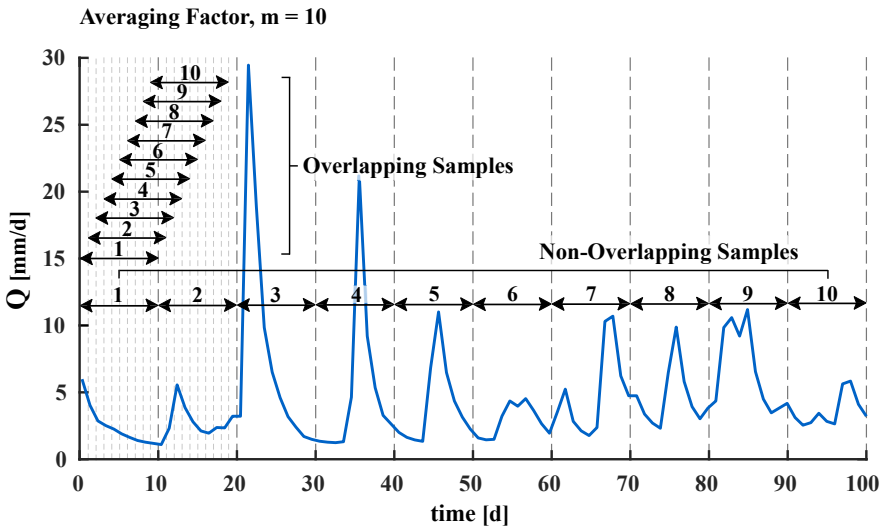

FIGURE 2.3: Comparison of non-overlapping and overlapping sampling.

In the following study, the frequency stability analysis of daily discharge time series recorded upstream and downstream of reservoirs is performed weekly and seasonally based on the overlapped Allan deviation. As a linear dependence between the Allan deviation and the averaging time is barely observed in a log-log plot when considering

streamflow records, the slope of $\sigma_A(\tau)$, α, is calculated locally as the slope of the line interpolating $\sigma_A(\tau)$ at the points τ_i and τ_{i+1} in the log-log plot:

$$\alpha_i = \frac{\log(\sigma_A(\tau_{i+1})/\sigma_A(\tau_i))}{\log(\tau_{i+1}/\tau_i)} \tag{2.17}$$

Values of α_i with $i < 10$ are thus considered to analyze the frequency stability of river flows at the weekly time scale, while values of α_i with $10 \leq i \leq 100$ are considered when working at the seasonal time scale. In this context, attention will be focused on three different noise types identified by a log σ_A versus log τ slope ranging between -0.5 and 0.5. According to the existing one-to-one correspondence between the slope of the log-log Allan deviation plot and specific spectral power law components, the considered noise types are: (i) White Noise, identified by $\alpha = -0.5$; (ii) Pink Noise, identified by $\alpha = 0.0$; (iii) Red Noise, identified by $\alpha = 0.5$. White noises represent random signals characterized by equal intensity at different frequencies and by a self-averaging behaviour, as $\alpha = -0.5$ implies that averages become steadily less variable over longer averaging time scale [Kirchner and Neal, 2013]. Differently, pink noises show more energy at lower frequency (i.e.,$1/f$ power spectral density) and a non-self-averaging behaviour, since the flat profile of the log-log Allan deviation plot implies that averages taken over longer and longer time intervals do not converge towards a stable value [Kirchner and Neal, 2013]. Finally, red noises show higher amount of energy associated to lower frequency than pink noises (i.e. $1/f^2$ power spectral density) and are characterized by a divergent behaviour, as $\alpha = 0.5$ implies that averages variability keep growing over longer averaging time scales.

2.3 Study Sites and Hydro-Climatic Data

This study investigates the downstream effect of a representative selection of dams distributed throughout the Central-Eastern United States. To ensure the reliability of our analysis, the considered sample only consists of structures meeting specific selection criteria. First, selected dams should be primarily operated to mitigate floods, supply fresh water or generate hydroelectric power, so that observed regulation impacts

could be associated to the above functions. Second, dams must impound poorly engineered rivers to avoid the misleading overlap between the effects of different hydraulic devices operating in cascade. Third, corresponding reservoirs must be characterized by a reasonably high storage capacity, exceeding 10^6 m^3, in order to be eligible to exert a significant impact on downstream hydrology. Lastly, dams must be located upstream of one or more flow gauges providing sufficiently long records of regulated streamflows. To capture the impact of regulation, no major tributaries can intervene between the selected dam and river gauges and their spacing, properly scaled to the drainage area, must be reasonably small. Overall, 47 isolated dams that appears to be sufficiently well distributed throughout the Central-Eastern United States are detected, thus spanning a wide range of hydro-climatic settings. Winters are long, severe and affected by relevant snow precipitation in the northern sites, while summers are great, hot and sometimes characterized by prolonged droughts in the southern sites; river flows are generally abundant in the eastern regions, while a significant tendency towards low flows is observed in the central regions, where annual water losses from evapotranspiration can be higher than the annual precipitation. As previously mentioned, the considered dams additionally span three different water uses, allowing for a detailed understanding of the correlation between regulation effects and specific reservoir management strategies (attention is focused on the effect of regulation for flood control, water supply and hydropower production).

Information about the 47 dams and reservoirs selected in this study are mainly found in the annual reports of the U.S. Army Corps of Engineers, the U.S. Federal Agency responsible for developing and managing several reservoir projects in the United States. Important exceptions are represented by reservoirs only used for water supply and/or hydropower production, as they are not owned and operated by the U.S. Army Corps of Engineers. Relevant pieces of information, that are taken into account during the selection of dams, concern project functions, total reservoir storage capacity and the year in which the dam was placed in operation. For all the considered sites, daily discharge records are collected by the United States Geological Survey (USGS), considering time series typically spanning several decades. With reference to discharge data, selected sites are divided into two sets: (i) 25 sites with known streamflow time series

both upstream and downstream of the reservoir; (ii) 22 sites where extensive hydrologic data are considered only for reservoir release. The opportunity for overcoming the need of discharge records upstream of reservoirs derives by the application of a physically-based model designed to characterize natural flow regimes in ungauged settings [Botter et al., 2009]. The model is first applied to the first set of sites to calibrate its parameters (i.e., the root zone depth, Z_R), and then to the second one for predicting unregulated flow regimes. Climatic and geomorphological data required by the model are acquired through different databases: (i) daily rainfall records are collected by the Global Historical Climatology Network (GHCL) and the American National Oceanic and Atmospheric Administration (NOAA); (ii) potential evapotranspiration data (i.e. PET) are provided by the "CGIAR-CSI Global-Aridity and Global-PET Database", a freely available dataset containing monthly and annual average values of PET for the entire world; (iii) digital elevation models (i.e. DEMs) characterized by an horizontal resolution of $30m$ are obtained by the United States Geological Survey (USGS).

Figures 2.4 and 2.5 show the spatial distribution of the 47 reservoirs selected in this study, properly stratified on the basis of their functions (Fig. 2.4) and of the considered discharge records (Fig. 2.5). Summary information about these reservoirs are presented in Table 2.1. In particular, Table 2.1 contains the name of each reservoir selected in the study, the US state where it is located, the name of the impounded stream, the year in which the structure was placed in operation, the area of the contributing catchment, total reservoir storage capacity and reservoir functions. Note that project functions are reported using the following nomenclature: (i) F = Flood Control; (ii) S = Urban Water Supply; (iii) P = Hydropower Production; (iv) A = Low Flow Augmentation; (v) N = Navigation; (vi) Q = Wildlife Preservation; (ix) X = Water Conservation and Sedimentation. Additionally, summary information about NOAA and USGS stations providing daily rainfall and streamflow time series are reported in Table 2.2. For each of the considered sites, stations are selected in order to have synchronous rainfall and streamflow records during a specific time period (time period of analysis). Rainfall stations are preferably located within the boundaries of the contributing catchment, while discharge stations are always located upstream and downstream of the considered reservoir.

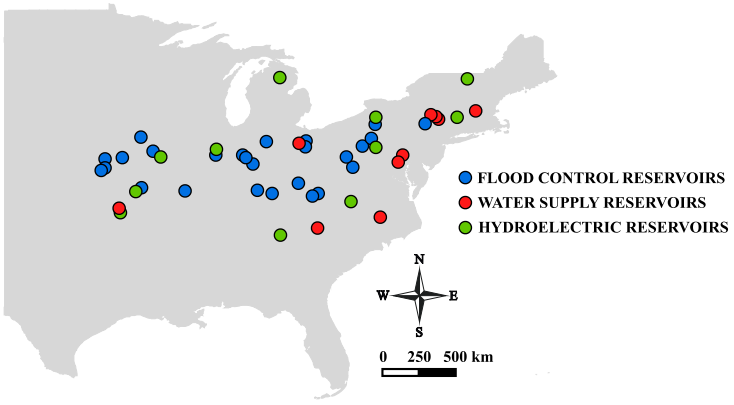

FIGURE 2.4: Spatial distribution of the 47 sites that were selected to investigate the downstream effect of dams on river flow regimes. Blue dots represent the 26 reservoirs primarily used for flood control, red dots show the 11 reservoirs only used for water supply and, finally, green dots represent the remaining reservoirs used for hydropower production.

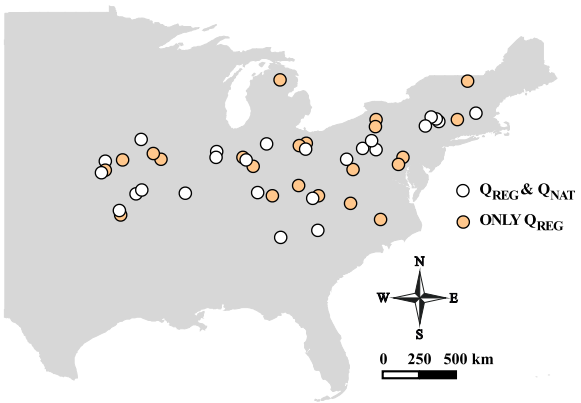

FIGURE 2.5: Spatial distribution of the 47 sites that were selected to investigate the downstream effect of dams on river flow regimes. White dots represents the 25 sites with known streamflow time series both upstream and downstream of the reservoir, while orange dots show the 22 sites where discharge records are considered only for regulated streamflows.

TABLE 2.1: Summary information about the 47 reservoirs selected in this study.

Reservoir	**State**	**Stream**	**Activation**	**Drainage Area [Mm^2]**	**Storage [Mm^3]**	**Project Functions**
Allegheny	PA	Allegheny River	1965	5646	1460	FPAQRW
Alum Creek	OH	Alum Creek	1975	319	166	FSRW
Buckhorn	NC	Contentnea Creek	1974	417	26	S
Cagles Mill	IN	Mill Creek	1952	764	281	FRX
Cannonsville	NY	WB Delaware River	1964	1181	362	S
Carters	GA	Coosawattee River	1975	1349	583	FPRW
Cave Run	KY	Licking River	1974	2142	757	FQRW
Clinton	KS	Wakarusa River	1977	1101	490	FSQRWX
C. M. Harden	IN	Big Racoon Creek	1960	575	164	FRX
Curwensville	PA	WB Susquehanna River	1965	945	153	FR
Decatur	IL	Sangamon River	1922	2430	24	S
Delaware	OH	Olentangy River	1961	987	337	FARW
EB Clarion	PA	EB Clarion River	1952	188	104	FAQRX
Eucha	OK	Spavinaw Creek	1952	930	99	S
Fishtrap	KY	Levisa Fork	1968	1023	205	FARW
J. W. Flannagan	VA	Pound River	1963	575	180	FAQR
Green River	KY	Green River	1969	1766	892	FSAQR
Loyalhanna	PA	Loyalhanna Creek	1942	751	118	FRW
Long Branch	MO	EF Lil Chariton River	1980	290	80	FSQRW
Mark Twain	MO	Salt River	1983	6086	1760	FNPRSW
Mio Pond	MI	Au Sable River	1917	3525	8	P
Monroe	IN	Salt Creek	1964	1119	544	FSAR
Neversink	NY	Neversink River	1954	240	132	S
Nolin	KY	Nolin River	1963	1821	752	FAR
O'Shaughnessy	OH	Scioto River	1925	2538	20	S
Pepaction	NY	EB Delaware River	1955	964	531	S
Perry	KS	Delaware River	1969	2955	950	FSRWX
Philpott	VA	Smith River	1951	557	393	FPR
Pomme de Terre	MO	Pomme de Terre River	1961	1593	802	FRWX
Pomona	KS	100 and 10 Mile Creek	1963	834	284	FSQRWX
Prettyboy	MD	Gunpouder Falls	1932	211	72	S
Prompton	PA	WB Lackawaxen River	1960	155	64	FQR
Quabbin	MA	Swift River	1939	490	1560	S
Rathbun	IA	Chariton River	1969	1422	681	FNQRWX
Raystown	PA	Juniata River	1973	2487	940	FPRW
Rocky Gorge	MD	Patuxent River	1952	342	21	S
Salomonie	IN	Salomonie River	1966	1432	325	FRW
Shelbyville	IL	Kaskaskia River	1970	2730	844	FSNRW
Smithville	MO	Little Platte River	1982	606	304	FSQRW
Stockton	MO	Sac River	1969	3005	2060	FPRW
Sutton	WV	Elk River	1960	1391	327	FARWX
Tenkiller	OK	Illinois River	1952	4183	1520	FP
Tygart	WV	Tygart Valley River	1938	3067	355	FANRX
Zoar	CT	Housatonic River	1919	3999	33	P
Wappapello	MO	St. Francis River	1941	3393	756	FR
Waterbury	VT	Little River	1938	288	46	FRP
W. C. Bowen	SC	Pacolet River	1960	549	28	S

TABLE 2.2: NOAA and USGS stations providing rainfall and discharge time series.

Reservoir	**State**	**Period**	**Rainfall Stations [GHCL]**	**Discharge Stations [USGS]**	
				$\mathbf{Q_{NAT}}$	$\mathbf{Q_{REG}}$
Allegheny	PA	1970-1990	USC00360868/00300766	-	03012550
Alum Creek	OH	2000-2015	USC00331404/00338951, USW00004855	03228750	03228805
Buckhorn	NC	1975-2000	USC00315123/00319476	-	02090380
Cagles Mill	IN	1970-2000	USC00123513/00125407	03358000	03359000
Cannonsville	NY	1970-1990	USC00302036/00302060/00308160	01423000	01425000
Carters	GA	1980-1997	USC00302036/00302060/00308160	02380500	02382500
Cave Run	KY	1975-1993	USC00157134/00153052	-	03249500
Clinton	KS	1985-2005	USC00141612/00140443	-	06891500
C. M. Harden	IN	1980-2000	USC00121873/00124356/00129300	-	03340900
Curwensville	PA	1970-1990	USC00361519/00365336/00365408	01541000	01541200
Decatur	IL	1982-2000	USC00113413/00115792, USW00014806	05572000	05573540
Delaware	OH	1995-2015	USC00333021/00334942	-	03225500
EB Clarion	PA	1970-1990	USC00363311	-	03027500
Eucha	OK	2000-2015	USC00032930/00034910	071912213	07191288
Fishtrap	KY	1971-1991	USC00152825/00443640	-	03208000
J. W. Flannagan	VA	1977-1997	USC00151120/00446173/00449215	03208950	03209000
Green River	KY	1973-1993	USC00154755/00150940	-	03306000
Loyalhanna	PA	1963-1990	USC00362108/00362183	03045010	03047000
Long Branch	MO	1999-2015	USC00235050, USW00014938	-	06906200
Mark Twain	MO	1985-2010	USC00234544/00235541/00235671	-	05507800
Mio Pond	MI	1998-2015	USC00203391/00203099	-	04136500
Monroe	IN	1970-2000	USC00120784/00127935/00121747	-	03372500
Neversink	NY	1970-1990	USC00301521/00307799	01435000	01436000
Nolin River	KY	1975-2000	USC00153252/00153929/00155684	03310300	03311000
O'Shaughnessy	OH	1995-2012	USC00336861/00334189/00334942	-	03221000
Pepaction	NY	1970-1990	USC00300254/00302036/00301860	01413500	01417000
Perry	KS	1975-2000	USC00143759/00143810/00149026	06890100	06890900
Philpott	VA	1970-2000	USC00446692/00443071/00449272	-	02072000
Pomme de Terre	MO	1970-2000	USC00230789/00231087/00235307	06921070	06921350
Pomona	KS	1970-1996	USC00142602/00143467/00146498	06911900	06912500
Prettyboy	MD	2000-2015	USC00185934	-	01581920
Prompton	PA	1986-2001	USC00364043/00367029	01428750	01429000
Quabbin	MA	1985-2005	USC00190408/00193401/00198573	01174500	01175500
Rathbun	IA	1970-2000	USC00131354/00131394/00136316	06903400	06903700
Raystown	PA	1988-2008	USC00361087/00362721/00369823	01562000	01563200
Rocky Gorge	MD	1978-1992	USC00181125	-	01592500
Salomonie	IN	1975-1989	USC00123777/00127069	03324300	03324500
Shelbyville	IL	1975-2000	USC00118740/00115792/00118684	05591200	05592000
Smithville	MO	1999-2015	USC00230143/00237862	-	06821150
Stockton	MO	1975-1988	USC00230657/00235027, USW00013995	06918440	06919000
Sutton	WV	1970-1991	USC00463798/00469086/00469333	-	03195500
Tenkiller	OK	1970-2010	USC00032444/00344672	-	07198000
Tygart	WV	1960-1980	USC00460633/00469086, USW00013729	03054500	03056000
Zoar	CT	1970-2000	USC00062658/00199371/00069775	-	01205500
Wappapello	MO	1989-2004	USC00230224/00232809/233038	07037500	07039500
Waterbury	VT	1990-2015	USC00435376/00435416	-	04289000
W. C. Bowen	SC	2000-2015	USC00381625/00318744	02154790	02155500

2.4 Model Calibration and Performances

The physically-based analytic model capable of predicting natural flow regimes in ungauged catchments relies on four parameters, whose values are estimated by coupling the considered method with the geomorphological recession flow model proposed by Biswal and Marani [2010] and the physically-based analytical stochastic model of soil moisture dynamics proposed by Porporato et al. [2004] (see section 2.2.2). The latter approach requires the calibration of the root zone depth, Z_R, to evaluate the frequency of streamflow-producing rainfall events, λ. As Z_R is assumed to be constant in time during each season, throughout the entire catchment and among different catchments, calibration is performed seasonally by means of a multisite framework based on the 25 sites with known time series of unregulated discharge. Moreover, as the main focus of this study is the analysis of the impact of regulation on streamflow variability, calibration of Z_R is performed by comparing modeled and observed coefficients of variation of daily flows, CV_Q. The physically-based analytic model is thus applied seasonally to the 25 catchments with known streamflow records upstream of the dams and, for each value of Z_R, accuracy is assessed through the Mean Squared Relative Error (MSRE) of estimated $CV_Q s$. Calibrated values of Z_R are those minimizing the the Mean Squared Relative Error, and are used for predicting unregulated flow regimes of catchments where streamflow time series are lacking. Note that calibrating Z_R using observed mean discharges instead of observed $CV_Q s$ would leads to similar results.

The calibration sites located in the Northeastern United States (see figure 2.5) are characterized by the highest latitudes and elevations, being located along the Appalachian Mountains, and thus experience relevant snow precipitation during the winter season. Therein, snowfall significantly impacts the water balance through accumulation and melting processes, thus increasing the catchment water storage in winter and the flow rate in spring and sometimes in summer. The hydrological model does not explicitly consider these phenomena; therefore, in these sites, the frequency of streamflow-producing events, λ, shall account for the carryover flows across seasons by suitably calibrating the value of the root zone depth, Z_R [Schaefli et al., 2013; Doulatyari et al., 2015]. Accordingly, during the calibration procedure, Northeastern sites (belonging to the 25

sites with known streamflow time series both upstream and downstream of dams) are considered separately, thus calibrating the seasonal value of the root zone depth for two different groups of dams. Table 2.3 reports the values of the catchment mean elevation and of the average annual snowfall for all the considered sites, confirming that Northeastern sites are those characterized by the highest values of the average annual snowfall ($> 1000\ mm$), at least in the period of analysis. Additionally, table 2.4 reports the calibrated values of Z_R.

As an example, figure 2.6 reports the comparison between observed and modeled PDFs of natural streamflow for two sites belonging to the two different catchment groups: the Spavinaw Creek Basin upstream of Eucha Lake, Oklahoma, and the East Branch Delaware River Basin upstream of Pepacton Lake, New York State. In both catchments, the frequency of flow producing events, and thus the likelihood of high flows, is greater in winter and spring. This reflects on streamflow PDFs, that appear to be hump-shaped in spring and winter seasons and monotonically decreasing in autumn and summer seasons. However, the Spavinaw Creek Basin is characterized by seasonal flow regimes with a higher degree of erraticity than those observed in the East Branch Delaware River Basin, as confirmed by the larger values of CV_Q (reported within each plot). Visual inspection reveals that the observed PDF of flows is well reproduced by the analytical model in all seasons and for both sites. This suggests the ability of the approach to characterize natural flow regimes across different hydro-climatic conditions.

Figure 2.7 shows the modeled seasonal coefficient of variation of daily discharge, CV_Q, plotted against the corresponding observed values for all the 25 study sites where discharge time series upstream of reservoirs are available. Modeled values of CV_Q are calculated numerically integrating eq. (2.2), where the parameter λ is obtained by eqs. (2.3) and (2.4) upon calibration of Z_R. The figure suggests the ability of the model to reproduce observed flow statistics in all seasons, even though some scatter is visible. In particular, the mean squared relative error of CV_Q is approximately equal to 0.08.

The obtained results suggest that the adopted approach is robust in reproducing the major features of natural flow regimes in different sites under a variety of climate and morphological conditions. Consequently, the model can be used to investigate the impact of dams on hydrological regimes.

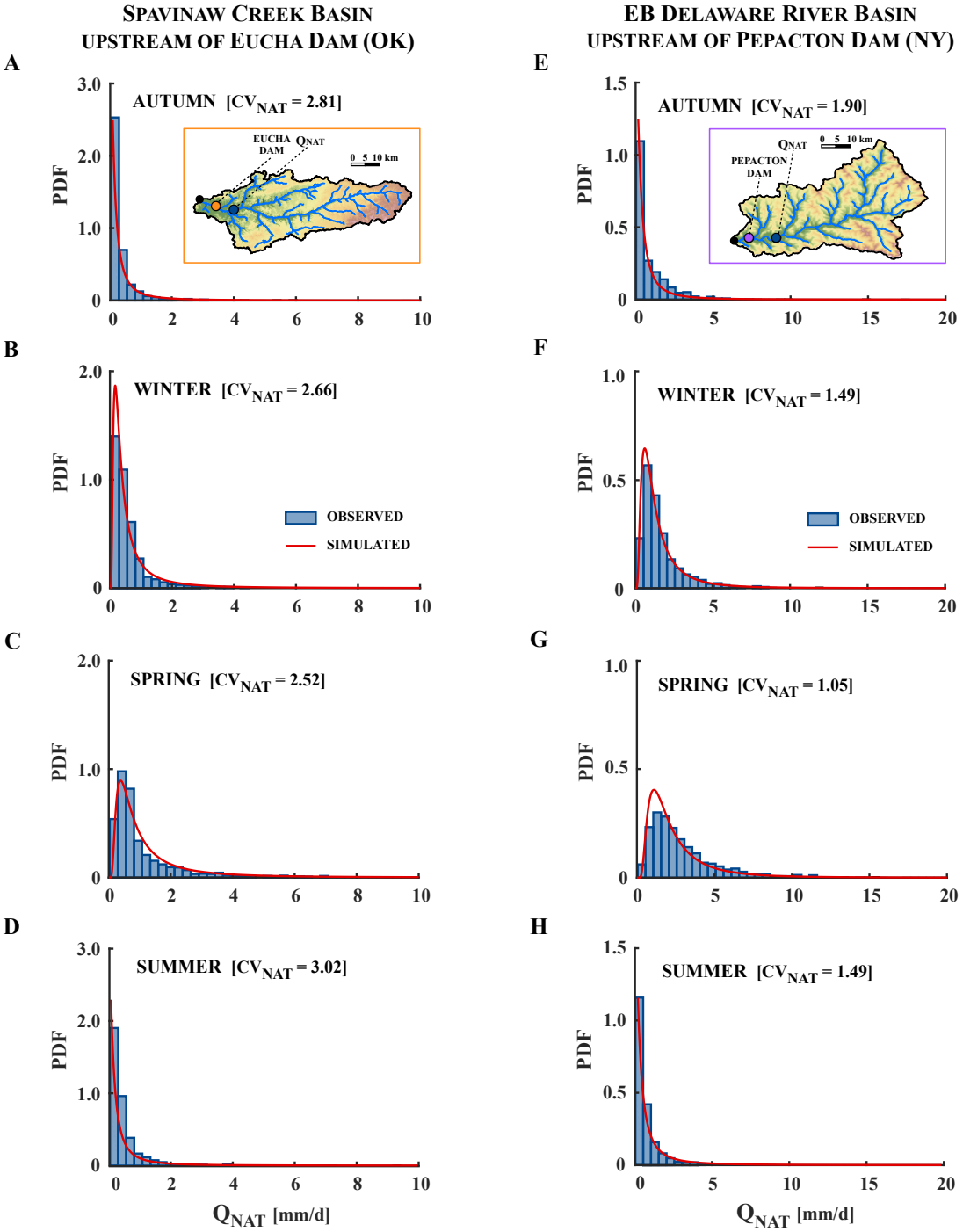

FIGURE 2.6: Observed (bar) and simulated (solid line) PDFs of natural streamflow for all seasons and two of the selected sites: the Spavinaw Creek basin upstream of Eucha lake ($A - D$), Oklahoma, and the East Branch Delaware River basin upstream of Pepacton lake ($E - H$), New York State.

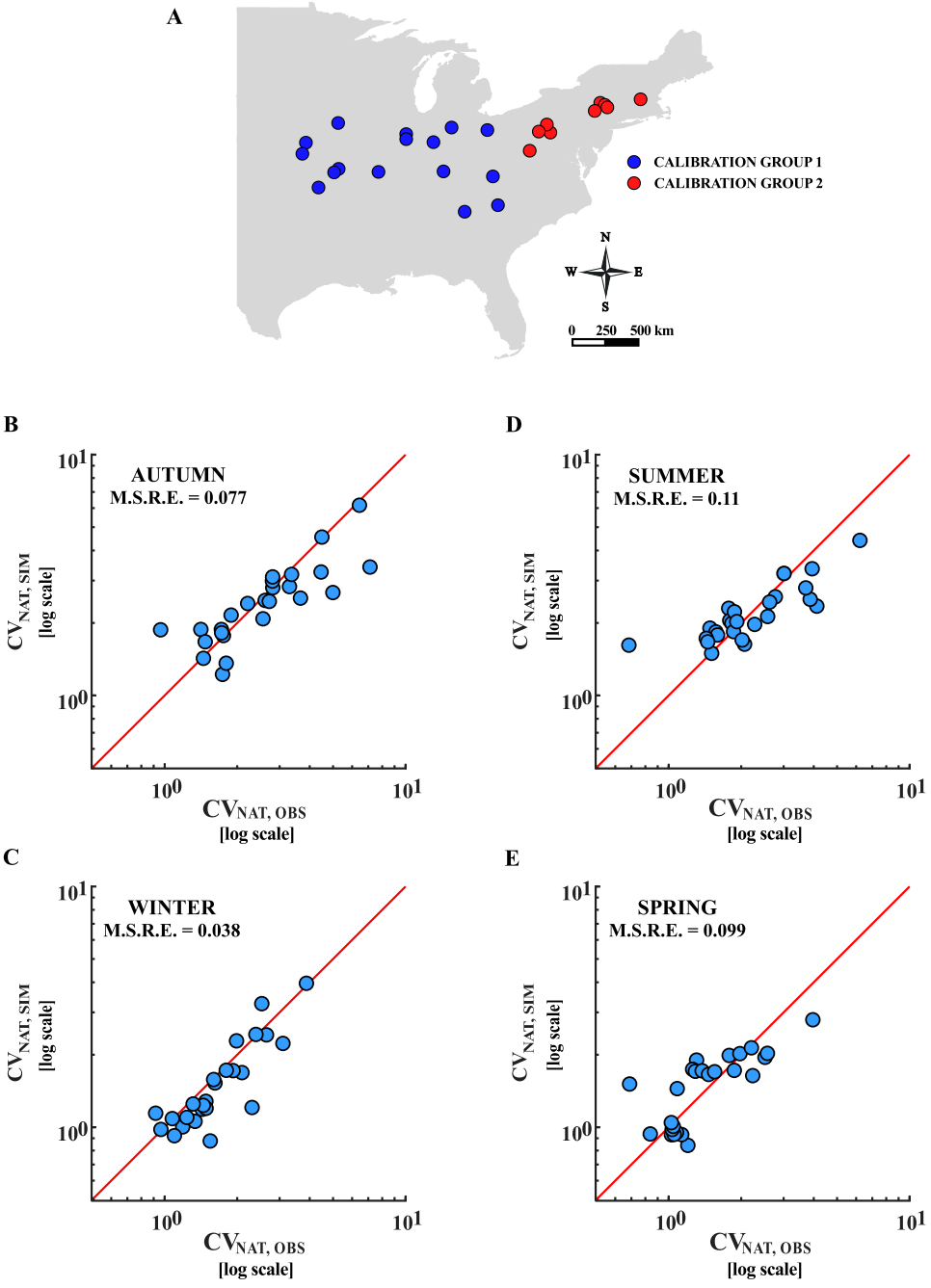

FIGURE 2.7: Model calibration. (A) Spatial distribution of the 25 sites used for the calibration of the root zone depth, Z_R, in the soil water balance. Red dots identify Northeastern catchments, characterized by the highest values of the average annual snowfall (> 1000 mm), while blue dots represent all the other catchments. ($B - E$) Scatter plots of observed vs. modeled coefficient of variation, CV_Q, for all seasons at the 25 test catchments. The Mean Squared Relative Error of estimated CV_Q is reported for each season.

TABLE 2.3: Catchment Mean Elevation and Average Annual Snowfall typical of the 25 sites considered during the calibration procedure.

Reservoir	**State**	**Catchment**	**Catchment Mean Elevation [m a.s.l.]**	**Average Annual Snowfall [m]**
Alum Creek	OH	Alum Creek Basin upstream of Alum Creek Lake	327	0.41
Cagles Mill	IN	Mill Creek Basin upstream of Cagles Mill Lake	237	0.60
Cannonsville	NY	WB Delaware River Basin upstream of Cannonsville Lake	579	1.47
Carters	GA	Coosawattee River Basin upstream of Carters Lake	548	0.11
Curwensville	PA	WB Susquehanna River Basin upstream of Curwensville Lake	493	1.48
Decatur	IL	Sangamon River Basin upstream of Decatur Lake	220	0.47
Eucha	OK	Spavinaw Creek Basin upstream of Eucha Lake	337	0.36
J. W. Flannagan	VA	Pound River Basin upstream of J. W. Flannagan Lake	607	0.84
Loyalhanna	PA	Loyalhanna Creek Basin upstream of Loyalhanna Lake	490	1.01
Neversink	NY	Neversink River Basin upstream of Neversink Lake	735	2.21
Nolin	KY	Nolin River Basin upstream of Nolin Lake	227	0.16
Pepaction	NY	EB Delaware River Basin upstream of Pepacton Lake	644	1.52
Perry	KS	Delaware River Basin upstream of Perry Lake	345	0.47
Pomme de Terre	MO	Pomme de Terre River Basin upstream of Pomme de Terre Lake	354	0.23
Pomona	KS	Hundred and ten miles Creek upstream of Pomona Lake	343	0.49
Prompton	PA	WB Lackawaxen River upstream of Prompton Lake	509	1.46
Quabbin	MA	Swift River upstream of Quabbin Lake	265	1.45
Rathbun	IA	Chariton River upstream of Rathbun Lake	316	0.69
Raystown	PA	Juniata River upstream of Raystown Lake	475	1.07
Salomonie	IN	Salomonie River upstream of Salomonie Lake	273	0.67
Shelbyville	IL	Kaskaskia River upstream of Shelbyville Lake	207	0.57
Stockton	MO	Sac River upstream of Stockton Lake	352	0.47
Tygart	WV	Tygart Valley River upstream of Tygart Lake	670	1.62
Wappapello	MO	St. Francis River upstream of Wappapello Lake	264	0.34
W. C. Bowen	SC	Pacolet River upstream of W. C. Bowen Lake	337	0.08

TABLE 2.4: Calibrated values of Z_R. Group 2 specifically refers to sites located in Northeastern US, while group 1 refers to all the others.

Season	**Z_R [mm]**	
	Group 1	**Group 2**
Winter	240	0.0
Spring	240	0.0
Summer	420	260
Autumn	1600	800

2.5 Results

Results are organized into three different sections. Section 2.5.1 describes the main findings obtained through the analysis of mean water availability and hydrological variability. Section 2.5.2 investigates the temporal trajectories of flow regimes by means of the autocorrelation and frequency stability analyses. Finally, section 2.5.3 reports some typical examples of flow regime alterations by dams.

2.5.1 Mean water availability and hydrological variability

The nature of flow regimes in regulated and unregulated reaches is characterized through the first two moments of the discharge frequency distribution. They provide and objective measure of the mean water availability and hydrological variability, and are main drivers of the ecological and geomorphological instream processes [Olden and Poff, 2003; Doyle et al., 2005], thus representing key attributes of managed rivers. $\overline{Q}$ and CV_Q of natural and regulated flow regimes are evaluated for each combination of site and season, thereby leading to 376 couples of values that represent the downstream impact of dams on water resources. Analyzing the effect of regulation at the seasonal time scale is necessary to capture the seasonality of natural flows [Botter et al., 2013] and the associated temporal patterns of hydrological alterations by dams, possibly amplified by the adoption of climate-dependent regulation strategies. Figures 2.8, 2.9, 2.10, 2.11 and 2.12 summarize the impact of dams on mean water availability and hydrological variability. Flow regimes upstream of flood control structures selected in this study are extremely heterogeneous in space and time. Most cases are characterized by erratic regimes ($CV_Q > 1$). These regimes are commonly found throughout the entire Central-Eastern United States, though an enhanced erraticity ($CV_Q > 3$) emerges in the Eastern Great

Plains, especially during summer and fall seasons. Nevertheless, persistent regimes ($CV_Q < 1$) are also observed, particularly in northeastern catchments during spring and winter. During high flow events, flood control dams store water that is then released during low flow periods with the goals of preserving the storage capacity of reservoirs and conveying water downstream for secondary uses, such as irrigation, navigation or wildlife preservation. Accordingly, regulation for flood control produces a negligible impact on mean water availability (figure 2.11, *A*). On the other hand, flood mitigation reduces the intra-seasonal variability of river flows during all seasons, and strongly lowers (by more than 60%) regional-scale differences typical of unregulated regimes (figure 2.10, *A*). These results comply with the findings reported by previous studies [Poff et al., 2007; Destouni et al., 2013; Jaramillo and Destouni, 2015].

Hydrological regimes upstream of the selected urban water supply reservoirs are relatively homogeneous: most cases are weakly erratic ($1 < CV_Q < 2$), especially during winter and spring seasons, when many intermediate regimes ($CV_Q \simeq 1$) are observed. Regulation for urban water supply is intended to intercept river flows and feed aqueduct systems. As a result, the mean seasonal discharge downstream is reduced proportionally to the relative amount of water withdrawn or diverted from reservoirs (figure 2.11, *B*), whereas the variance of flows (that is more sensitive to high flows) is less impacted [Döll et al., 2009]. Accordingly, water supply reservoirs typically produce an increase of the relative streamflow variability downstream of the dam, with regulated regimes that generally exhibit a more erratic behaviour (larger CV_Q). Moreover, damming enhances inter-catchment heterogeneity of flow variability by almost 50% in response to diversified exploitation strategies across different reservoirs (figure 2.10, *B*). During winter and spring, the increase of daily streamflow variability downstream of dams and the effect of streamflow differentiation at the regional scale are particularly evident (red dots in figure 2.10, *B*). In these seasons, the inter-catchment heterogeneity of CV_Q in dammed rivers is almost four times larger than that of natural flow regimes. This is due to the lower variability of natural river flows from November to April, which conceals the unavoidable confounding effect of flood lamination by dams during high flow events.

Natural flow regimes upstream of the selected hydroelectric reservoirs are extremely heterogeneous. Persistent regimes ($CV_Q < 1$) are observed in eastern catchments, especially

during winter and spring, while erratic regimes ($CV_Q > 1$) characterize catchments in the Central US. Differently from regulation for flood control and water supply, typical patterns in flow regime alterations prove difficult to find downstream of reservoirs used for hydropower production. As most of the considered reservoirs are managed for multiple purposes, including flood control, regulation produces a general decrease of daily streamflow variability. Though, the magnitude of regime alterations may be constrained by the reduced effective capacity of reservoirs, as implied by the compliance of a minimum stage necessary to sustain the hydraulic head during hydropower production (i.e., capacity allocated to power generation). Overall, the reduction of streamflow variability is visible when natural flow regimes are erratic, while it is less significant in case of more persistent regimes (figure 2.12, *A*). Concurrently, the impact on mean water availability is negligible, since only nonconsumptive water uses are involved (figure 2.12, *B*).

The reservoir main function and the natural streamflow variability are not the unique determinants of the extent of river flow regime alterations. Other quantitative descriptors need to be introduced to better understand the link between anthropogenic water uses and hydrologic alterations by dams. Figure 2.10, *A* suggests that the observed reduction of CV_Q downstream of flood control dams is roughly proportional to the natural variability of discharges. However, the decrease of the relative streamflow variability is also modulated by the storage capacity allocated to flood control scaled to the mean annual inflow (i.e., the number of consecutive days for which the mean flow can be stored in the reservoir assuming no releases downstream), here defined as reservoir regulation capacity, R_C. As expected [Graff, 1999], the higher the regulation capacity, the more enhanced the reduction of streamflow variability. On the other hand, the downstream effect of water supply reservoirs depends on seasonal patterns of water consumption (i.e., the relative amount of inflows withdrawn from the reservoir), here defined as the degree of exploitation of a reservoir, R_E. This is particularly true in winter and spring season, when the confounding effect of flood mitigation is not visible (red dots in figure 2.10, *B*). In particular, it is proved empirically that the increase of the relative streamflow variability downstream of water supply dams grows with the degree of exploitation of the corresponding lakes. Figure 2.13 graphically shows the relationships here explained, while table 2.5 reports values of R_C and R_E for flood control and water supply dams.

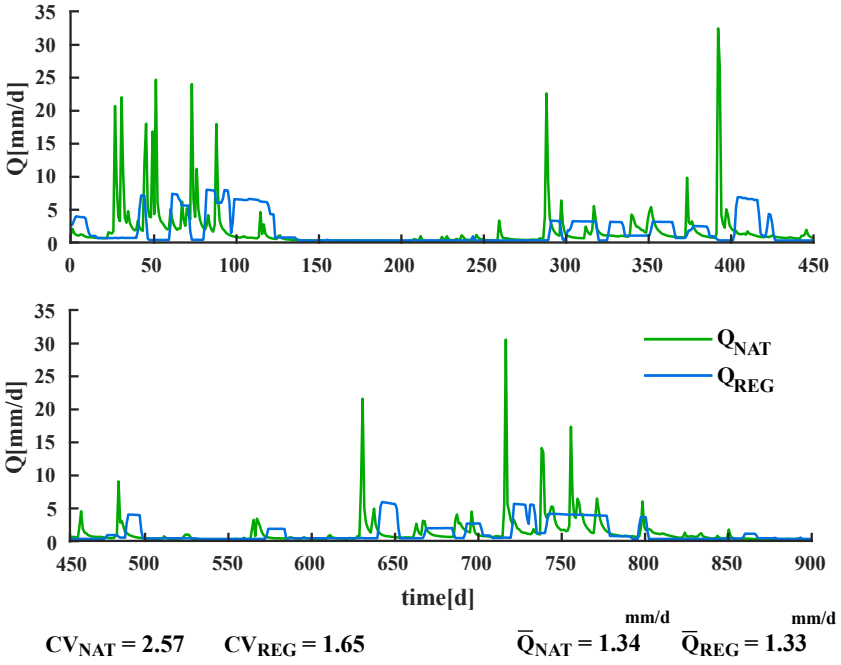

FIGURE 2.8: Typical impact of flood control structures on the temporal dynamics of river flows: the case of the Pomme de Terre dam (MO).

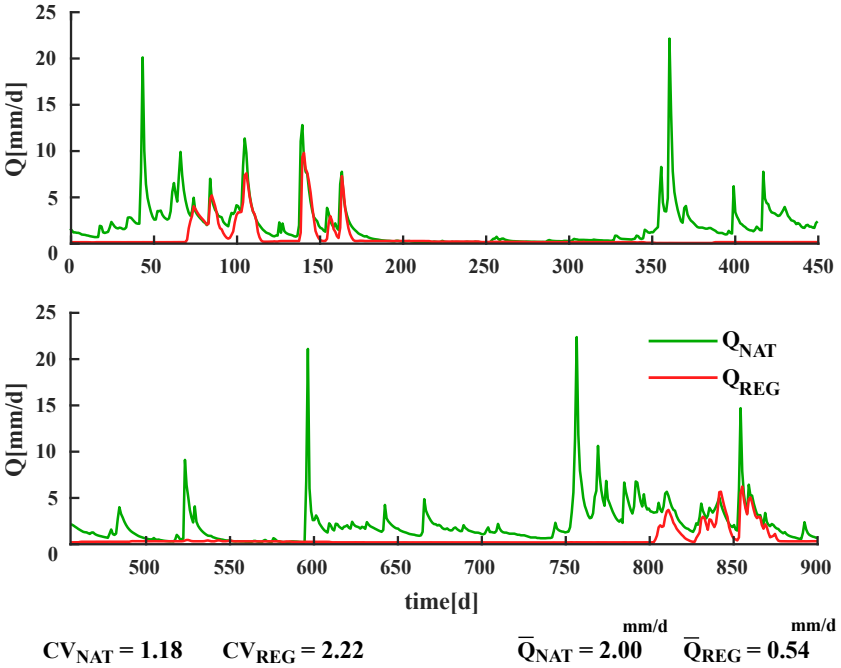

FIGURE 2.9: Typical impact of water supply structures on the temporal dynamics of river flows: the case of the Pepacton dam (NY).

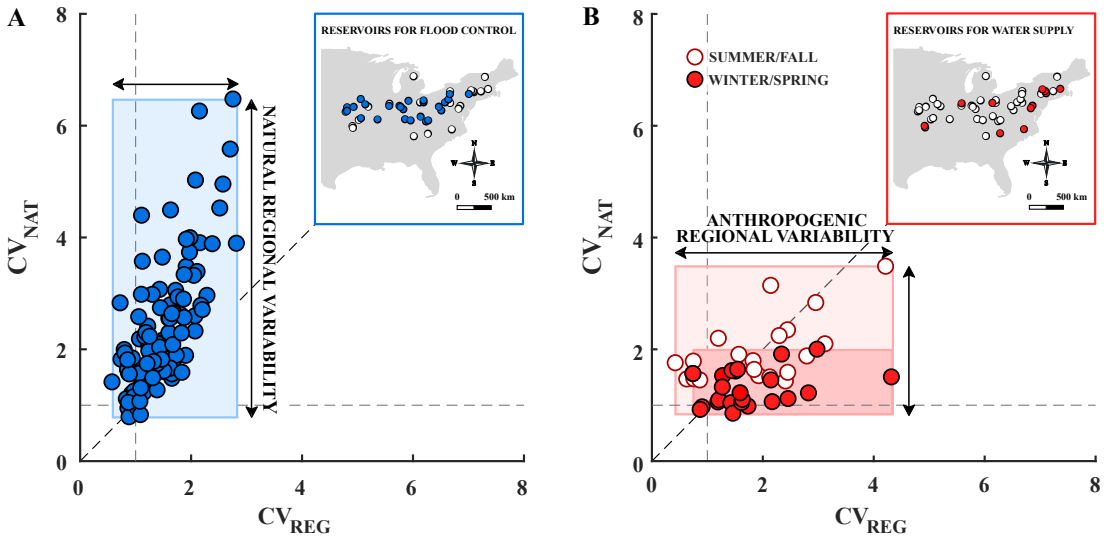

FIGURE 2.10: Seasonal coefficient of variation of natural river flows, CV_{NAT}, plotted against the corresponding value associated to regulated flows, CV_{REG}, for all the flood control (A) and water supply (B) dams considered in this study. The insets show the geographical location of the selected dams.

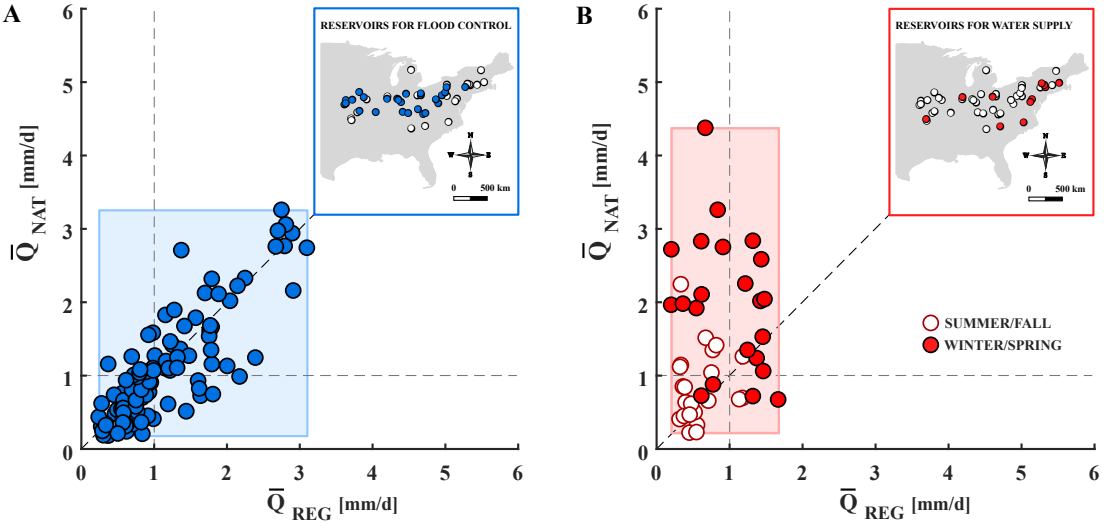

FIGURE 2.11: Seasonal mean discharge of natural river flows, $\overline{Q}_{NAT}$, plotted against the corresponding value associated to regulated flows, $\overline{Q}_{REG}$, for all the flood control (A) and water supply (B) dams considered in this study. The insets show the geographical location of the selected dams.

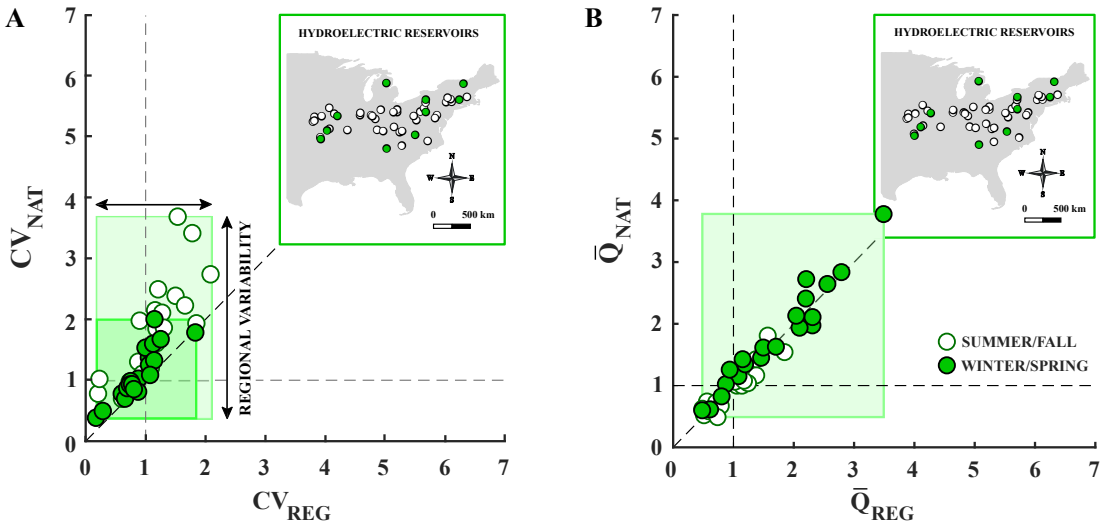

FIGURE 2.12: Impact of hydroelectric reservoirs on river flow regimes. Seasonal coefficient of variation (A) and mean discharge (B) characterizing natural river flows, CV_{NAT} and $\overline{Q}_{NAT}$, plotted against the corresponding value associated to regulated flows, CV_{REG} and $\overline{Q}_{REG}$. The insets show the geographical location of the selected dams.

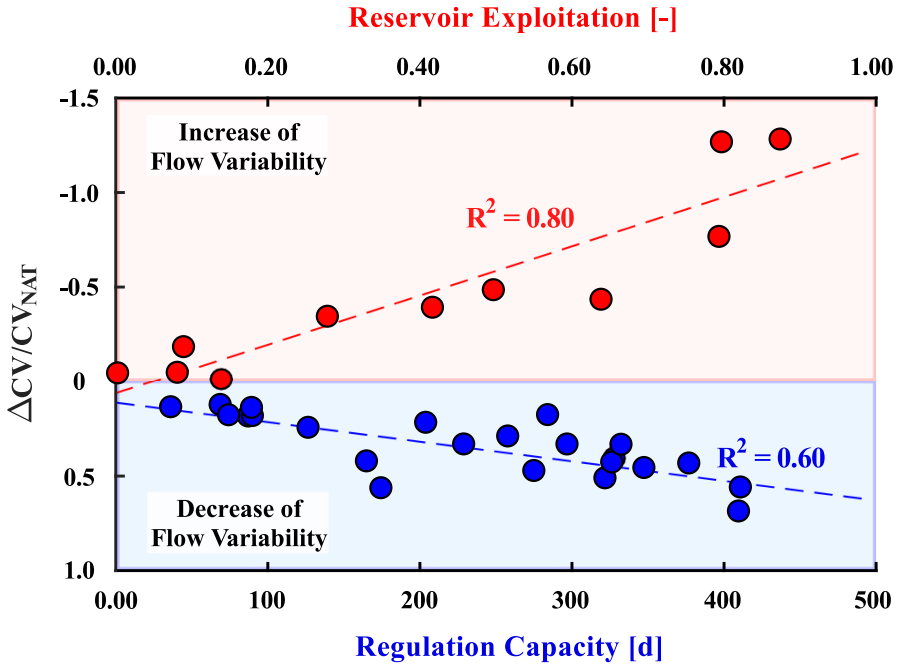

FIGURE 2.13: Reservoir regulation capacity and reservoir exploitation control the relative magnitude of flow regime alterations (i.e., difference between the value of CV_Q upstream and downstream of the dam scaled to the variability of natural streamflows, here indicated as $\Delta CV/CV_{NAT}$) downstream of flood control and water supply structures, respectively. Blue dots represent the behaviour of flood control structures, while red dots are related to water supply dams.

TABLE 2.5: Regulation capacity, R_C, and reservoir exploitation, R_E, typical of flood control and water supply structures, respectively.

Reservoir	**Functions**	**Regulation Capacity** [d] [1]	**Reservoir Exploitation** [–] [2]
Alum Creek	FSRW	242	-
Buckhorn	S	-	0.10
Cagles Mill	FRX	297	-
Cannonsville	S	-	0.50
Cave Run	FQRW	327	-
Clinton	FSQRWX	- [3]	-
C. M. Harden	FRX	275	-
Curwensville	FR	88	-
Decatur	S	-	0.10
Delaware	FARW	204	-
EB Clarion	FAQRX	75	-
Eucha	S	-	0.60
Fishtrap	FARW	127	-
J. W. Flannagan	FAQR	- [3]	-
Green River	FSAQR	348	-
Loyalhanna	FRW	90	-
Long Branch	FSQRW	166	-
Monroe	FSAR	377	-
Neversink	S	-	0.87
Nolin	FAR	284	-
O'Shaughnessy	S	-	0.01
Pepaction	S	-	0.80
Perry	FSRWX	328	-
Pomme de Terre	FRWX	322	-
Pomona	FSQRWX	411	-
Prettyboy	S	-	0.15
Prompton	FQR	90	-
Quabbin	S	-	0.80
Rathbun	FNQRWX	410	-
Rocky Gorge	S	-	0.40
Salomonie	FRW	258	-
Shelbyville	FSNRW	229	-
Smithville	FSQRW	333	-
Sutton	FARWX	69	-
Tygart	FANRX	37	-
Wappapello	FR	175	-
W. C. Bowen	S	-	0.30

[1] Reservoir regulation capacity is calculated as the storage capacity allocated to flood control, V_{FC}, scaled to the mean annual inflow, $R_C = V_{FC}/\overline{Q}_{NAT}$ with $\overline{Q}_{NAT} = \sum_{i=1}^{365} Q_{NAT,i}/365$.

[2] Reservoir exploitation is calculated as the average relative amount of inflows withdrawn from the reservoir at the annual time scale, $R_E = \sum_{i=1}^{365} \left(\frac{Q_{NAT,i} - Q_{REG,i}}{Q_{NAT,i}} \right) / 365$.

[3] Regulation capacity is not evaluated due to the absence of information about the storage capacity allocated to flood control, V_{FC}.

2.5.2 Autocorrelation and frequency stability analysis

Besides alterations to the frequency distribution of streamflows, dams and reservoirs significantly impact the temporal trajectories of downstream releases across a broad range of time scales (from daily to yearly), with relevant modifications of the predictability of flow rates in regulated reaches. These modifications might create adverse conditions for autochthonous riverine ecosystems and threaten anthropogenic uses in dammed rivers. In this study, the autocorrelation and frequency stability analyses are implemented to investigate the memory and fractal properties of flow patterns upstream and downstream of the selected dams, properly stratified according to their main characteristics (i.e., main use, regulation capacity, degree of exploitation). Note that autocorrelation and frequency stability analyses are only performed for sites where streamflow time series are considered both upstream and downstream of the reservoir (see table 2.2).

Figure 2.14 shows the comparison between the observed PDFs of the integral scale typical of hydrologic regimes upstream (pink) and downstream (light blue) of reservoirs for flood control (A and B) and water supply (C and D). Reservoirs for flood control increases downstream flow correlation consistently with their ability to store large amount of water through time. Storages with sufficiently high regulation capacity ($R_C > 150d$; see table 2.5) are able to produce more persistent flow patterns up to seasonal and annual time scales, inducing an increase of the mean integral scale of flows, $\overline{T}$, greater than 130% (from 6.5 to 15.2 days). This is approximately nine times higher than the increase of $\overline{T}$ generated by low regulation capacity reservoirs (from 10.5 to 11.4 days). Overall, the observed increase of downstream flow correlation is consistent with the reduction of discharge variability operated by flood control dams, with higher low flows and smoothed peaks in regulated regimes. Regulation for water supply exhibits a similar behaviour with only a slight reduction of its magnitude. Strongly exploited reservoirs ($R_E > 0.5$; see table 2.5) induce an increase of the integral scale from 11.9 to 17.4 days, on average. Conversely, meaningful differences are lacking for weakly exploited dams.

Figure 2.15 shows the impact of hydroelectric reservoirs on downstream flow correlation. As most of the considered structures include flood control among their project functions, regulation still determine more persistent flow patterns, with the mean integral scale increasing from 14 to 16.5 days. However, it should be noted that this is

not the typical impact of reservoirs only used for hydropower production, whose effect on stream correlation appears to be negligible or slightly counterposed to that of flood control (see figure 2.22, *B*).

Figure 2.16 represents the results of frequency stability analysis for flood control reservoirs, properly stratified according to their regulation capacity (*A*, *B* and *C* $R_C > 150d$, *D*, *E* and *F* $R_C < 150d$). Results reveal that the overall unpredictability of regulated streamflows downstream of flood control structures is always reduced if compared to natural conditions, as inferred by the lower values of the Allan deviation. However, regulation for flood control determines an increase of the slope of the log-log Allan deviation plot, α, which is roughly proportional to reservoir regulation capacity, thus enhancing the multifractality of natural flows. In particular, reservoirs with a high regulation capacity ($R_C > 150d$; see table 2.5) typically induce a negative-positive transition of α for averaging times up to 100 days (*A*, *B* and *C*). Although the self-averaging behaviour of natural flows is slower than that of an ideal white noise ($\alpha = -0.5$), their unpredictability typically decreases over longer time intervals ($\alpha < 0$ in 95% of cases). Instead, the unpredictability of regulated hydrographs downstream of large flood control structures increases for longer time intervals up to the seasonal time scale ($\alpha > 0$ in 55%of cases), sometimes originating a red-noise signal. The increase of downstream flow unpredictability over longer averaging time periods is most likely due to the variety of social requirements that must be satisfied by reservoir release; in fact, most of the largest flood control structures in the US are multipurpose and, thus, convey water to downstream users for water supply, irrigation, navigation or wildlife preservation. Different functions, each one requiring different type of releases in specific circumstances, follow each other and reservoir releases tend to shift accordingly. The resulting hydrograph appears as a square-wave with unsteady frequency and amplitude. For this reason, regulated streamflows show an increasing unpredictability over longer time period, but their overall variability is reduced compared to natural conditions because of the smoothed peaks of the signal (i.e. the log-log Allan deviation curve typical of regulated flows is always shifted downward with respect to that of natural flows). Conversely, the impact of low regulation capacity reservoirs ($R_C < 150d$; see table 2.5) on the stability of river

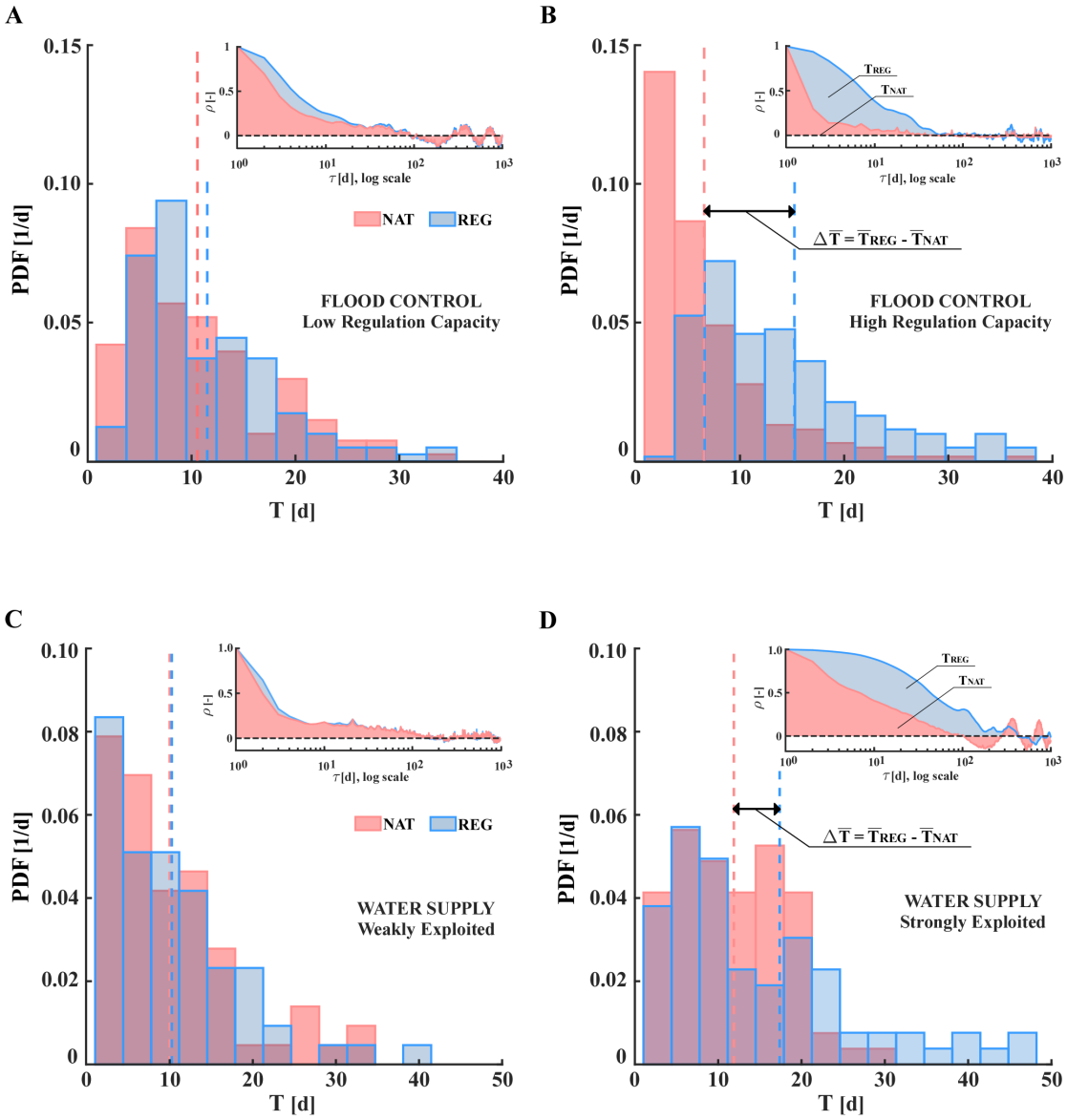

FIGURE 2.14: Comparison between the observed PDFs of the integral scale typical of hydrologic regimes upstream (pink) and downstream (light blue) of reservoirs. Vertical dashed lines indicate the mean integral scale of river flow regimes in natural (pink) and regulated (light blue) reaches. (*A* and *B*) Low and high regulation capacity structures operated to mitigate floods. (*C* and *D*) Weakly and strongly exploited reservoirs operated to supply fresh water. The insets show the typical behaviour of the autocorrelation functions upstream and downstream of considered dams.

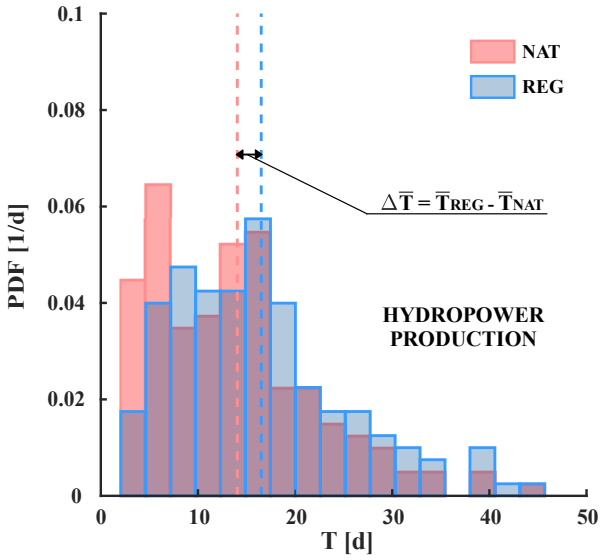

FIGURE 2.15: Comparison between the observed PDFs of the integral scale typical of hydrologic regimes upstream (pink) and downstream (light blue) of hydroelectric reservoirs. Vertical dashed lines indicate the mean integral scale of river flow regimes in natural (pink) and regulated (light blue) reaches.

flows is only visible at the weekly time scale, when these structures determine an increase of the slope of the log-log Allan deviation plot, α. At the seasonal scale, regulated river flows typically exhibit a non-self averaging behaviour ($\alpha \approx 0$), which turns into a self-averaging behaviour ($\alpha < 0$) at longer time scales (D, E and F).

The increase of flow multifractality is less evident downstream of water supply dams. On the other side, the frequency stability analysis reveals a reduction of the unpredictability of regulated streamflows (i.e. lower values of the Allan deviation), which is roughly proportional to the degree of exploitation. This is evident from the examples reported in section 2.5.3 (see comparison between figure 2.19, B and figure 2.20, B).

2.5.3 Emblematic examples of river flow regime alterations by dams across different water uses

Figures 2.17, 2.18, 2.19, 2.20, 2.21 and 2.22 represent streamflow memories and fractal properties alterations downstream of a set of representative case studies, coupled with the typical impact of regulation on the temporal dynamics of river flows. Specifically, in all figures, plots A show the geographical location of selected dams, plots B show the autocorrelation function, $\widehat{\rho}(\tau)$, and log-log Allan deviation plot, σ_A, typical of flow

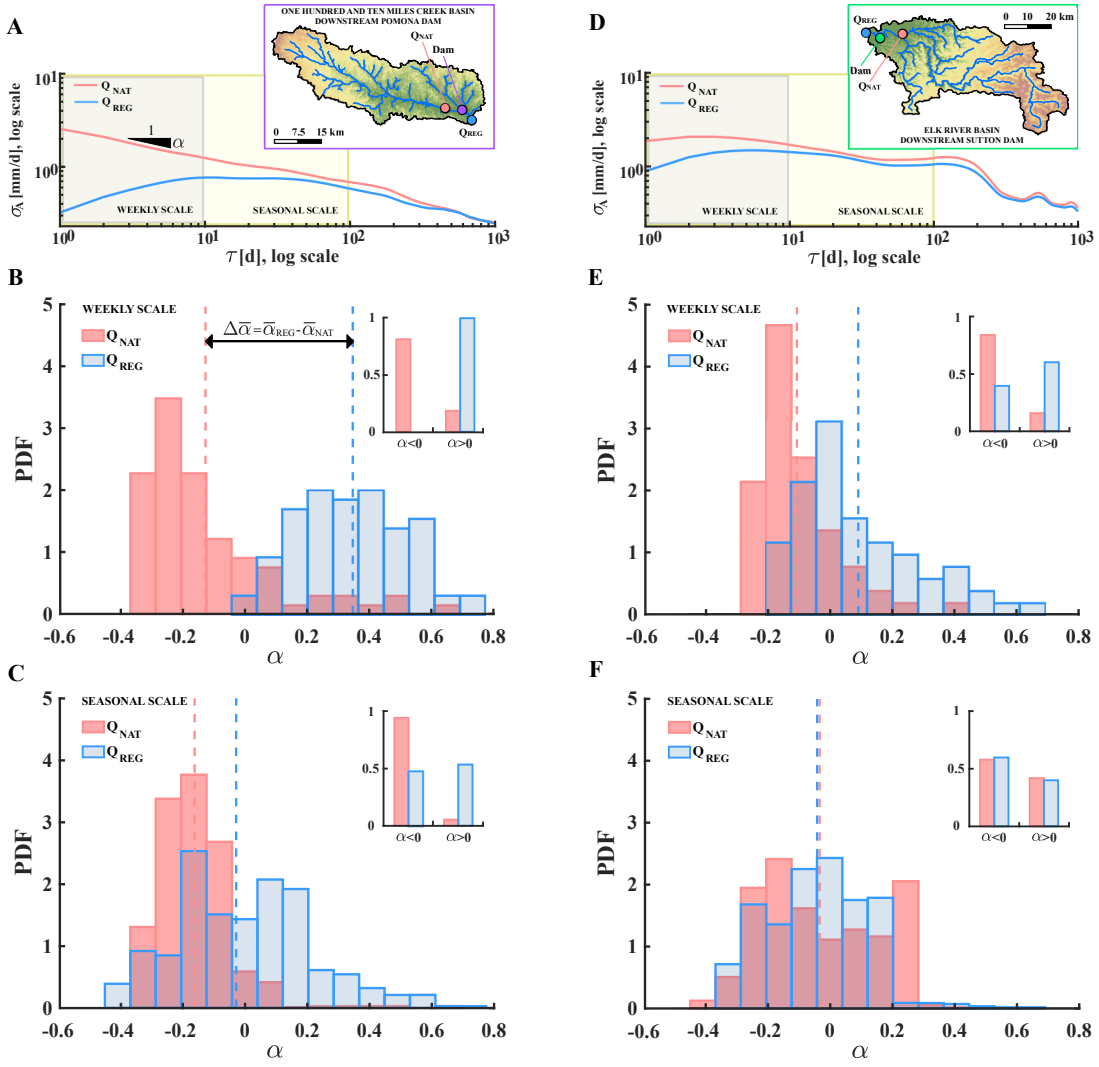

FIGURE 2.16: Frequency stability analysis of daily discharge time series recorded upstream and downstream of flood control reservoirs, properly stratified according to their regulation capacity (A, B and C high regulation capacity, D, E and F low regulation capacity). (A and D) Typical behaviour of the log-log Allan deviation plot upstream (pink) and downstream (light blue) of flood control dams. (B, C, E and F) Observed frequency distribution (PDFs) of the slope characterizing the log-log Allan deviation plot, α, upstream (pink) and downstream (light blue) of dams (B and E weekly time scale, C and F seasonal time scale).

regimes upstream (pink) and downstream (light blue) of the same structures, and plots *C* report the temporal dynamics of natural (Q_{NAT}) and regulated (Q_{REG}) river flows. Figures 2.17 and 2.18 are focused on results obtained for two different flood control structures: Pomme de Terre dam and Curwensville dam. The former is an earth and rockfill structure impounding the main stem of the Pomme de Terre River in Hickory County, Missouri. Since October 1961, it has provided a storage capacity of 802 millions m^3, of which 502 millions m^3 are allocated to flood control. The latter is an earthfill structure located on the West Branch Susquehanna River, approximately four kilometers upstream of Curwensville, in Clearfield County (PA). Since it has been placed in operation, in 1965, it has provided a storage capacity of 150 millions m^3, entirely allocated to flood control. These two reservoirs represent a typical example of the observed regional variation in the regulation capacity of flood control dams, that increases westward to the Central United States [Graff, 1999, 2006]. Pomme de Terre dam and Curwensville dam are characterized by a regulation capacity of 322 d and 87 d, respectively. This implies that the former can store water, on average, for much longer time periods. Accordingly, Pomme de Terre dam, in Missuori, has the capability to alter significantly the downstream hydrology. The regulated hydrograph appears as a square-wave with unsteady frequency and amplitude, and flows stability and temporal correlation are significantly increased at the seasonal scale (figure 2.17). Differently, Curwensville dam, in Pennsylvania, exerts a more limited impact on downstream flow regimes, that only exhibit higher low flows and more smoothed peaks with respect to natural ones. In this case, streamflow uniformity and temporal correlation are only increased at the weekly time scale (figure 2.18).

Figures 2.19 and 2.20 focus on Pepacton and William C. Bowen dams, two water supply projects. Pepacton dam has impounded the East Branch Delaware River since 1955, creating one of the largest reservoirs operated to transfer water from the upper tributaries of the Delaware river to the city of New York. William C. Bowen dam has served as a public drinking water supply for the northern Spartanburg County (SC) since 1960, when it was constructed on the Pacolet river to meet a steadily increasing water demand. These two water supply structures are characterized by a different degree of exploitation, with the Pepacton reservoir being a heavily exploited storage used

to accommodate the population increase and economic growth that took place in New York city during the 20th century. The autocorrelation function and the log-log Allan deviation plot reveal a limited effect of the William C. Bowen dam on downstream flows (figure 2.20, *B*), implying that regulated regimes maintain pre-dam characteristics with the exception of a slight reduction of the mean discharge induced by water withdrawals (figure 2.20, *C*). Conversely, the frequency stability analysis in the Pepacton reservoir reveals a significant decrease of streamflow variability caused by water supply regulation (figure 2.19, *B*). This is explained by the huge volumes of water extracted from the lake, which induces a drastic flattening of downstream hydrograph (figure 2.19, *C*).

Figures 2.21 and 2.22 show a comparison between the downstream impact of two different reservoirs used for hydropower production: Stockton lake and Zoar lake. The former was placed in operation in December 1969, after impounding the Sac river through a rock-shell dam in Cedar County (MO). Total reservoir storage capacity consists of 955 millions m^3 allocated to flood control and 1079 millions m^3 allocated to power generation, thus feeding the 45200 kilowatt power installation on the Stockton dam. The latter was built in 1919 impounding the Housatonic river through the Stevenson dam, whose hydroelectric plant is currently characterized by a capacity of 28900 kilowatt. This lake is located downstream a second power project named Lillinonah reservoir: both lakes are used only for hydropower generation, thus contributing similarly to the overall alteration of the flow regime. Figures 2.21 and 2.22 shed light on the differential influence of multipurpose regulation, including flood control, and regulation only performed for power production. The downstream impact exerted by Stockton dam shows some of the typical features of flow regime alterations induced by flood control. The alteration of downstream hydrology is similar to that observed in the case of Pomme de Tere dam, and still produce the increase of discharge correlation and an enhanced uniformity of downstream flows (figure 2.21). This behaviour is not observed in the case of Zoar lake, whose unique function is energy production (figure 2.22). Note that, in both cases, the temporal dynamics and the autocorrelation function of regulated streamflow show the oscillations typical of hydropower production, which are related to the weekly and seasonal periodicity characterizing the behaviour of the energy market [Zolezzi et al., 2009].

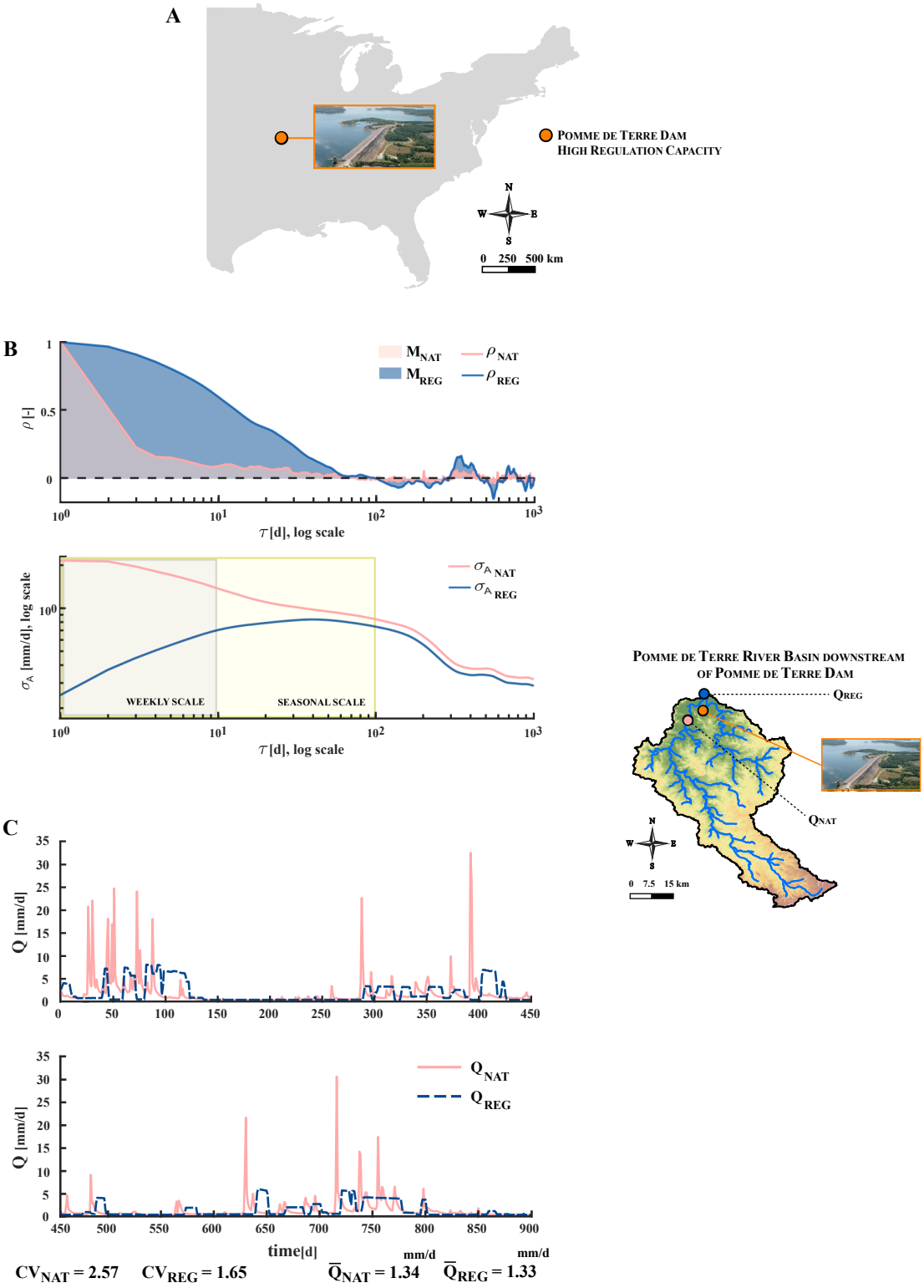

FIGURE 2.17: Typical impact of flood control structures characterized by a high regulation capacity: the case of Pomme de Terre dam ($R_C = 322d$).

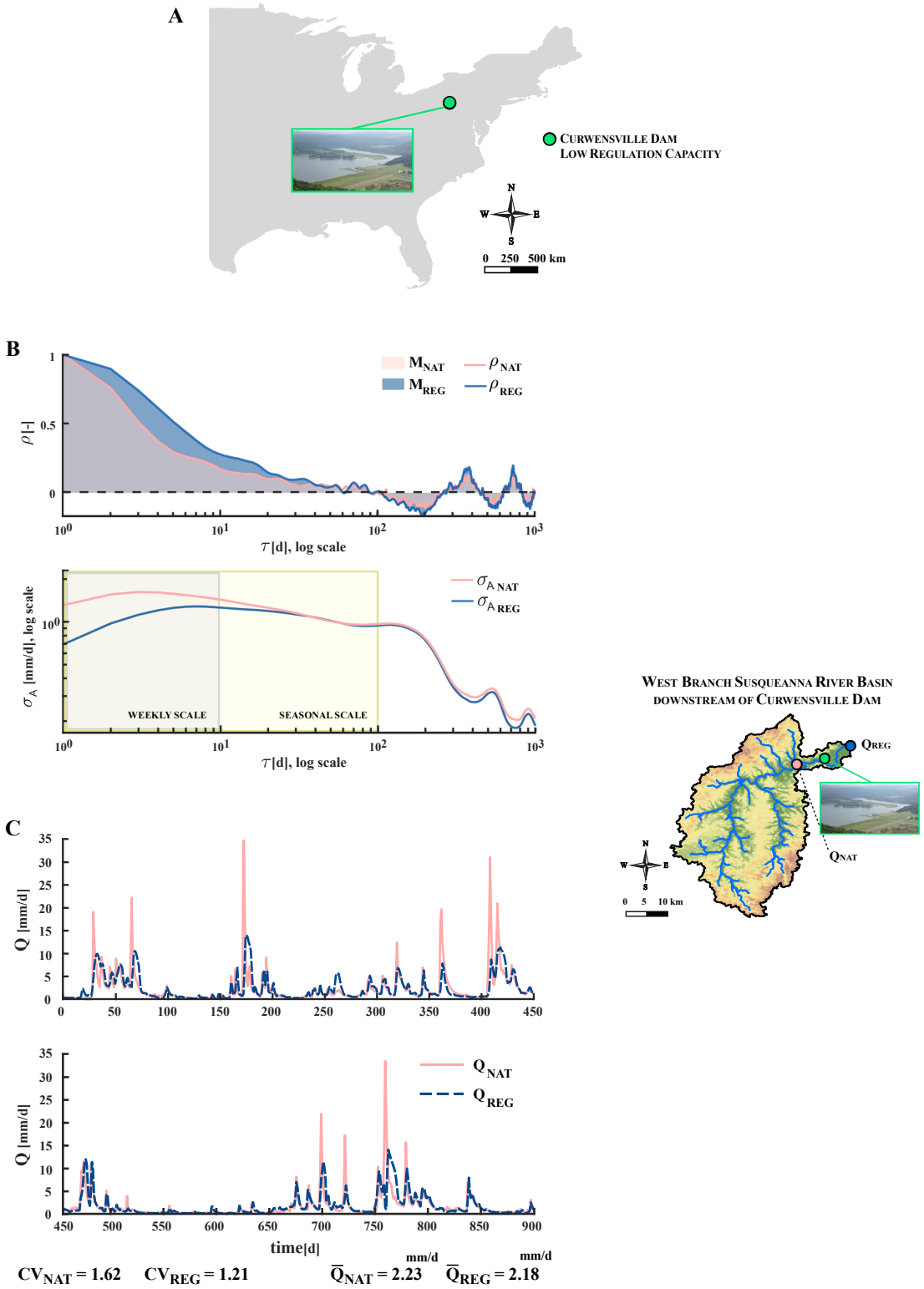

FIGURE 2.18: Typical impact of flood control structures characterized by a low regulation capacity: the case of Curwensville dam ($R_C = 87d$).

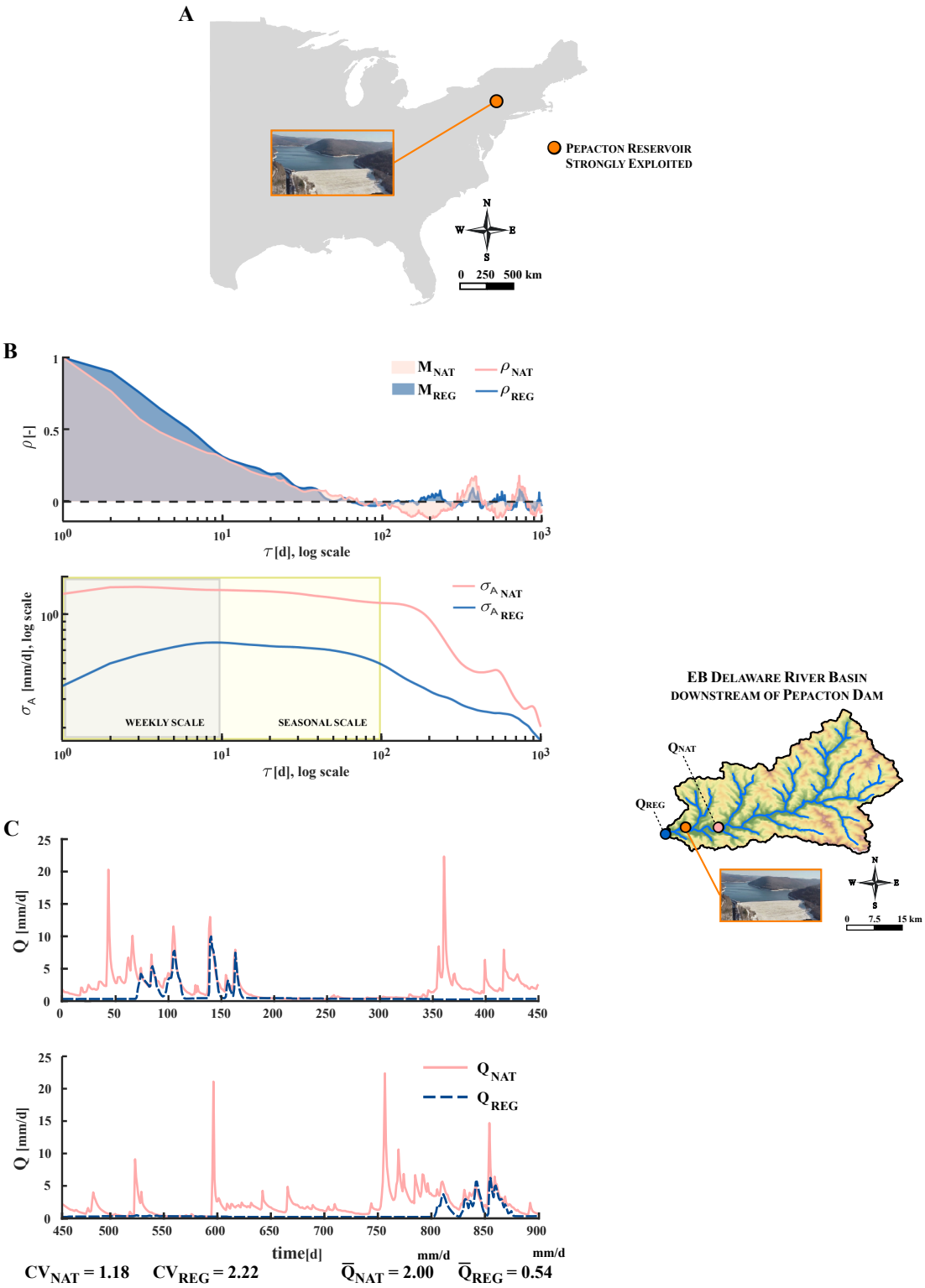

FIGURE 2.19: Typical impact of water supply structures characterized by a high degree of exploitation: the case of Pepacton dam ($R_E = 0.8$).

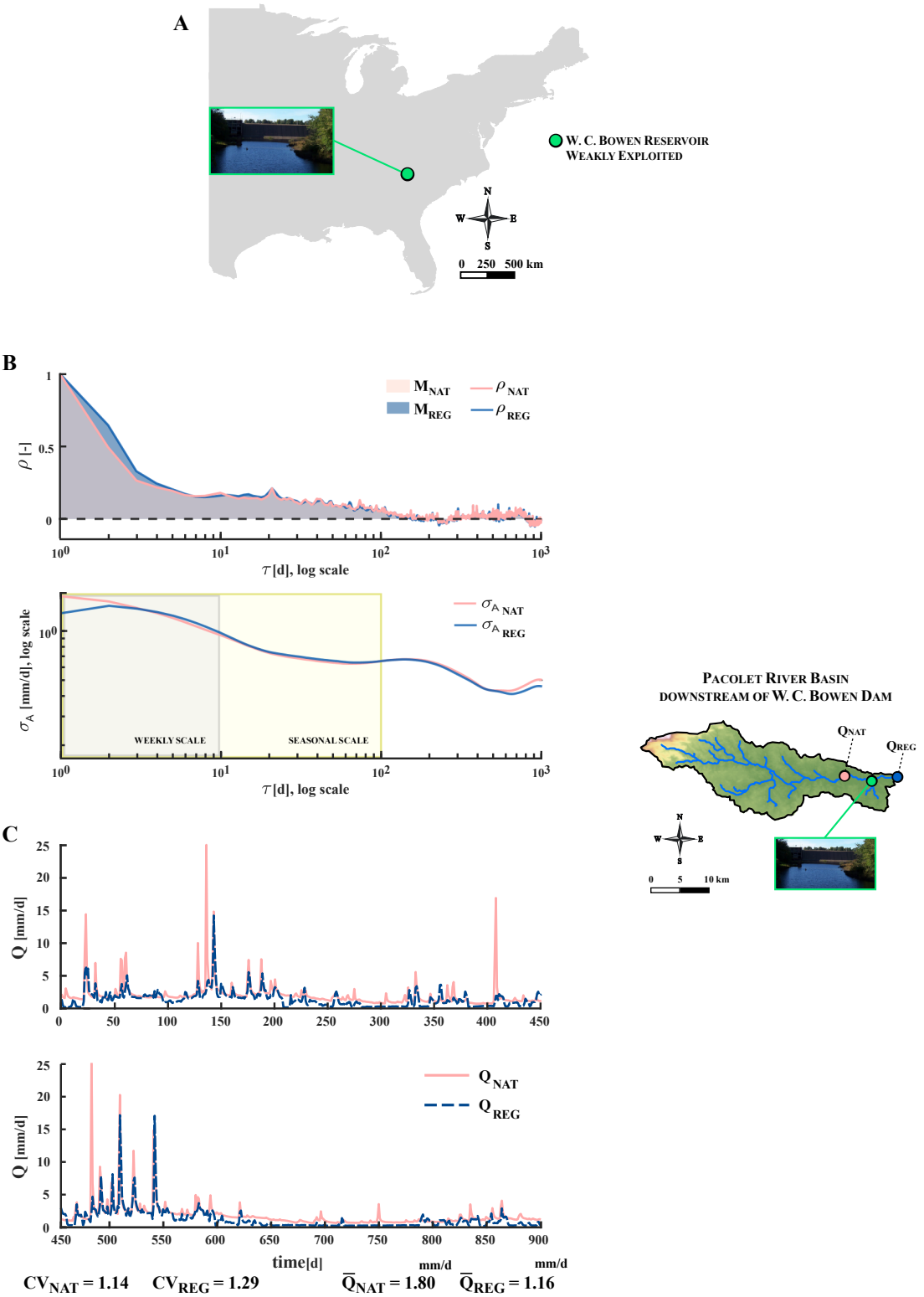

FIGURE 2.20: Typical impact of water supply structures characterized by a low degree of exploitation: the case of W. C. Bowen dam ($R_E = 0.3$).

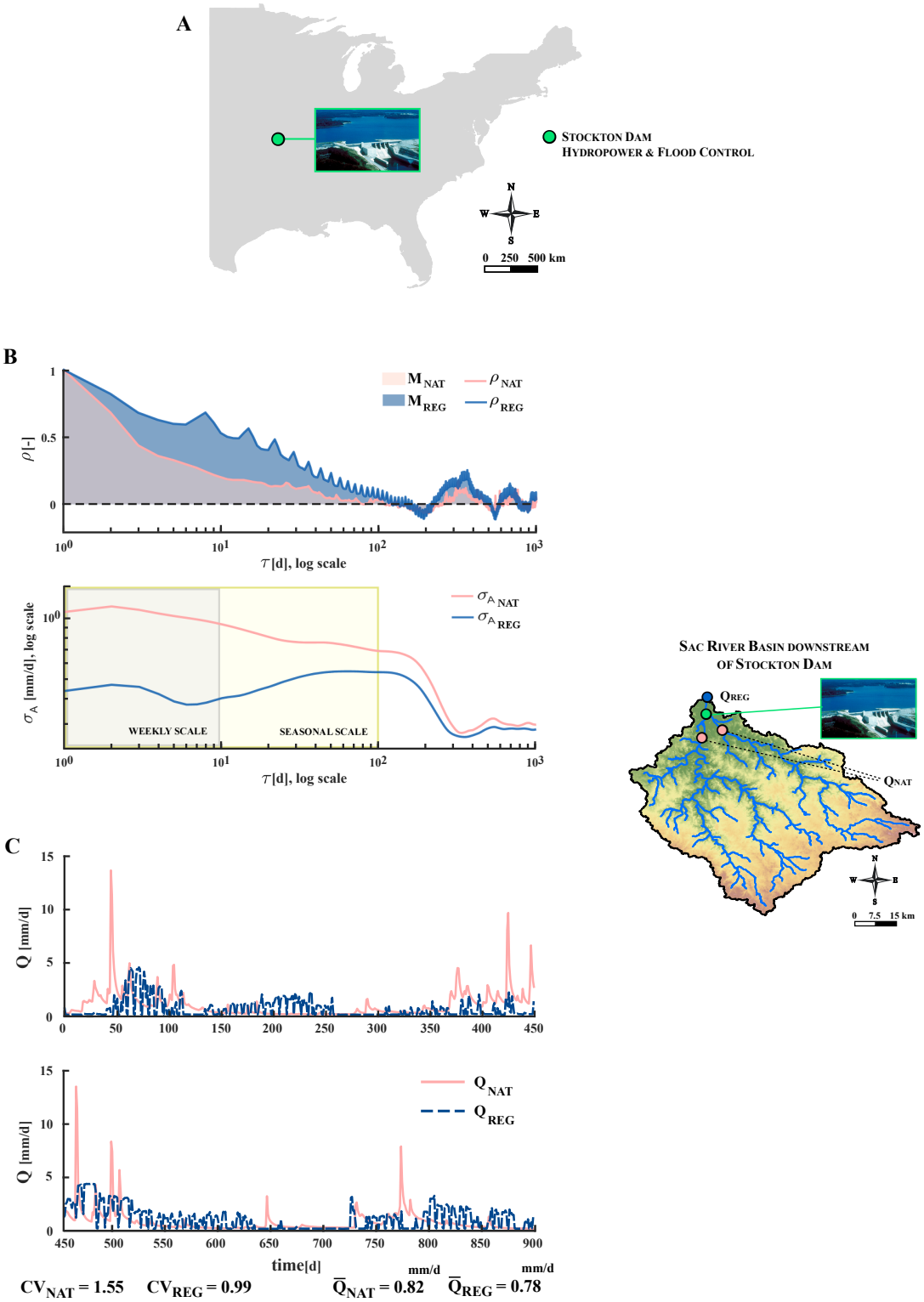

FIGURE 2.21: Typical impact of hydroelectic structures including flood control among its functions: the case of Stockton dam.

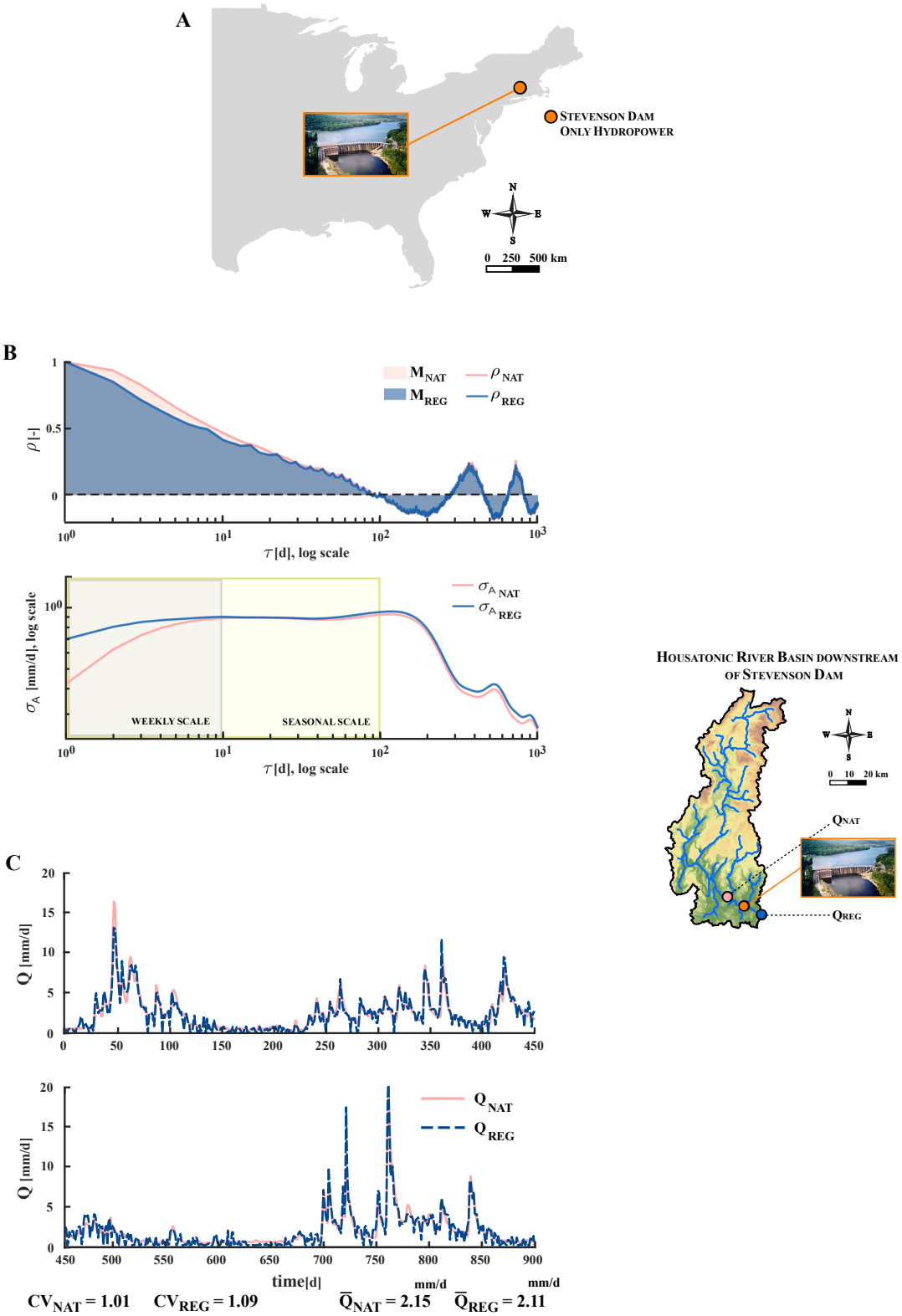

FIGURE 2.22: Typical impact of structures only used for hydropower production: the case of Stevenson dam.

2.6 Discussion

The obtained results reveal that reservoirs devoted to flood control and those operating for water supply produce distinctive impacts on flow regimes. Flood control through dams does not alter the mean discharge downstream, but decreases the intra-seasonal variability of streamflows and, therefore, homogenize regional flow dynamics. Water supply, instead, reduces the mean discharge of regulated reaches but increases the relative streamflow variability, thereby enhancing the regional heterogeneity of discharge fluctuations.

The reduction of river flow variability induced by flood control is mirrored by a lowered diversity of aquatic habitats, which promotes the flourishing of non-native organisms of fewer species [Poff et al., 2007; Moyle and Mount, 2007]. The case of the Upper Allegheny River Basin (see table 2.1) is emblematic of the type of ecological impacts produced by flood control dams. Therein, flow regime alterations downstream of the Kinzua Dam were responsible for endangering several plant, mussel and fish native species, concurrently promoting the settlement of non-native riparian plants [Cowell and Stoudt, 2002]. On the other hand, the reduction of mean discharge and the abrupt sporadic changes in flow magnitude downstream of water supply structures affect the carrying capacity of regulated streams and inevitably alter key physical and biological attributes of riverine habitats, such as velocity, temperature, depth, nutrient and sediment loads [Dewson et al., 2007; Petts, 1994]. Typical examples of the resulting negative effects on aquatic and riparian ecosystems have been documented in the Upper Delaware River Basin, where three water supply structures (Cannonsville, Pepacton and Neversink, see table 2.1) divert up to 85% of the annual inflow to supply the city of New York [Baldingo and Schuler, 2002; Harman, 1974]. Persistent droughts interlaced by sporadic high flow events in the regulated reaches of the Delaware River have reduced the ecosystem size and have limited spawning and outmigration, thereby leading to scarce and less diverse populations of fishes, benthic invertebrates and mussels. However, there is no evidence of the flourishing of invasive species in that river - a circumstance shared by all the regulated reaches downstream of the 11 water supply dams considered in this study. Nevertheless, results suggest that regional scale heterogeneity of flow variability might

be enhanced by regulation for water supply (figure 2.10, *B*), with a compensatory effect against the loss of diversity of river regimes induced by flood control dams, and potentially beneficial consequences for large-scale biodiversity.

Multipurpose structures partly devoted to water supply are, in most cases, primarily built for flood control, and they are classified accordingly also in this study. Results from the presented analysis show that regulation through multipurpose reservoirs produces downstream patterns of discharge that differ from those observed downstream of reservoirs operated only to mitigate floods. The overall magnitude of flow regime alterations downstream of multipurpose dams is reduced by the distinctive, compensatory effect of water supply, that partly counterbalance the decrease of flow variability typical of flood control dams, especially during seasons with significant withdrawals and limited floods (winter and spring). Figure 2.23, *A* shows the comparison between the effects of regulation in two adjacent catchments. The first one is closed in coincidence to the Alum Creek Dam (right), originating a multipurpose reservoir devoted to flood control and water supply, while the second one is closed in coincidence to the Delaware Dam (left), which is only designed for flood protection. The reduction of river flow variability observed downstream of the Alum Creek Dam is less significant than that observed downstream of the Delaware Dam (particularly in spring and winter), confirming the counterbalancing effect of water supply on the decrease of flow variability due to flood mitigation. Overall, it is proved empirically that the relative reduction of CV_Q induced by flood control decreases by 30% when reservoirs are also used for water supply (see section 2.2.3).

On the other side, large multipurpose reservoirs are able to impact the autocorrelation structure of downstream flows beyond the timescale of single events. This implies that, at seasonal and annual time scales, regulated hydrographs behave more as an autocorrelated red noise rather than as an uncorrelated white noise – as some natural rivers do [Kirchner and Neal, 2013]. Discharge color, as well as its variability, is known to affect riverine ecosystems, exerting a significant impact on population dynamics and persistence [Sabo and Post, 2008; Petchey et al., 1997]. Overall, the reddening of river flow regimes downstream of large multipurpose dams might enhance the likelihood of prolonged detrimental environmental conditions, which endanger short-lived organisms

and promote the settlement of long-lived fishes [Sabo and Post, 2008; Schwager et al., 2006].

Public supply withdrawals in the United States have more than tripled since 1950, jumping from 13.6 Bgal/d to 42 Bgal/d in 2010 (USGS, 1950–2010; figure 2.23, *B*). Public supply from surface water provides approximately two-thirds of the total consumption for municipal uses, particularly in large metropolitan areas [USGS, 1950–2010; Sankarasubramanian et al., 2017]. Since the early 20*th* century, water supply systems have undergone substantial expansion to sustain the increasing demand of fresh water associated to population growth and economic development. Initially, new dams were constructed and operated to supply fresh water [Fitzhugh and Richter, 2004], while more recently it has become increasingly widespread to allocate a fraction of the capacity of existing storages to water supply. Accordingly, while the number of flood control structures remained relatively stable over time, the number of reservoirs devoted to water supply increased by 50% in the last 30 years [USACE, 1980–2010]. In support of this, figure 2.23, *C* shows the temporal trend and spatial distribution in the number of reservoirs managed by the U.S. Army Corps of Engineering, distinguishing between structures including and not-including water supply among their project functions.
In the light of this findings, it follows that the current increase of water demand for public supply might generate a possible shift in the cumulative effect of dams at regional and global scales. Enhancing the water supply function of multipurpose dams might potentially compensate (and even reverse) the impact of flood control on relative discharge fluctuations, thereby leading to smoothed alterations of the internal variability and the regional diversity of flow regimes. Obtained results also indicate that massive constructions of new dams operated mainly for water supply could impact more severely the mean discharge of dammed rivers and might generate more heterogeneous and variable flow regimes in the future. An increased erraticity of regulated flow regimes might exacerbate water conflicts in socially unstable regions [Müller and Levy, Submitted], and originate distinctive trajectories of ecologic and morphological alterations downstream of water supply dams. These alterations are likely to be driven by the duration of persistent droughts induced by water abstractions and the frequency and timing of sporadic

high flow events bypassing the dam. These results bring important clues for understanding the nature of anthropogenic alterations of river flow regimes, possibly helping the development of flexible and targeted strategies for a sustainable management of water resources. The awareness of the connection between flow regime alterations and anthropogenic water uses might be of particular importance in developing countries, where a dramatic increase of water use is expected to take place to sustain population growth and economic development. This is especially true in areas where signs of water scarcity have been already appeared, as well as in tropical regions, where rainfall is abundant but unevenly distributed in space and time and massive infrastructures would be necessary to optimize anthropogenic exploitation of water resources.

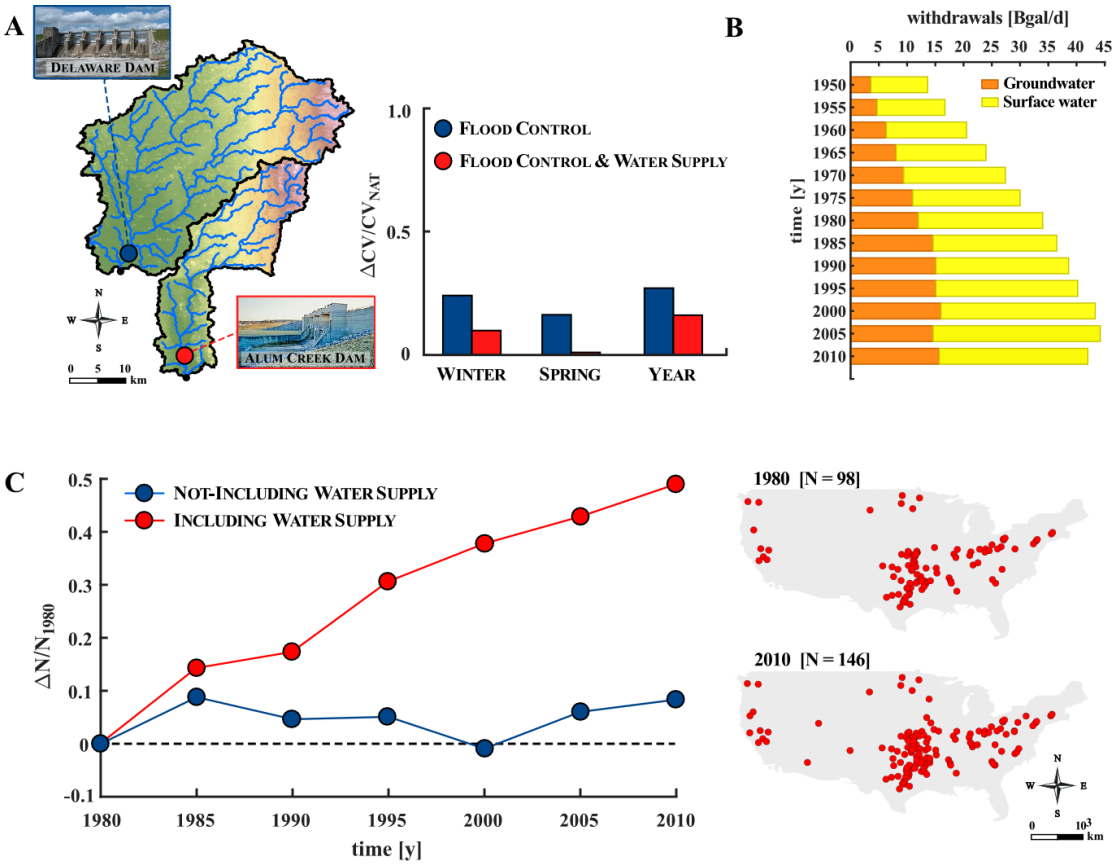

FIGURE 2.23: Impact of regulation on flow regimes and temporal patterns of public water supply withdrawals in the United States. (A) Impact of regulation in two adjacent catchments characterized by the presence of reservoirs with different functions: the Alum Creek lake, devoted to flood control and water supply, and the Delaware lake, only used for flood control. (B) Temporal trend in public supply water withdrawals in the United States: since 1950, public supply withdrawals have more than tripled. (C) Temporal trend and spatial distribution in the number of reservoirs managed by the U.S. Army Corps of Engineers including and not-including water supply among their project functions.

Chapter 3

Climatic signatures in regulated flow regimes

3.1 Introduction

Natural and human induced climate patterns are producing significant alterations of the hydrologic cycle at global scale, endangering riverine ecosystems as well as anthropogenic water uses [Lettenmaier et al., 1994; Groisman et al., 2001; Milly et al., 2005]. On account of dams ability to enable anthropogenic freshwater exploitation, the number of engineering structures could further increase in the near future because of the revamping of old dams and the construction of new infrastructures designed to mitigate the risk induced by fluctuations in climate drivers [ICOLD, 2014; Poff et al., 2015]. Despite this emerging intent, almost nothing is known about the sensitivity of regulated flow regimes to climate drivers, with the exception of a recent study by Ficklin et al. [2018], highlighting the similarity of the response of natural and anthropogenic flow regimes to climate change. In this context, understanding the combined contribution of river regulation through dams and changing climate patterns to flow regime alterations is going to play a key role in water planning and management [Patterson et al., 2013; Ficklin et al., 2016; Chen and Olden, 2017]. This is particularly true due to the indiscriminate growth of engineered rivers, where infrastructures aimed at the exploitation of running water are often built in cascade also downstream of existing dams [Lebel et al., 2005; Lazzaro et al., 2013]. Accordingly, this chapter aims to provide a clear understanding on the relation between the potential presence of climate signatures in regulated regimes and reservoir functions. Particular emphasis is placed on the relative roles of

climate variability and dam operations in controlling the long-term variability of regulated streamflow. These issues are addressed by using a data-driven approach. First, the sensitivity of unregulated and regulated flow regimes to climate forcings is investigated through the evaluation of specific indexes based on a limited number of climate variables (i.e., precipitation, temperature and potential evapotranspiration) [Abatzoglou et al., 2014]. Second, the interaction between climate variability and reservoir operations is studied by investigating the long-term patterns of the occurrence probability of specific flow ranges. Differently from Ficklin et al. [2018], who compare two disjoint sets of catchments representing natural and regulated rivers, here, temporal patterns of flow regimes upstream and downstream of isolated dams distributed throughout the Central-Eastern United States are compared. In order to capture the heterogeneity of hydro-climatic patterns and reservoir functions [Carey et al., 2010; Patterson et al., 2012; Botter et al., 2013], the analysis spans a wide range of climatic settings and the same water uses analyzed in Chapter 2 (namely flood control, water supply and hydropower production).

3.2 Theoretical Framework

The primary purpose of this chapter is to identify and describe the nature of climatic controls on river flow regimes. This issue is first addressed through the similarity framework presented by Berghuijs et al. [2014], allowing for the characterization of the seasonal water balance behaviour and of the impact of such seasonal water balance on streamflow variability. The approach identifies three dimensionless indexes expressing the primary role of climate in controlling the seasonal water balance and, thus, the hydrologic regime: the aridity index, ϕ, the timing of precipitation, δ_P^*, and the fraction of precipitation falling as snow, f_S (hereafter referred to as "snowiness"). Aridity shapes the partitioning of precipitation into evapotranspiration and drainage [Budiko, 1974; Milly, 1994; Porporato et al., 2004], precipitation timing strongly affects the dynamics of the catchment water storage, that ultimately contributes to streamflow, while precipitation falling as snow is responsible for carryover flows across seasons through accumulation and melting processes and, thus, causes delayed streamflow peaks [Woods, 2009; Doulatyari et al.,

2015; Schaefli et al., 2013]. Accordingly, in this study, climate is first investigated and described through ϕ, δ_P^* and f_S. Additionally, rainfall frequency, λ_P, is considered to account for the daily variability of river flows and, thus, to comply with the classification of streamflow regimes used in chapter 2 (see section 3.2.2). The nature of climatic control on unregulated and regulated river flow regimes is further investigated by organizing a representative selection of catchments into different groups on the basis of values assumed by the considered climate indexes (i.e., δ_P^*, f_S, ϕ and λ_P). The emergence of hydrologically coherent clusters should reveal the governing role of climate on streamflow regimes. This approach agrees with a large body of literature using clustering schemes to identify the relationship between the hydrologic response and physical drivers [Coopersmith et al., 2012; Ye et al., 2012; Sawicz et al., 2011; Berghuijs et al., 2014].

The analysis is complemented by an objective characterization of the impact of dams on the response of regulated regimes to inter-annual fluctuations of climate and hydrologic properties. The latter is obtained by investigating the occurrence probability of small flows and the magnitude of river flows able to buffer long term fluctuations in hydroclimatic forcings, hereafter termed resilient flows.

3.2.1 Climatic Indexes

Three climatic indexes (aridity, precipitation timing and snowiness) are evaluated assuming that the seasonal variability of precipitation, $P(t)$, air temperature, $T(t)$, and potential evapotranspiration, $PET(t)$, can be approximated by a sine curve [Milly, 1994; Potter et al., 2005; Woods, 2009]. This is a reasonable assumption at extratropical locations, where most of the climatic variables are characterized by a dominant period of one year due to the seasonality of the solar irradiance normal to the top of the atmosphere [Trewartha, 1954]. In particular, $P(t)$, $T(t)$ and $PET(t)$ are expressed via the following equations:

$$\begin{aligned} P(t) &= \overline{P}(1 + \delta_P sin(2\pi(t - s_P)/\tau_P)) = \\ &= \overline{P} + \Delta_P(sin(2\pi(t - s_P)/\tau_P) \end{aligned} \tag{3.1}$$

$$\begin{aligned} T(t) &= \overline{T}(1+\delta_T sin(2\pi(t-s_T)/\tau_T)) = \\ &= \overline{T}+\Delta_T(sin(2\pi(t-s_T)/\tau_T) \end{aligned} \tag{3.2}$$

$$\begin{aligned} PET(t) &= \overline{PET}(1+\delta_{PET} sin(2\pi(t-s_{PET})/\tau_{PET})) = \\ &= \overline{PET}+\Delta_{PET}(sin(2\pi(t-s_{PET})/\tau_{PET}) \end{aligned} \tag{3.3}$$

In eqs. (3.1), (3.2) and (3.3), t is the time expressed in days, overlined letters are the time-averaged values of the considered climatic variables, Δ is the seasonal amplitude of the harmonics, δ is the ratio between Δ and the corresponding average, s is phase shift in days, τ is the duration of the seasonal cycle (365 days) and $2\pi/\tau$ is a scaling factor that allows s to be measured in days rather than in radians.

Differently from the parametric representation of $P(t)$, $T(t)$, $ET(t)$ proposed by Milly [1994], the one considered in this study [Potter et al., 2005; Woods, 2009; Berghuijs et al., 2014] adds an arbitrary shift among the considered climatic variables (i.e., $s_P \neq s_T \neq s_{ET}$), thus allowing their maximum to occur at arbitrary time during the year.

Analytical expressions for the precipitation timing, δ_P^*, the snowiness, f_S, and the aridity index, ϕ, derive from eqs. (3.1), (3.2) and (3.3). Precipitation timing can be evaluated as follows [Woods, 2009; Berghuijs et al., 2014]:

$$\delta_P^* = \delta_P sgn(\Delta_T) cos(2\pi(s_P - s_T)/\tau) \tag{3.4}$$

δ_P^* ranges between -1 and 1 and describes the seasonality of precipitation, including information related to the phase shift between precipitation and the other climatic variables (assuming that $s_T \approx s_{PET}$). In particular, $\delta_P^* = -1$ indicates winter-dominant precipitations, out of phase with temperature and potential evapotranspiration, while $\delta_P^* = 1$ indicate summer-dominant precipitation, in agreement with T and PET. Finally, $\delta_P^* = 0$ is typical of areas where precipitation is uniformly distributed throughout the entire year.

The snowiness, f_S, identifies the fraction of precipitation falling as snow and is defined

through the following equation [Woods, 2009; Berghuijs et al., 2014]:

$$f_S = \frac{1}{2} - \frac{sin^{-1}(\overline{T^*})}{\pi} - \frac{\delta_P^*}{\pi}\sqrt{1-\overline{T^*}} \qquad \overline{T^*} = \frac{\overline{T} - T_0}{|\Delta_T|} \tag{3.5}$$

where T_0 is the temperature below which precipitation falls as snow. f_S ranges from 0 to 1, where $f_S = 0$ and $f_S = 1$ mean that all the precipitation falls as rain and snow, respectively.

The aridity index is defined as [Budiko, 1974] :

$$\phi = \frac{\overline{PET}}{\overline{P}} \tag{3.6}$$

ϕ is a dimensionless index (as both precipitation and potential evapotranspiration are expressed in mm/d) that theoretically ranges from 0 to ∞.

Note that parameters of eq. (3.1) are evaluated based on daily precipitation values characterizing the average year of a given time window. Because of the focus on the seasonal water balance, the considered time series is smoothed by means of a 45 days moving average; this timespan is chosen to filter out the short-term variability of precipitation, though preserving its seasonal behaviour. Consequently, parameters $\overline{P}$, δ_P and s_P of the best-fitting sinusoid are evaluated solving a least-square minimization problem through the Newton-Raphson method [Stoer and Bulirsch, 1993]. The same procedure is used to evaluate parameters of eqs. (3.2) and (3.3), though considering daily temperature and evapotranspiration values, respectively.

Finally, the frequency of rainfall events, λ_P, is evaluated as detailed in Chapter 2, thus computing the relative number of days with a rainfall depth equal to or higher than 1 mm [Doulatyari et al., 2017].

3.2.2 Construction of Coherent Clusters

The representative selection of dams considered in this study is divided into groups of hydrologically-similar sites. Each group of catchments is obtained by mean of the cluster analysis. The approach is based on the averaged values of the four climatic indexes and treats each catchment as an object with a specific location in the climatic indexes space. Grouping is performed through the evaluation of the euclidean distance between objects

[Wilks, 2011]:

$$d_{AB} = \sqrt{\sum_{n=1}^{4}(X_{A,ci} - X_{B,ci})^2} \tag{3.7}$$

where $X_{A,ci}$ and $X_{B,ci}$ represents the coordinates of objects A and B defined by the climate index ci, respectively. Objects located close to each other and far from the other form a group.

To assess the hydrological similarity of each cluster, mean water availability ($\overline{Q}$) and hydrological variability (CV_Q) typical of each catchment are evaluated and compared at both the inter-seasonal and intra-seasonal time scales (see section 2.2.3). Moreover, the RMSE-observations standard deviation ratio (hereafter referred to as "RSR") is estimated for each couple of clusters based on discharge time series [Moriasi et al., 2007]:

$$RSR_M^K = \frac{1}{N}\sum_{n=1}^{N}\frac{\sqrt{\sum_{i=1}^{365}(Q_i^n - Q_i^{\overline{k}})^2}}{\sqrt{\sum_{i=1}^{365}(Q_i^n - \overline{Q^k})^2}} \tag{3.8}$$

In eq. (3.8), the time series of streamflow are those characterizing the average year of each catchment. Therein, M is the considered cluster, K is the cluster to which each catchment belonging to cluster M is compared, N is the number of catchments characterizing cluster M, i is the day of the year, Q_i^n is the value of streamflow for catchment n on day i, $Q_i^{\overline{k}}$ is the average streamflow typical of catchments characterizing cluster K on day i and, finally, $\overline{Q^k}$ is the annual average of $Q_i^{\overline{k}}$. The goal is to obtain the lowest values of RSR_M^K when $M = K$ and the largest when $M \neq K$; in fact, this confirms that the variance between river flow regimes within a single cluster is lower than that among different clusters. Therefore, under these circumstances, the considered group of catchments is made of hydrologically similar sites.

To assess whether or not climatic signatures are still visible downstream of reservoirs and whether this is dependent on the type of regulation, natural and regulated flow regimes of specific groups are compared. This is done to devise a link between river flow regimes in unregulated and regulated reaches, that implicitly define the relation between regulated flow regimes and climatic conditions. Mean water availability, $\overline{Q}$, and hydrological variability, CV_Q, are evaluated upstream and downstream of dams for the period of time in which sites are characterized by synchronous records of unregulated

and regulated streamflows (see table 3.1). Moreover, the value of RSR_M^K based on regulated discharge time series is estimated.

3.2.3 Small Flows Stability and Resilient Streamflows

Temporal trajectories of river flow regimes are investigated resembling the theory of superstatistics [D'Odorico et al., 2000; Porporato et al., 2006]. Accordingly, the period of record is divided into disjointed sub-periods, and changes of the flow regime between couples of contiguous sub-periods are analyzed. The aggregation time scale of discharge time series used in our analysis is three years, so as to ensure a reasonable ergodicity of river flows during each sub-period though simultaneously allowing for the identification of recognizable internal fluctuations within the period of record [Botter et al., 2013; Botter, 2014]. Our attention is focused on the sustainable management of hydraulic infrastructures for the exploitation of running water in the context of long-term streamflow variability. Inter-annual changes of river regimes in natural and regulated reaches are studied in terms of the stability of streamflows. Streamflow stability quantifies the ability of flow regimes to buffer their responsiveness to long term fluctuations of the hydroclimatic forcing, which is related to the time-invariant fraction of the discharge frequency distribution, $p(Q)$. River flows characterized by high stability are able to buffer inter-annual changes in climate and hydrologic properties and, thus, are observed with the same probability regardless of the underlying climatic conditions. These flows are termed resilient streamflows [Botter et al., 2013].

In particular, in the presented approach inter-annual changes of flow regimes are analyzed by means of two synthetic indexes: the low-flow stability, LS, and the magnitude of resilient flows, Q_R. LS is evaluated as the difference between the cumulative non-exceedance probability of streamflows observed across each couple of subsequent three-year sub-periods, with specific reference to a threshold discharge Q^*. In other words, the low-flow stability quantifies the difference in the occurrence probability of flows smaller than Q^* (figure 3.1, A and B):

$$LS = \int_0^{Q^*} (p_{i+1}(Q) - p_i(Q))dQ \tag{3.9}$$

In eq. (3.9), $p_i(Q)$ and $p_{i+1}(Q)$ represent the discharge frequency distributions in the contiguous sub-periods i and $i+1$, respectively. Uncertainty may arise on how to define the upper integration limit in eq. (3.9), Q^*. Here, the threshold Q^* is set equal to $0.25\,mm/d$ ($\approx 3\,l/s\,km^2$). This discharge value might have the same order of magnitude of a minimum flow discharge, and it is then taken here as a proxy for the minimum river discharge necessary to trigger any abstraction device located alongside the river (e.g., for irrigation, urban water supply or energy production). This way, LS become representative of the variations in the percentage of time during which certain ecological and human water uses can be guaranteed. High and low streamflow stability are identified by low and high absolute values of LS, respectively.

The magnitude of resilient flows, instead, is evaluated by identifying the values of Q that are characterized by a time-invariant probability density function across subsequent sub-periods (figure 3.1, C and D). Formally, Q_R obeys to the following equation:

$$\Delta p(Q_R) = p_{i+1}(Q_R) - p_i(Q_R) = 0 \tag{3.10}$$

which is solved numerically based on the observed time series of discharge. In particular, two cycles of smoothing are applied to the observed differences PDFs, $\Delta p_i(Q)$, as follows:

$$\Delta p_i^j(Q) = \frac{\Delta p_{i-1}^{j-1}(Q) + \Delta p_i^{j-1}(Q) + \Delta p_{i+1}^{j-1}(Q)}{3} \qquad j = 1, 2 \tag{3.11}$$

where $\Delta p_i^0(Q)$ coincides with the unsmoothed differences PDF and j is the smoothing cycle number. These cycles isolate the most significant patterns from spurious fluctuations due to the non-ergodic nature of time series. Negative/positive or positive/negative transitions in the differences of PDFs after the smoothing represent resilient streamflows, Q_R.

Small flow stability and resilient streamflows are detected for each couple of three-year intervals belonging to the period of record of each case study, and are then used to calculate the frequency distribution of the quantities of interest (i.e., $p(LS)$ and $p(Q_R)$). To quantify the effect of regulation on the sensitivity of flow regimes to inter-annual fluctuations of hydroclimatic forcings, these PDFs are calculated both upstream and downstream of each reservoir and then compared.

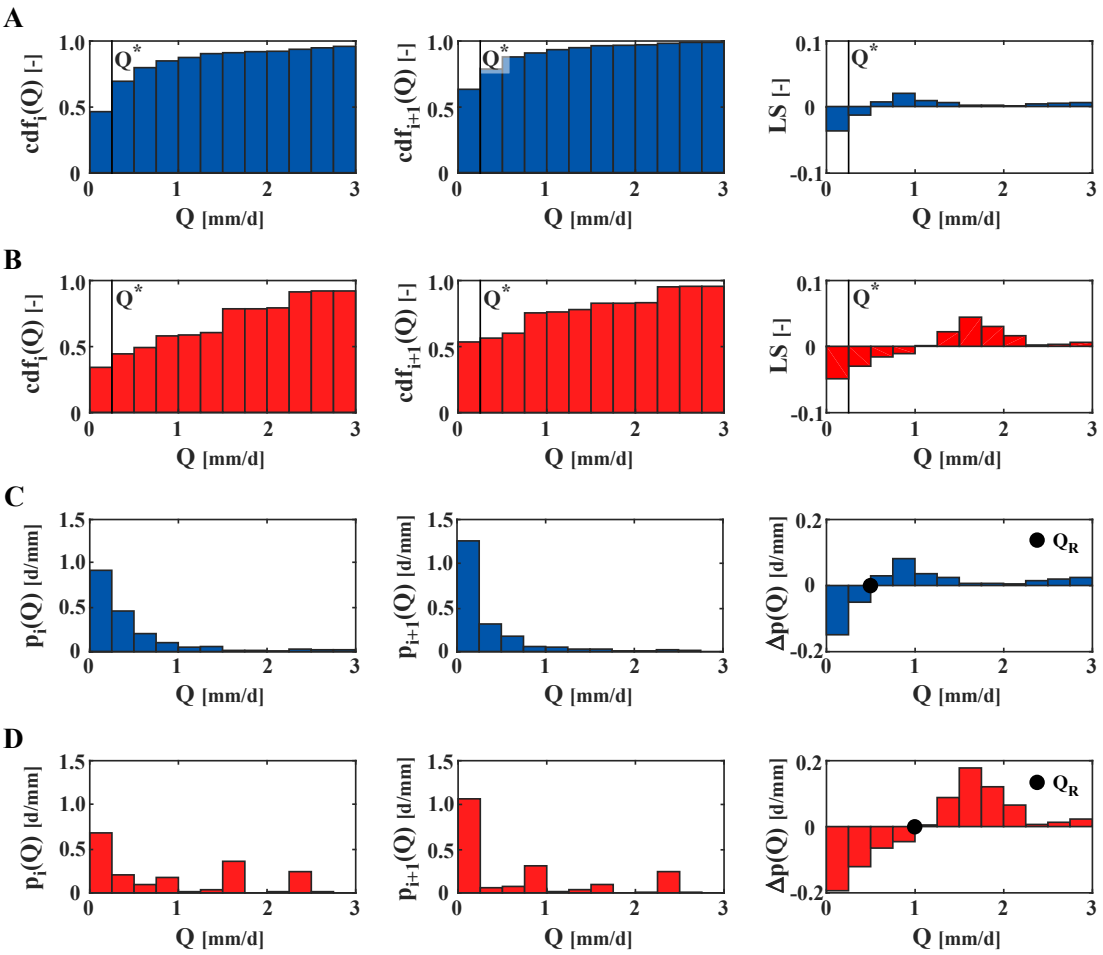

FIGURE 3.1: Graphical representation of the approach used to investigate the stability of small flows (A and B) and the magnitude of resilient streamflows (C and D). Blue and red bars are used to represent the cumulative non-exceedance probability and the frequency distribution of natural (A and C) and regulated (B and D) streamflows, respectively. It is noteworthy to point out changes undergone by hydrological properties across different sub-periods (column 1 vs. column 2) and through river flows regulation (rows A and C vs. rows B and D).

3.3 Study Sites and Hydro-Climatic Data

This study investigates the downstream effects of a representative selection of dams distributed throughout the Central-Eastern United States. Study sites are recovered from chapter 2 and summary information about dams can be found in table 2.1. The analysis performed in this chapter is exclusively based on observed discharge records. Daily streamflow time series are collected by the US Geological Survey and typically span several decades (see table 3.1). For the characterization of daily temperature and precipitation of each catchment, the spatially explicit "Daymet V3" database is used. This data set provides gridded estimates ($1\ km\ \times\ 1\ km$ spatial resolution) of the aforementioned variables for the entire North America between 1980 and 2017. Daily temperature and precipitation values are used to evaluate ϕ, λ_P, δ_P^* and f_S. Potential evapotranspiration data are further required to evaluate ϕ (see eq. (3.6)), and they are obtained by the "CGIAR-CSI Global-Aridity and Global-PET Database", a data set containing monthly and annual average values of PET for the entire world. Estimation is performed across the contributing catchment of each dam with a spatial resolution of $1\ km\ \times\ 1\ km$. High resolution digital elevation models (i.e., DEMs) allowing for the extraction of the contributing catchments by suitable GIS-based manipulations are collected by the U.S. Geological Survey.

On account of the hydroclimatic similarities characterizing groups of sites belonging to the considered selection (see sections 3.4.1 and 3.4.2), the analysis of small flow stability and the magnitude of resilient streamflow is performed by focusing on a subset of reservoirs spanning the entire Central-Eastern United States (see figure 3.2).

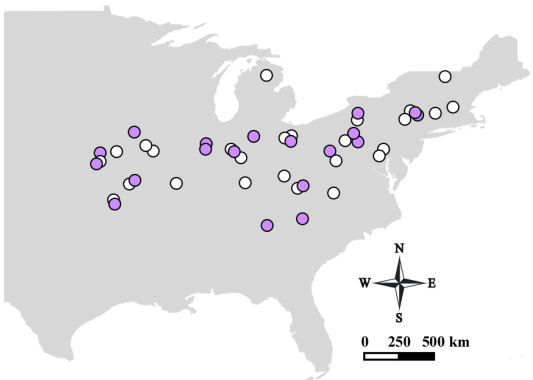

FIGURE 3.2: Lilac dots represent the spatial distribution of the aforementioned subset of reservoirs.

TABLE 3.1: USGS stations providing discharge time series.

Reservoir	**State**	**Natural Streamflow [Q_{NAT}]**		**Regulated Streamflow [Q_{REG}]**	
		USGS Station	Timespan	USGS Station	Timespan
Allegheny	PA	03010500	1980-2017	03012550	1980-2017
Alum Creek	OH	03228750	2000-2017	03228805	2000-2017
Cagles Mill	IN	03358000	1980-2017	03359000	1980-2002
Cannonsville	NY	01423000	1980-2017	01425000	1980-2017
Carters	GA	02380500	1980-2017	02382500	1980-2017
Cave Run	KY	03248300	2001-2017	03249500	1980-2017
Clinton	KS	06891260	2002-2017	06891500	1980-2017
C. M. Harden	IN	03340800	1980-2017	03340900	1980-2001
Curwensville	PA	01541000	1980-2017	01541200	1980-2017
Decatur	IL	05572000	1982-2017	05573540	1980-2017
Delaware	OH	03223000	1980-1998	03225500	1980-2017
Eucha	OK	07191220	1980-2017	07191288	2001-2017
EB Clarion	PA	03026500	1980-2017	03027500	1980-2017
Fishtrap	KY	03207800	1980-2017	03208000	1980-2000
J. W. Flannagan	VA	03208950	1980-2017	03209000	1980-2017
Green River	KY	03305000	1980-2017	03306000	1980-1994
Loyalhanna	PA	03045010	1980-2017	03047000	1980-2017
Long Branch	MO	06906150	2001-2017	06906200	1980-2017
Mark Twain	MO	05502300	1980-2017	05507800	1980-2017
Mio Pond	MI	04135700	1980-2017	04136500	1980-2017
Neversink	NY	01435000	1980-2017	01436000	1980-2017
Nolin River	KY	03310300	1980-2017	03311000	1980-2004
O'Shaughnessy	OH	03219500	1980-2017	03221000	1980-2017
Pepaction	NY	01413500	1980-2017	01417000	1980-2017
Perry	KS	06890100	1980-2017	06890900	1980-2017
Philpott	VA	02071530	1995-2017	02072000	1980-2017
Pomme de Terre	MO	06921070	1980-2017	06921350	1980-2017
Pomona	KS	06911900	1980-2017	06912500	1980-2017
Prettyboy	MD	01581810	2000-2017	01581920	2000-2017
Prompton	PA	01428750	1986-2017	01429000	1980-2017
Quabbin	MA	01174500	1980-2017	01175500	1980-2017
Rathbun	IA	06903400	1980-2017	06903700	1980-2017
Raystown	PA	01562000	1980-2017	01563200	1980-2017
Rocky Gorge	MD	01591000	1980-2017	01592500	1980-2017
Salomonie	IN	03324300	1980-2017	03324500	1980-2002
Shelbyville	IL	05591200	1980-2017	05592000	1980-2017
Smithville	MO	06821080	1999-2017	06821150	1980-2017
Stockton	MO	06918440	1980-2017	06919000	1980-1990
Sutton	WV	03194700	1980-2017	03195500	1980-1992
Tenkiller	OK	07196500	1980-2017	07198000	1980-2017
Tygart	WV	03054500	1980-2017	03056000	2000-2017
Zoar	CT	01200500	1980-2017	01205500	1980-2017
Wappapello	MO	07037500	1980-2017	07039500	1980-2017
Waterbury	VT	04288225	2000-2017	04289000	1980-2017
W. C. Bowen	SC	02154790	1989-2017	02155500	1980-2017

3.4 Results

Results are organized into four different sections. Section 3.4.1 firstly describes the behaviour of climatic indexes across a representative selection of catchments distributed throughout the Central-Eastern Unites States; secondly, it presents the grouping of the considered catchments, here performed on the basis of climatic indexes by mean of the cluster analysis. Section 3.4.2 analyzes the climate dependent nature of natural flow regimes by unravelling the hydrological similarities and differences typical of catchments belonging to different groups. Section 3.4.3 describes the link between natural and regulated flow regimes of specific catchment groups, assessing whether climatic signatures are still visible in regulated regimes and whether this is dependent on the type of regulation. Finally, section 3.4.4 analyzes the responsiveness of regulated flow regimes to inter-annual changes of climatic and hydrological properties.

3.4.1 Climatic indexes and catchment classification

Climatic indexes are spatially-evaluated across the considered catchments for the period of time ranging between 1980 and 2017. As an example, figure 3.3 shows the spatial patterns of each climatic index across the Delaware river basin upstream of Perry lake, Kansas. The obtained results suggest that all the considered indexes are characterized by a pronounced inter-catchment variability and large-scale patterns. Catchments in the Eastern US tend to be humid, with low values of the aridity index, ϕ, and high values of the rainfall frequency, λ_P. Moving towards the Central US, catchments become more arid, with higher values of ϕ and lower values of λ_P. In the case of precipitation timing, catchments in Southeastern US tend to have uniform precipitation throughout the entire year, with values of δ_P^* approximately ranging between -0.10 and 0.10, whereas catchments in Northeastern US exhibit slightly higher values of δ_P^*, from 0.10 to about 0.20. However, the highest values of δ_P^* (i.e., $\delta_P^* > 0.5$) are observed in Central US, where the considered catchments experience relevant summer-dominant precipitation. Finally, the snowiness, f_S, increases while moving north, but only catchments in the north-east have a non-negligibe fraction of precipitation falling as snow, with values of f_S ranging between 0.20 and 0.35. These patterns are confirmed by table 3.2, reporting

the geographical location and the spatial average of the four climatic indexes for each of the considered catchment.

Spatially averaged values of ϕ, λ_P, δ_P^* and f_S are used to perform the cluster analysis. Clustering of catchments is first performed over the entire period of analysis, ranging between 1980 and 2017, and is then repeated over three different sub-periods (i.e., 1980-1992, 1993-2005 and 2006-2017) to verify whether the obtained classification is time invariant. This is necessary because of the occasional absence of complete discharge time series between 1980 and 2017 (see table 3.1), preventing the consequent assessment of catchment hydrological similarities over the entire period of analysis. During clustering, three sites are disregarded from the analysis because of significant climate dissimilarities with respect to all the other (i.e., Eucha and Tenkiller lake, Oklahoma, and Mio Pond, Michigan), as highlighted by their distance from the median location of the assigned cluster (in the climatic indexes space), that is approximately 200% greater than the average distance calculated on the basis of the remaining catchments. Figure 3.4 shows the obtained groups of catchments, as well as their geographic spread and organization. Catchments are grouped into four different clusters that appear to be almost time invariant: just two of the considered catchments move from a certain group to another and this happens only in one of the three sub-periods. In agreement with the spatial patterns shown by the four climatic indexes, clusters exhibit a remarkable spatial coherence. Apart from sporadic exceptions, catchments belonging to class 1 and 2 are distributed throughout the Northeastern and Southeastern US, respectively, while catchments forming class 3 and 4 are located in the Midwestern and Central US, respectively. Finally, figure 3.5 displays the ranges of ϕ, λ_P, δ_P^* and f_S typical of each cluster. Catchments exhibit remarkable climatic similarities within specific groups and remarkable variations between different groups. Sites in class 1 are humid, with the highest values of λ_P and the lowest of ϕ, and exhibit the largest snowmelt component and mild in-phase seasonality of precipitation. Conversely, sites in class 4 are arid, with the lowest values of λ_P and the highest of ϕ, and are characterized by a negligible fraction of precipitation falling as snow and significant in-phase rainfall seasonality. Class 2 and 3 mainly display intermediate features, though the absence of any snowmelt component and precipitation seasonality is typically observed in catchments of class 2.

TABLE 3.2: Spatially averaged values of ϕ, λ_P, δ_P^* and f_S across the selected catchments.

Catchment	**Lat [DD]**	**Long [DD]**	**Aridity Index** [ϕ]	**Precipitation Timing** [$\delta_{\mathbf{P}}^*$]	**Snowiness** [$\mathbf{f_S}$]	**Rainfall Frequency** [$\lambda_{\mathbf{P}}$]
Allegheny	42.1°	−78.5°	0.76	0.20	0.28	0.40
Alum Creek	40.4°	−82.9°	0.98	0.20	0.18	0.31
Cagles Mill	39.5°	−86.7°	0.92	0.17	0.16	0.29
Cannonsville	42.2°	−75.0°	0.68	0.19	0.30	0.37
Carters	34.7°	−84.5°	0.78	-0.10	0.00	0.30
Cave Run	38.0°	−83.3°	0.95	0.09	0.00	0.31
Clinton	38.9°	−95.6°	1.16	0.54	0.07	0.21
C. M. Harden	39.9°	−86.9°	0.92	0.20	0.18	0.28
Curwensville	40.7°	−78.7°	0.83	0.16	0.24	0.37
Decatur	40.1°	−88.6°	1.05	0.27	0.17	0.26
Delaware	40.6°	−82.9°	0.99	0.22	0.19	0.31
EB Clarion	41.6°	−78.5°	0.73	0.18	0.29	0.40
Eucha	36.4°	−94.7°	1.03	0.16	0.00	0.23
Fishtrap	37.3°	−82.1°	0.90	0.13	0.03	0.34
J. W. Flannagan	37.1°	−82.5°	0.89	0.10	0.00	0.35
Green River	37.3°	−85.0°	0.85	-0.01	0.00	0.31
Loyalhanna	40.3°	−79.3°	0.82	0.14	0.21	0.38
Long Branch	40.0°	−92.5°	1.02	0.44	0.13	0.24
Mark Twain	39.6°	−92.0°	1.05	0.38	0.12	0.24
Mio Pond	44.6°	−84.5°	1.03	0.28	0.29	0.33
Neversink	42.0°	−74.5°	0.55	0.13	0.32	0.35
Nolin River	37.5°	−86.0°	0.89	-0.02	0.00	0.28
O'Shaughnessy	40.2°	−83.1°	1.02	0.22	0.18	0.30
Pepaction	42.1°	−74.7°	0.62	0.17	0.31	0.37
Perry	39.5°	−95.6°	1.20	0.60	0.08	0.21
Philpott	36.8°	−80.0°	0.96	0.11	0.01	0.28
Pomme de Terre	37.6°	−93.3°	1.01	0.25	0.01	0.24
Pomona	38.7°	−95.8°	1.18	0.53	0.08	0.21
Prettyboy	39.7°	−76.8°	0.88	0.09	0.12	0.29
Prompton	41.7°	−75.4°	0.72	0.15	0.29	0.33
Quabbin	42.5°	−72.2°	0.74	0.09	0.29	0.32
Rathbun	40.9°	−93.3°	1.03	0.60	0.13	0.25
Raystown	40.2°	−78.5°	0.96	0.15	0.20	0.31
Rocky Gorge	39.2°	−77.1°	0.93	0.09	0.04	0.29
Salomonie	40.6°	−85.4°	0.98	0.24	0.19	0.29
Shelbyville	39.7°	−88.6°	1.06	0.22	0.16	0.26
Smithville	39.5°	−94.4°	1.06	0.54	0.10	0.22
Stockton	37.4°	−93.6°	1.00	0.25	0.00	0.24
Sutton	39.6°	−80.4°	0.69	0.09	0.20	0.42
Tenkiller	36.1°	−94.6°	0.99	0.15	0.00	0.23
Tygart	39.0°	−80.0°	0.74	0.21	0.33	0.42
Zoar	42.1°	−73.3°	0.71	0.13	0.26	0.32
Wappapello	37.4°	−90.5°	0.98	0.04	0.03	0.25
Waterbury	44.5°	−72.7°	0.60	0.21	0.33	0.42
W. C. Bowen	35.1°	−82.2°	0.92	0.02	0.00	0.29

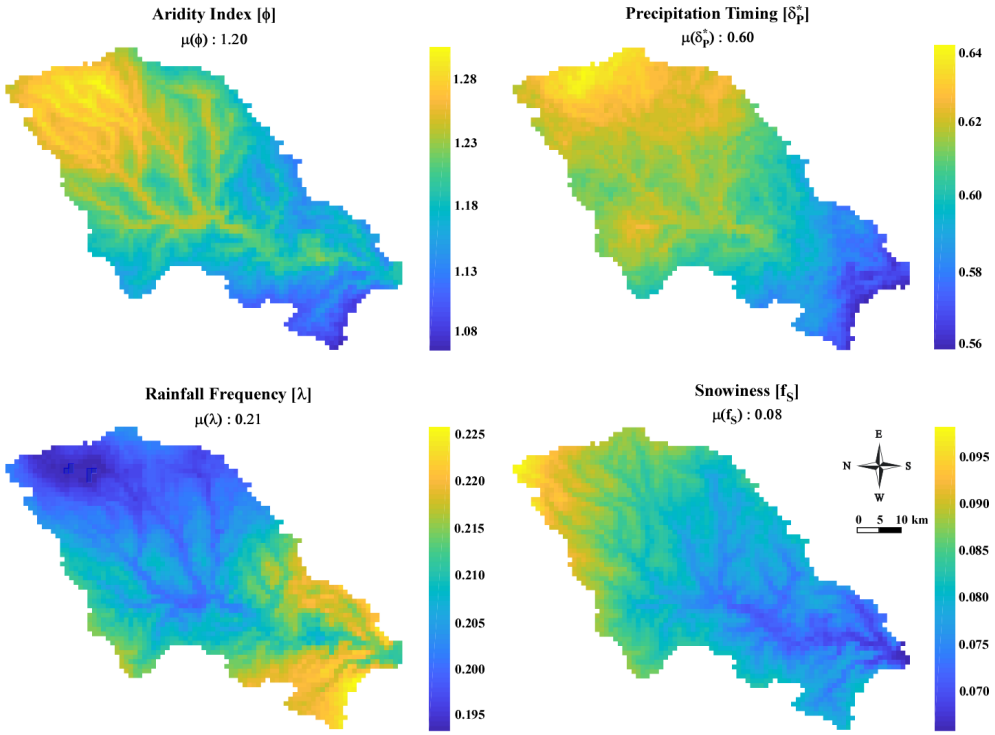

FIGURE 3.3: Spatial indexes across the Delaware river basin upstream of Perry lake, KS.

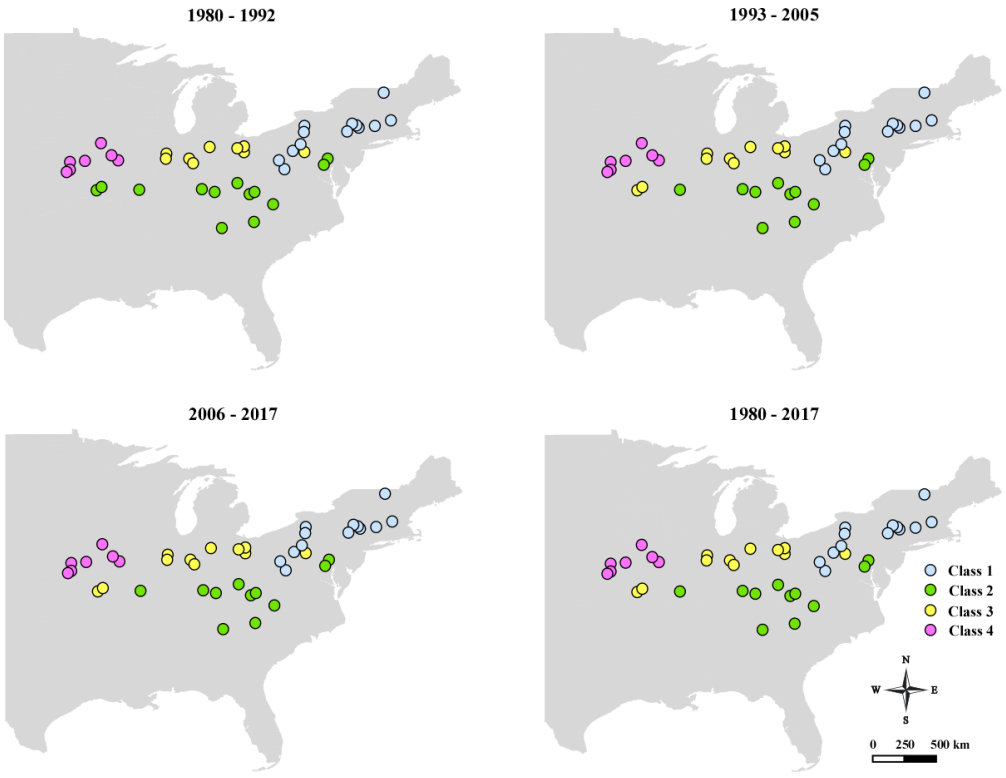

FIGURE 3.4: Groups of catchments obtained by mean of the cluster analysis for each of the considered periods of time.

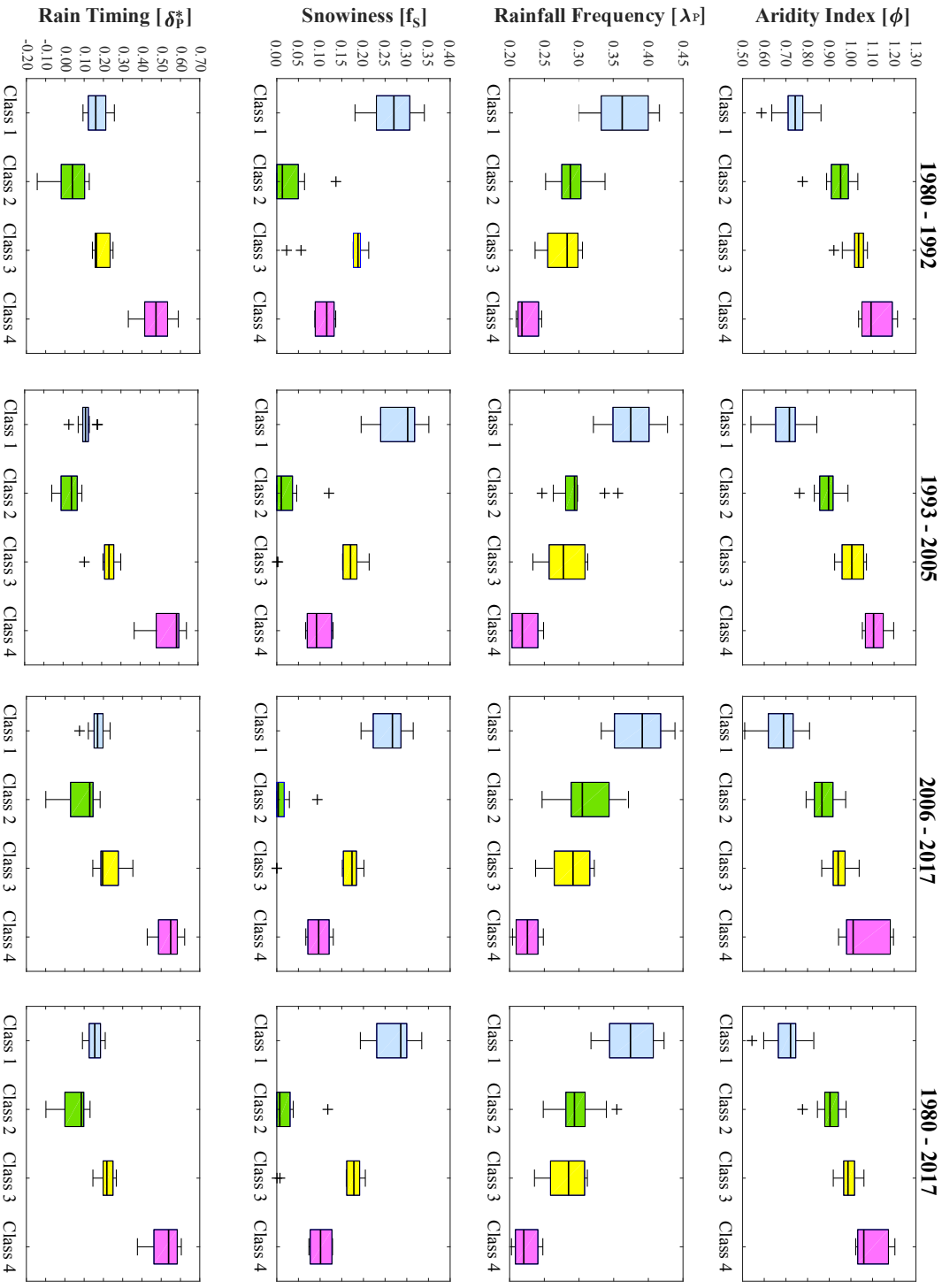

FIGURE 3.5: Behaviour of the four climatic indexes in each of the considered periods of time.

3.4.2 Analysis of climatic signatures in natural flow regimes

Within-cluster hydrological similarities and between-cluster differences are investigated through the evaluation of the mean water availability, $\overline{Q}$, and hydrological variability, CV_Q, characterizing the natural flow regimes of the study catchments. Figure 3.6 shows results obtained at the annual time scale, displaying the ranges of $\overline{Q}$ and CV_Q within each cluster by means of suitable box plots. As expected [Berghuijs et al., 2014], the average discharge and the coefficient of variation observed in catchments belonging to the same cluster are quite similar, while significant variations exist between the values of $\overline{Q}$ and CV_Q characterizing catchments of different groups. The annual average discharge decreases from the left to the right, displaying the maximum values for class 1 and the minimum for class 4 (figure 3.6, left), while the annual coefficient of variation shows an opposite trend (figure 3.6, right), in agreement with previous studies [Botter et al., 2013; Destouni et al., 2013]. The within cluster variability of $\overline{Q}$ and CV_Q exhibit comparable patterns, with class 1 and 4 being characterized by the highest within cluster variability of $\overline{Q}$ and CV_Q respectively. These trends mainly results from the superposition of aridity, rainfall frequency and precipitation timing, based on which clusters are obtained. Catchments belonging to class 1 display the lowest interarrivals and water losses from evapotranspiration (see figure 3.5). Accordingly, they exhibit the most abundant and less variable river flows, owing to an almost persistent supply of water to streams from the catchment soil. Conversely, catchments belonging to class 4 are characterized by the least frequent rainfall events and the greatest water losses through evapotranspiration, due to the highest values of the aridity index and seasonal precipitation in phase with potential evapotranspiration (see figure 3.5). As a result, these catchments can dry significantly in between events, producing limited and fluctuating streamflows. Catchments belonging to class 2 and 3 display intermediate behaviours, though the coefficient of variation of class 2 is similar to that of class 1. As the CV_Q is quite strongly anticorrelated with the mean discharge [Destouni et al., 2013], the fluctuations of river flows must be particularly weak in catchments of class 2 with respect to class 1. This peculiarity is explained by the precipitation timing, which is always slightly higher than zero in class 1 and close to zero in class 2 (see figure 3.5). Catchments belonging to class 2 respond slowly to rainfall events and are baseflow dominated, with most of the discharge coming

from the groundwater and being almost uniform in response to the time-invariant level of groundwater and, thus, to the uniform precipitation throughout the year ($\delta_P^* \simeq 0$). Figure 3.7 shows that annual patterns are maintained seasonally. At this time scale, it is also possible to appreciate the influence of the snowiness on natural flow regimes, as it is responsible for carryover flows across seasons through accumulation and melting processes [Schaefli et al., 2013]. In particular, it is evident that the average streamflow of catchments belonging to class 1 (the only sites with a non-negligible fraction of precipitation falling as snow, see figure 3.5) is remarkably increased by melting processes during the spring season, as inferred by the significant difference observed in this season between the mean water availability of class 1 and that of the other classes.

Within-cluster hydrological similarities and between-cluster differences are further investigated by estimating the value of RSR_M^K (eq. 3.8) based on unregulated discharge time series. Table 3.3 shows the obtained results for each of the 16 couples of clusters M and K. As expected, the lowest values of RSR_M^K are obtained when comparing streamflow time series of catchments belonging to the same cluster ($M = K$, diagonal terms of table 3.3), while larger values are obtained comparing streamflow time series of catchments belonging to different clusters ($M \neq K$, off-diagonal terms of table 3.3). This analysis further confirms that the variance between river flow regimes within a specific class is always lower than that between different classes and, thus, that each climate-based cluster is hydrologically coherent.

These results display a remarkable correlation between natural flow regimes and climatic conditions (here described through ϕ, λ_P, δ_P^* and f_S), proving the climate dependent nature of flows in unregulated rivers, and comply with the findings of previous works [Pike, 1964; Budiko, 1974; Dooge, 1992; Milly and Dunne, 2002; Carmona et al., 2014].

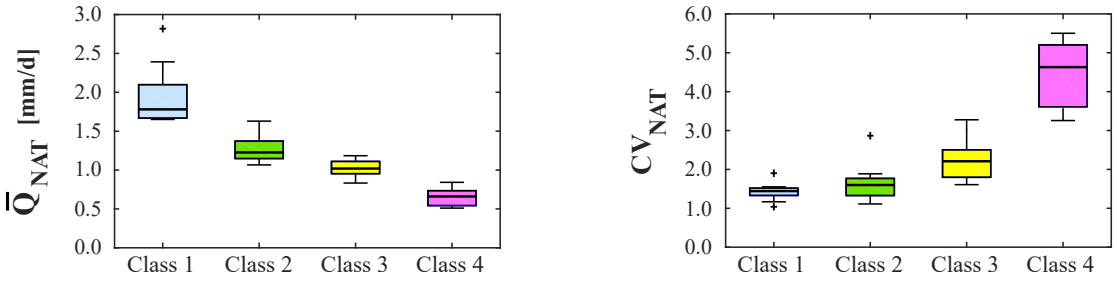

FIGURE 3.6: Behavior of $\overline{Q}$ and CV_Q observed for each cluster at the annual time scale

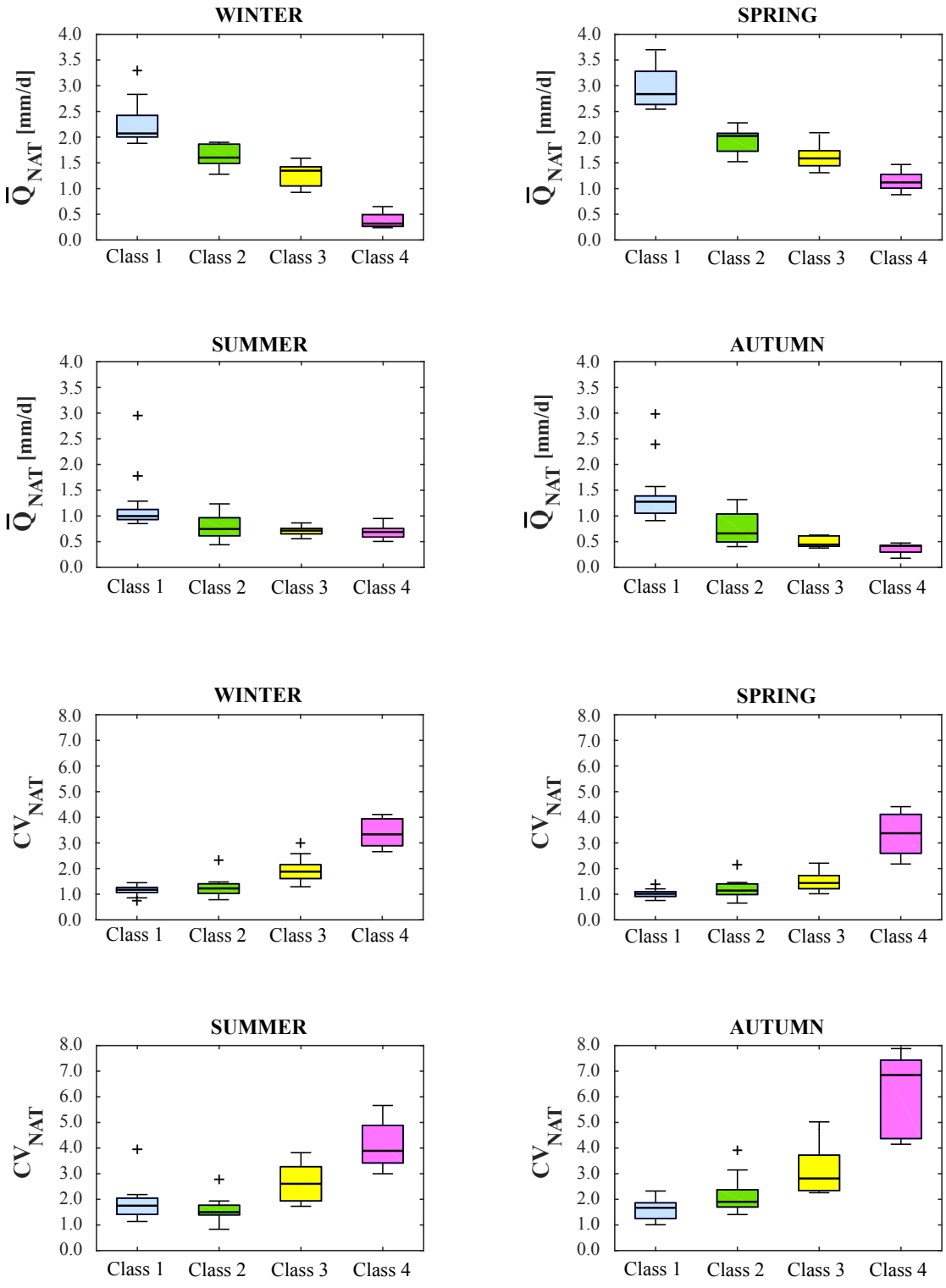

FIGURE 3.7: Behavior of $\overline{Q}$ and CV_Q observed for each cluster at the seasonal time scale

TABLE 3.3: The RSR_M^K values of the 16 couples of clusters

	Class 1	**Class 2**	**Class 3**	**Class 4**
Class 1	0.55	1.00	1.02	1.12
Class 2	0.73	0.63	0.78	1.10
Class 3	0.83	0.76	0.56	1.06
Class 4	1.00	1.05	1.04	0.68

3.4.3 Analysis of climatic signatures in regulated flow regimes

The link between natural and regulated flow regimes of catchments belonging to each group is investigated to assess whether climatic signatures are still visible in regulated discharge time series. The analysis is performed by comparing annual and seasonal values of the mean water availability, $\overline{Q}$, and hydrological variability, CV_Q, typical of river flows upstream and downstream of the considered selection of reservoirs. To assess the correlation between the impact of dams on the climate dependent nature of river flows and specific water uses, the analysis is performed on flood control and multipurpose structures, and separately including reservoirs only operated to supply freshwater (see table 2.1). This is done on the basis of findings reported in chapter 2 (see section 2.5.1), that reveal significant differences between the effect of water supply dams on flow regimes and that produced by other types of reservoirs.

Figure 3.8 shows results obtained at the yearly time scale, displaying ranges of $\overline{Q}$ (top) and CV_Q (bottom) observed upstream (A) and downstream (B and C) of dams for each cluster. Note that results presented in plots B are those obtained through the analysis of flood control and multipurpose structures, while those shown in plots C include reservoirs only operated for water supply. Firstly, attention is focused on the comparison between plots A and B. The annual average discharge in natural and regulated reaches is comparable, owing to the reduced impact of flood control and multipurpose structures on the mean discharge (see section 2.5.1). On the other hand, the annual coefficient of variation is significantly reduced in response to flood mitigation (see section 2.5.1). This decrease occurs proportionally among classes. Accordingly, CV_{REG} displays the trend across different classes observed upstream of reservoirs, but inter-cluster variability and within-cluster variability are smoothed. This behaviour is explained by the average regulation capacity, $\overline{R}_C$, typical of reservoirs of different groups, whose value modulate

the actual magnitude of flow regime alterations (see section 2.5.1). $\overline{R}_C$ exhibits an increasing trend between class 1 and 4 (see blue bars in figure 3.8, *B*), implying that the ability of reservoirs to lower the variability of river flows is enhanced while moving form class 1 to class 4. Secondly, attention is focused on the comparison between plots *A* and *C*. Including reservoirs only operated to supply freshwater, class 1 turns out to be characterized by the presence of strongly exploited reservoirs, $R_E > 0.5$, used to transfer water to the city of New York and Boston, while class 2, 3 and 4 only include weakly exploited reservoirs (see red bars in figure 3.8, *C*). Water supply reduces the mean discharge of regulated reaches, increasing the relative streamflow variability and enhancing the heterogeneity of streamflow at the regional scale (see section 2.5.1). Accordingly, including these structures, alterations in the inter-cluster trend of $\overline{Q}$ and CV_Q observed downstream of reservoirs are visible, with the average discharge and coefficient of variation of class 1 displaying a non-negligible decrease and increase, respectively.

Figures 3.9 and 3.10 show the seasonal behaviour of the mean water availability, $\overline{Q}$, and hydrological variability, CV_Q, upstream (left) and downstream (right) of flood control and multipurpose reservoirs. Figure 3.9 shows a general reduction of $\overline{Q}$ by dams during the spring season, when the highest water availability is typically observed. This is clearly related to reservoir operation. In fact, during high flow periods, dams store water that is then released with the goal of preserving the storage capacity of reservoirs and conveying water downstream for ecosystems preservation or secondary uses. Overall, inter-cluster trends of $\overline{Q}$ and CV_Q observed at the annual time scale are maintained seasonally, with the single exception of the summer season. In this period, the average discharge of classes 2, 3 and 4 turns out to be comparable both upstream and downstream of dams (figure 3.9), probably leading to similar values of CV_{REG} observed in the same classes (figure 3.10). This might imply that the widespread reduction of streamflow fluctuations due to reservoirs operations largely link regional-scale differences of regulated streamflow to the mean water availability.

Overall, these findings indicate that within-cluster hydrological similarities observed in unregulated reaches are largely maintained downstream of reservoirs and, thus, display a correlation between regulated flow regimes and climatic conditions. This is particularly true for flood control and multipurpose structures, while regulation for water supply can

mask climatic signatures typical of natural river flows.

Finally, the RSR_M^K values of the 16 couples of clusters are reported in tables 3.4 and 3.5. Table 3.4 shows the outcomes of the analysis considering only regulated flow regimes downstream of flood control and multipurpose structures. Values of RSR_M^K agree with the results obtained in term of mean water availability and hydrological variability. The hydrological coherence of each climate-based cluster persist downstream of dams, even if it slightly decreases. In fact, diagonal terms are always lower than extra-diagonal terms, though differences are reduced with respect to the analysis of unregulated flow regimes (see table 3.3). Table 3.5 shows the outcomes of the analysis including regulated streamflows downstream of reservoirs only operated to supply freshwater. In agreement with previous findings, values of RSR_M^K indicate a much important reduction of the hydrological coherence typical of each cluster when considering regulated reaches downstream of water supply structures. RSR_1^1 and RSR_2^2 largely increase from table 3.4 to table 3.5, reducing their distance from extra-diagonal terms, as ten water supply reservoirs are distributed across class 1 and 2. Particularly, the most significant increase is exhibited by RSR_1^1 due to the presence of four strongly exploited structures in class 1.

TABLE 3.4: The RSR_M^K values of the 16 couples of clusters. Evaluation is performed considering regulated flows downstream of flood control and multipurpose reservoirs.

	Class 1	**Class 2**	**Class 3**	**Class 4**
Class 1	0.71	0.89	1.00	1.14
Class 2	0.84	0.73	0.92	1.26
Class 3	0.90	0.80	0.73	1.24
Class 4	1.02	1.05	1.06	0.64

TABLE 3.5: The RSR_M^K values of the 16 couples of clusters. Evaluation is performed including regulated flows downstream of water supply reservoirs.

	Class 1	**Class 2**	**Class 3**	**Class 4**
Class 1	0.84	0.89	0.93	1.13
Class 2	0.90	0.82	0.84	1.23
Class 3	0.98	0.86	0.70	1.26
Class 4	1.02	1.06	1.05	0.64

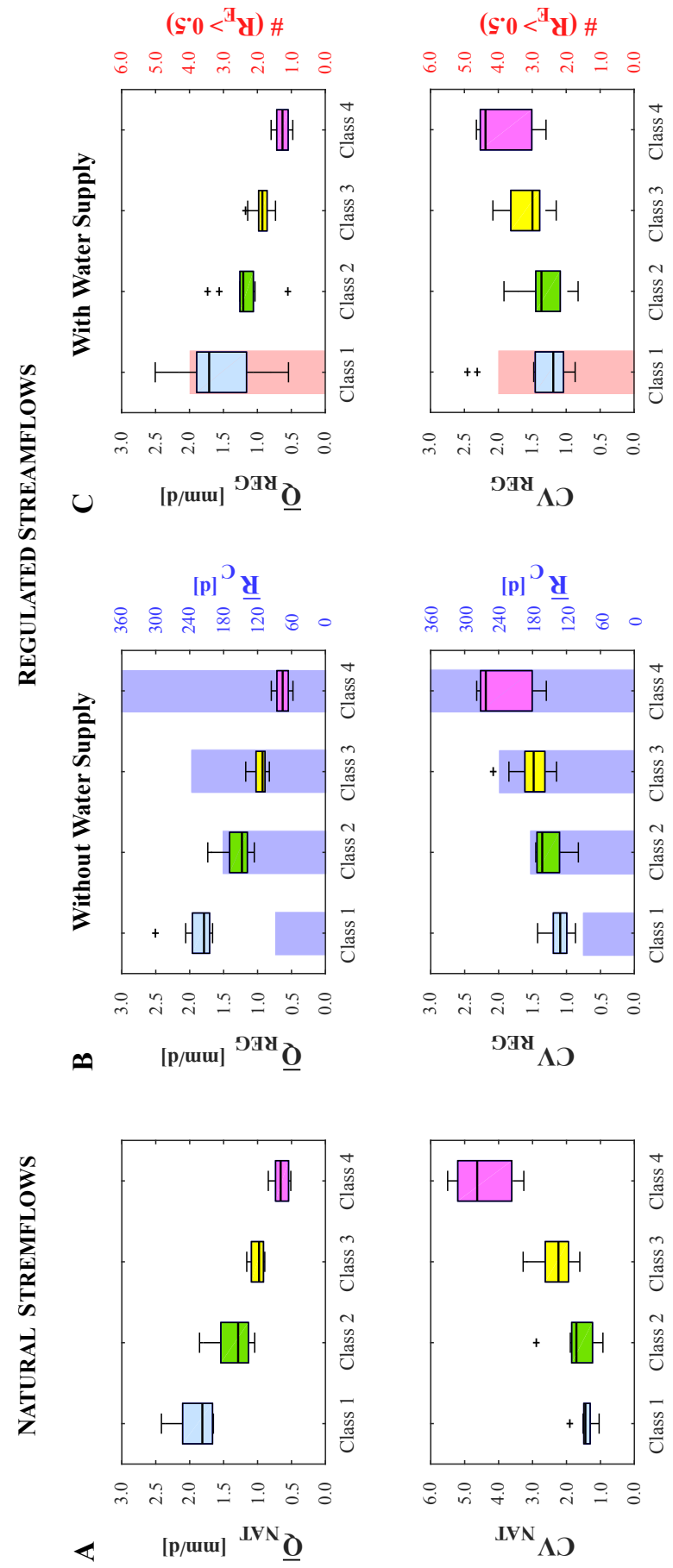

FIGURE 3.8: Annual behaviour of $\overline{Q}$ (top) and CV_Q (bottom) observed upstream (A) and downstream (B and C) of dams for each cluster. Plots B are obtained through the analysis of flow regimes downstream of flood control and multipurpose structures, while plots C show the ranges of $\overline{Q}$ and CV_Q obtained including reservoirs only operated for water supply. Note that blue bars in plots B indicate the average regulation capacity characterizing reservoirs of each class, while the red bar in plots C indicate the number of dams with a degree of exploitation higher than 0.5 (only class 1 is characterized by the presence of such structures). Note also that the scale of the Y-axis changes.

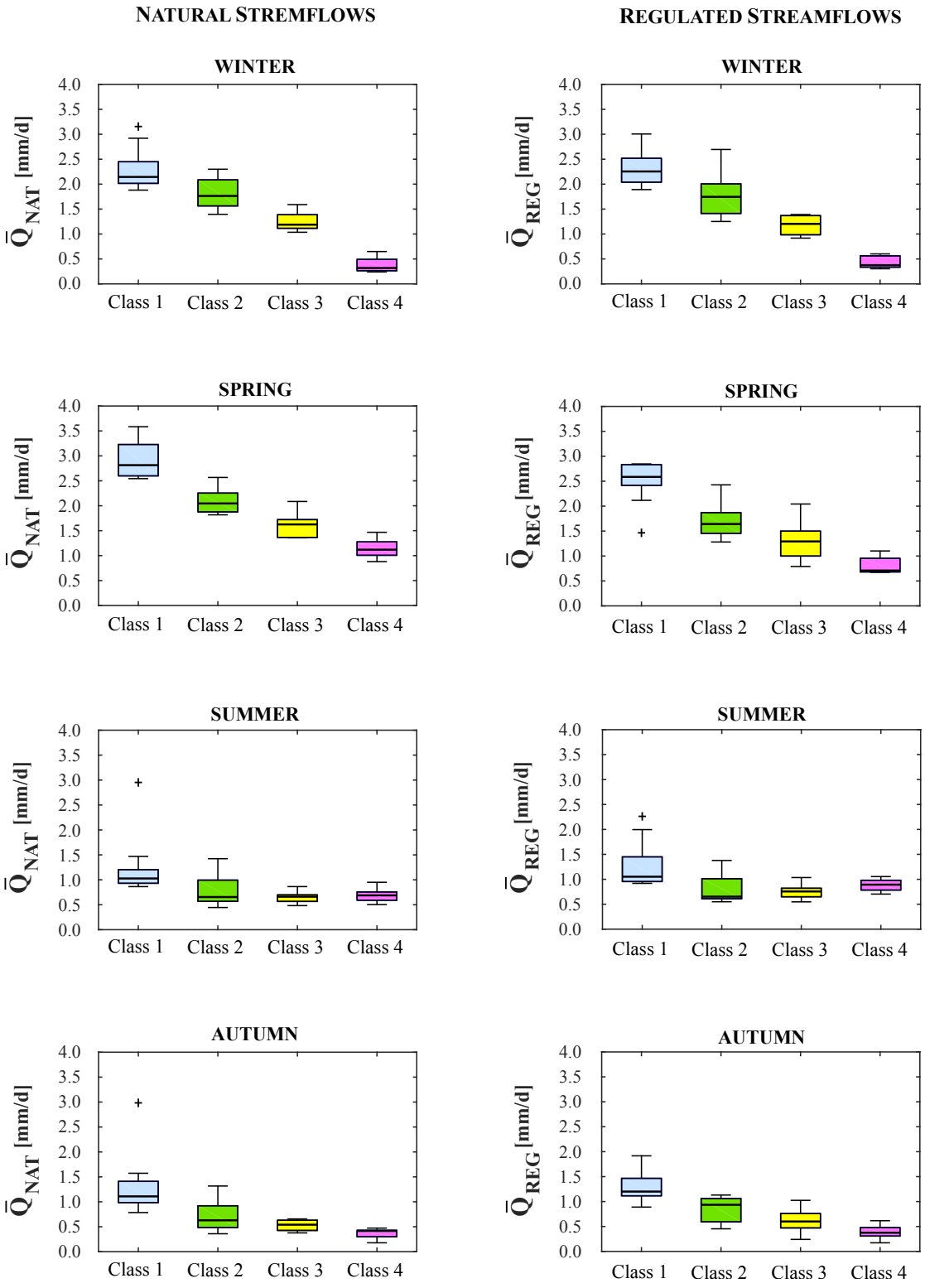

FIGURE 3.9: Seasonal behaviour of $\overline{Q}$ observed upstream (left) and downstream (right) of flood control and multipurpose structures for each cluster.

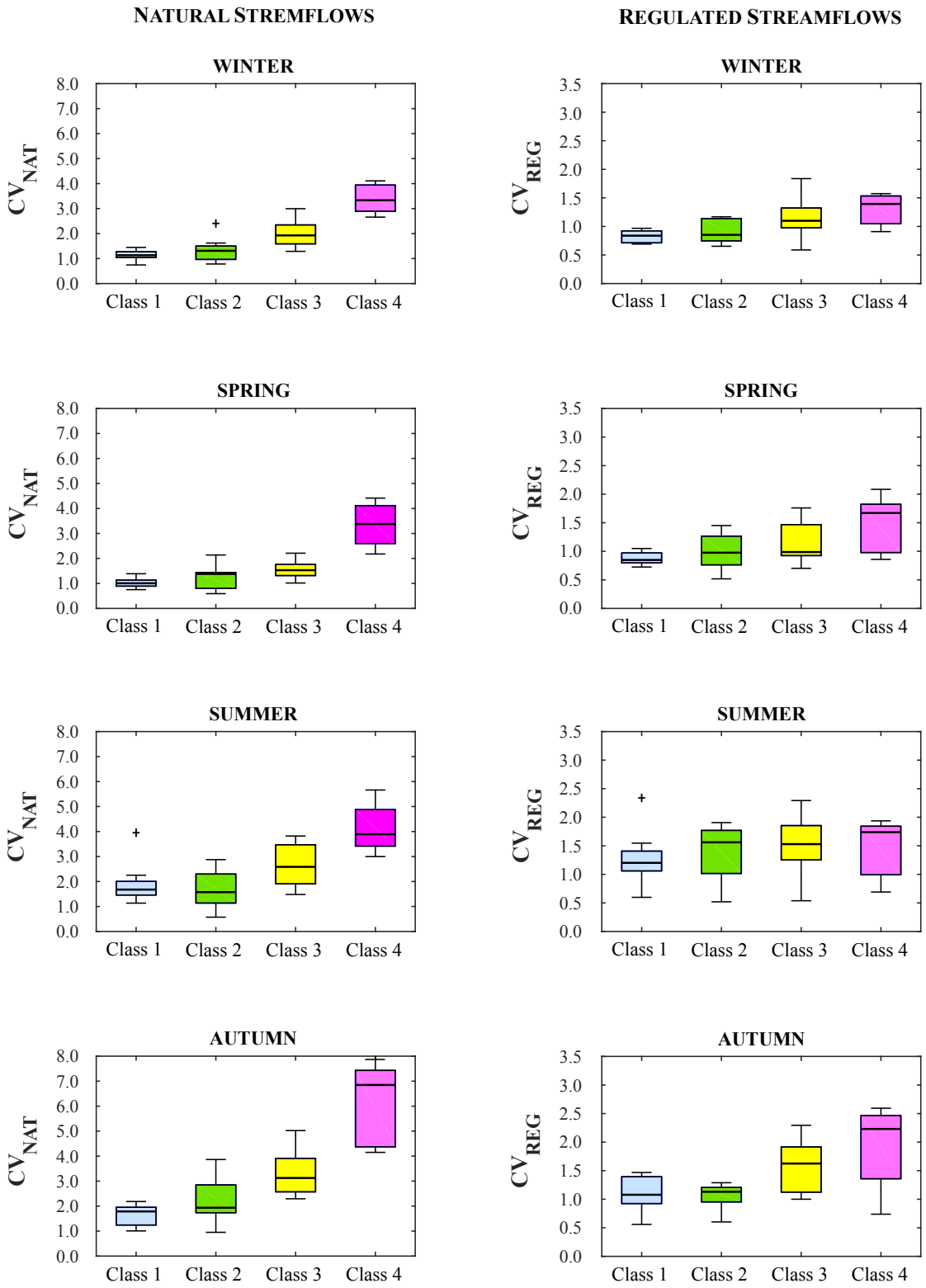

FIGURE 3.10: Seasonal behaviour of CV_Q observed upstream (left) and downstream (right) of flood control and multipurpose structures for each cluster. Note that the scale of the Y-axis changes.

3.4.4 Hydroclimatic fuctuations and inter-annual variability of regulated flow regimes

The analysis of temporal trajectories of river flow regimes reveals a significant within-catchment inter-annual variability in seasonal flow regimes of unregulated rivers. This is due to the ubiquitous fluctuations of hydroclimatic drivers. Inter-period changes of the probability associated to different flow intervals can vary significantly across flow magnitudes, indicating a heterogeneous sensitivity of various discharge levels to the underlying hydroclimatic fluctuations. In some cases, the inter-annual changes of $p(Q)$ are even comparable to the corresponding probability density (figure 3.1, *C*). However, the largest differences typically emerge from the comparison of hydrological regimes in unregulated and regulated reaches as a byproduct of dams operations (figure 3.1, *C* and *D*). Dams for flood control and hydropower production typically exert a small influence on the mean flow, but significantly decrease daily streamflow variability through flood lamination. Therefore, they homogenize regional flow dynamics (Graff [2006]; Poff et al. [2007]; Destouni et al. [2013]; Jaramillo and Destouni [2015]; see figure 2.10, *A*). On the other hand, reservoirs only operated to supply freshwater reduce the average discharge downstream proportionally to water withdrawals and, thus, usually increase the relative streamflow variability (see figure 2.10, *B*).

Figure 3.11 shows the frequency distribution of small flow variations in unregulated (blue) and regulated (red) reaches. The analysis of the low-flow stability reveals that variations of natural small flows are mainly concentrated between -0.05 and $+0.05$, a range of values comparable to the non-exceedance probability typically associated to Q^*, thus suggesting a poor ability of small flows to buffer inter-annual changes in climate and hydrologic properties (figure 3.11, blue bars). Additionally, the analysis indicates that low-flow stability is unlikely to be affected by regulation through dams, as observed variations of unregulated and regulated small flows exhibit very similar frequency distributions (figure 3.11, comparison between blue and red bars). Despite the heterogeneity of climate patterns, regime types and reservoir functions, this behaviour is observed ubiquitously throughout our representative selection of structures, without notable exceptions. This result can be explained as follows. River regulation through

dams typically obey to fixed time-invariant operating schemes, that have been developed based on the specific water uses of each reservoir. Accordingly, reservoirs can significantly impact the frequency distribution of discharge, but they are unlikely to mitigate the responsiveness of river flows to hydroclimatic fluctuations, that would require a self-adapting dynamic regulation strategies. Therefore, temporal patterns of regulated flow regimes across subsequent sub-periods are eventually governed by the inter-annual variability of flow regimes upstream of the dams.

Figure 3.12 shows the frequency distribution of the resilient discharges scaled to the mean flow, $\widetilde{Q} = Q_R/\overline{Q}$, upstream (blue) and downstream (red) of selected dams. The analysis of unregulated regimes reveals that resilient flows are typically lower than $\overline{Q}$, with the largest probabilities for $0.25\overline{Q} < Q_R < \overline{Q}$. With regard to regulated regimes, different classes of behaviour can be recognized, depending on the reservoir main use and regulation capacity, R_C (i.e., storage volume allocated to flood lamination scaled to the mean annual inflow). Resilient streamflows exhibit very similar frequency distributions upstream and downstream of flood control reservoirs with low regulation capacity (i.e., $R_C < 200\ d$). These structures can only store water during high flow events, producing more smoothed peaks in downstream reaches. Therefore, they are unlikely to alter the magnitude of resilient streamflows, Q_R, that are typically lower than the average discharge. Conversely, the magnitude of resilient flows increases in reservoirs with a high regulation capacity (i.e., $R_C > 300\ d$), as shown by the larger probabilities associated to high values of $\widetilde{Q}$ downstream of the Perry, Pomona, Pomme de Terre and Rathbun dams. This is due to the ability of these structures to support social and ecological requirements (i.e., irrigation, navigation, fish and wildlife preservation) by conveying water downstream during dry seasons, which is in turn related to their capacity to store water through time. Hence, the responsiveness of flows regimes to long-term changes in climate drivers is mitigated. Nevertheless, the largest differences between the PDFs of $Q_R/\overline{Q}$ upstream and downstream of the dam are observed in water supply dams. These differences are mainly attributable to the impact of regulation for water supply on the mean discharge $\overline{Q}$.

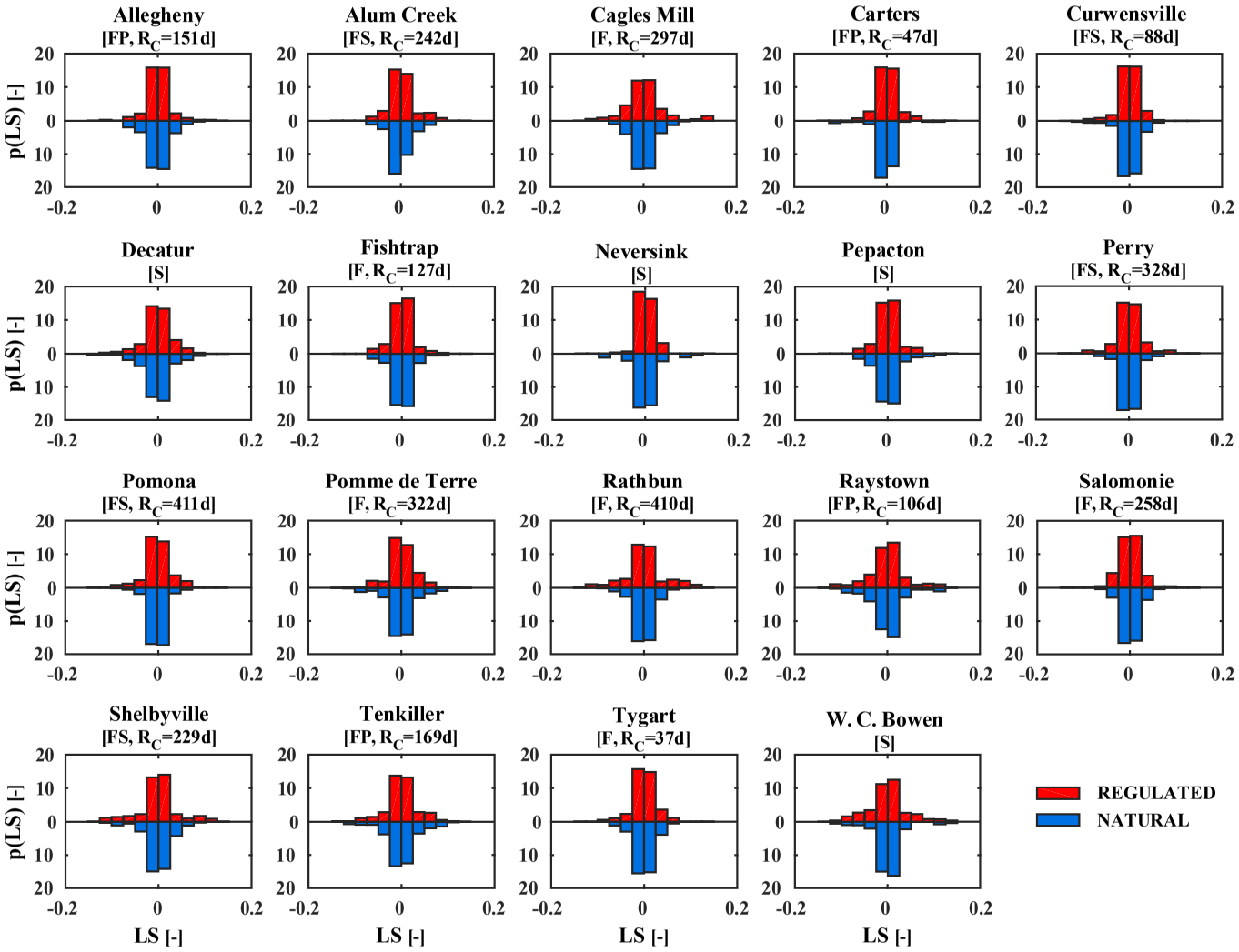

FIGURE 3.11: Upstream (blue) and downstream (red) PDFs of small flow variations for each dam. The header of each plot reports the name of the considered structure, major reservoir functions (nomenclature follows the rules explained in section 2.3) and, in case of flood control structure, the reservoir regulation capacity, R_C.

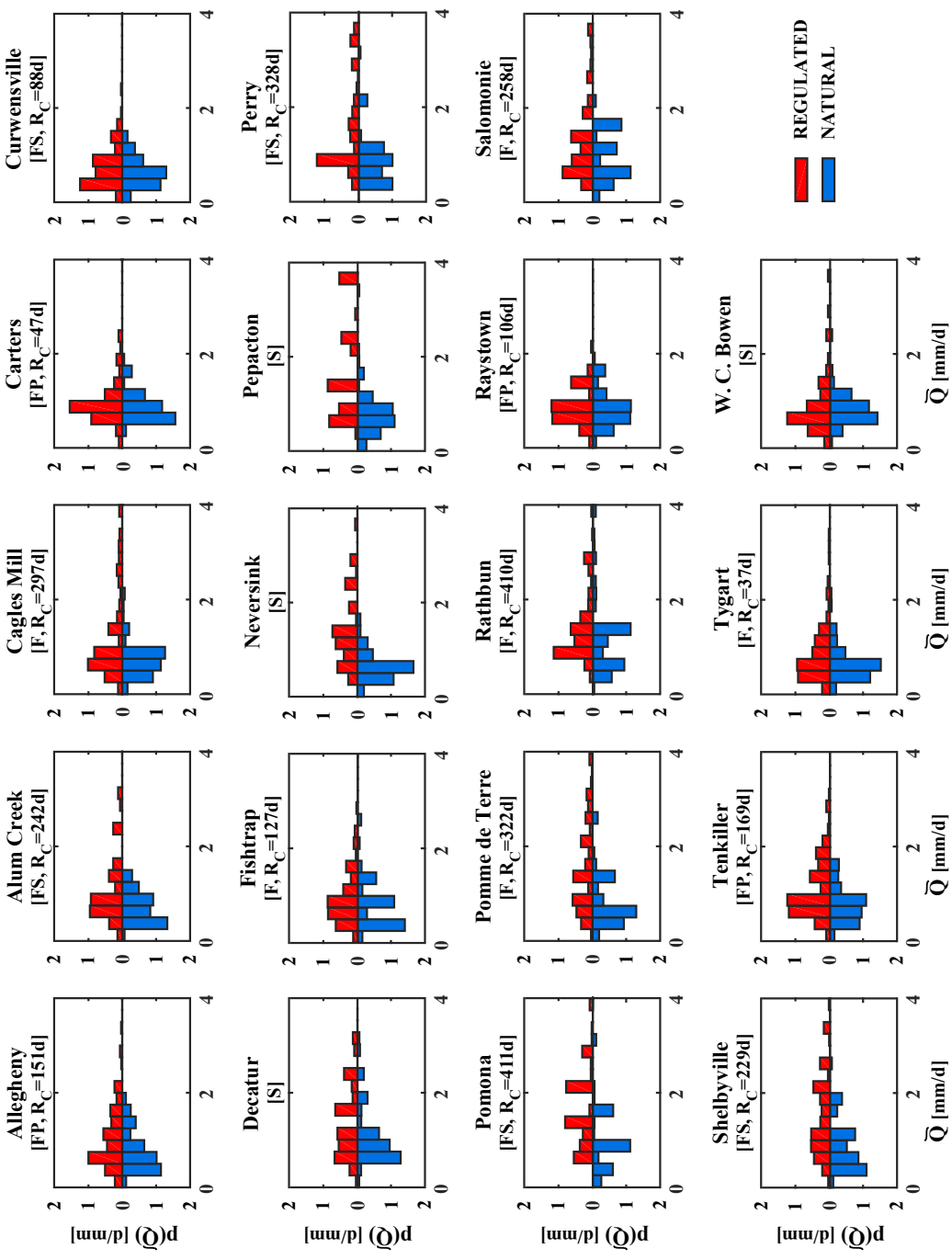

FIGURE 3.12: Upstream (blue) and downstream (red) PDFs of resilient flows, properly scaled to the mean discharge, $\widetilde{Q}$, for each dam. The header of each plot reports the name of the considered structure, major reservoir functions (nomenclature follows the rules explained in section 2.3) and, in case of flood control structure, the reservoir regulation capacity, R_C.

Figure 3.13 shows the upstream (blue) and downstream (red) average PDFs of small flow variations and $\widetilde{Q}$ across all sites. The similarity between the average frequency distribution of $\widetilde{Q}$ in unregulated and regulated reaches reveals that observed changes in $\widetilde{Q}$ across specific study sites are very mild. This is especially true in the light of the strong modifications induced by regulation on $p(Q)$.

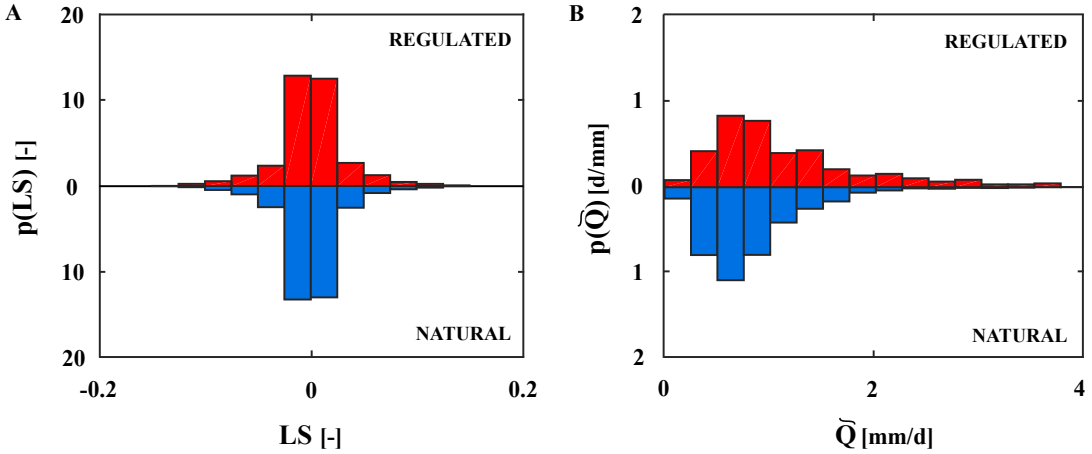

FIGURE 3.13: Impact of regulation across all study sites. (A) Upstream (blue) and downstream (red) average PDF of small flow variations. (B) Upstream (blue) and downstream (red) average PDF of resilient flows, properly scaled to the mean discharge.

Investigations on low flow stability and the magnitude of resilient flows allow a visual inspections of inter-period differences in streamflow probability, $\Delta p(Q)$, observed upstream and downstream of selected dams. Interestingly, inter-annual variability of climatic and hydrologic features appears responsible for shaping the changes in the frequencies of the entire spectrum of streamflows, as the shape of $\Delta p(Q)$ in regulated and unregulated reaches is very similar. Figures 3.14 and 3.15 report some examples of the observed behaviour. Note that regulation for flood control through high regulation capacity reservoirs slightly enhances observed differences in streamflow probability due to the uneven reduction of high flows and increase of low ones across contiguous sub-periods (figure 3.15, C and D). On the other side, a moderate smooth of $\Delta p(Q)$ is observed when regulation is performed to supply freshwater, as withdrawals for public supply can severely reduce the frequency associated to the large majority of flow ranges, with the exception of the smallest ones (figure 3.15, E and F).

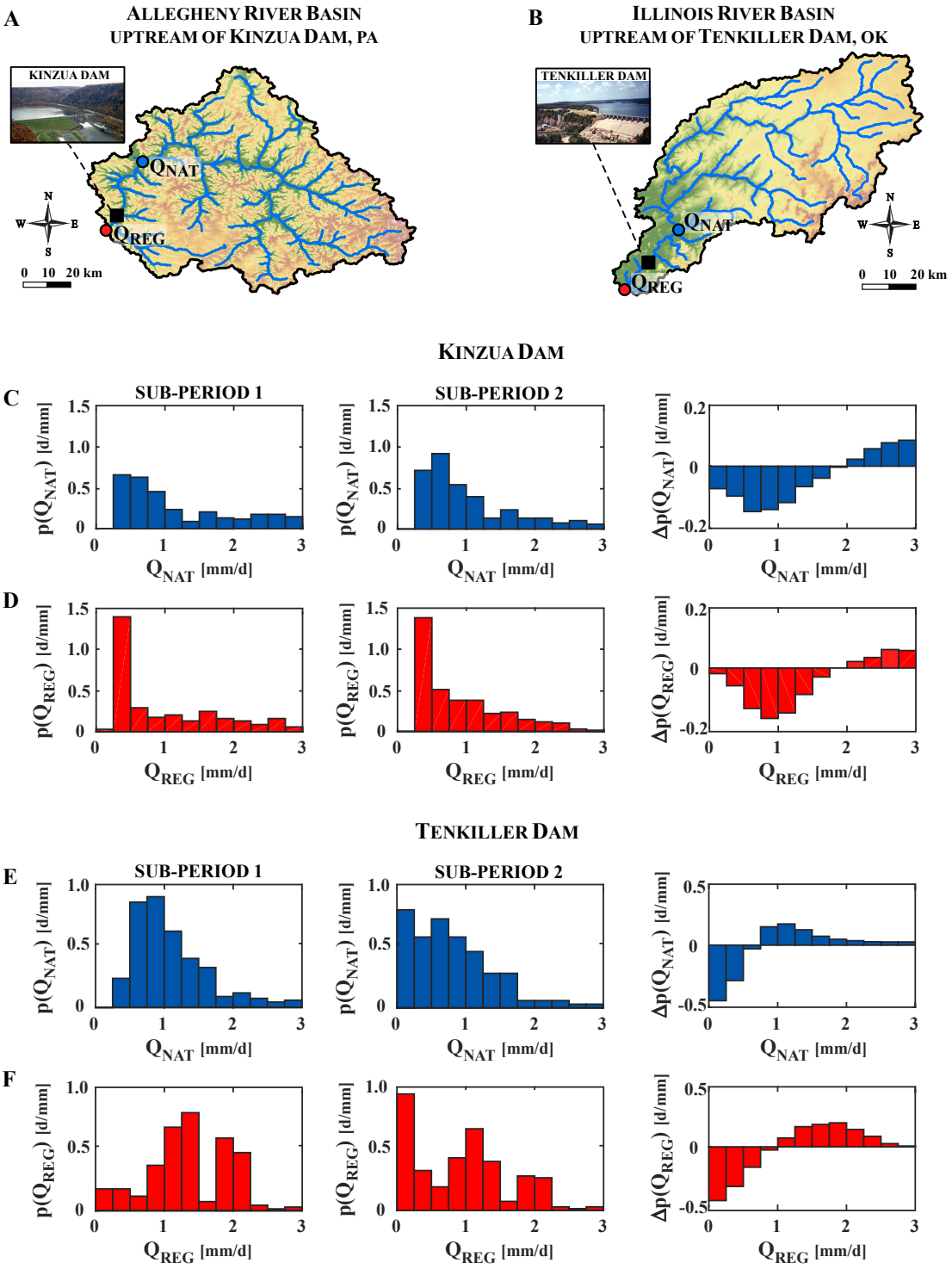

FIGURE 3.14: Typical behaviour of the inter-period differences in streamflow probability. (*A* and *B*) Selected study sites. (*C* and *D*) Changes in the spring flow regime of the Allegheny river upstream (*C*) and downstream (*D*) of Kinzua dam (R_C = 151d). (*E* and *F*) Changes in the spring flow regime of the Illinois river upstream (*E*) and downstream (*F*) of Tenkiller dam (R_C = 169d).

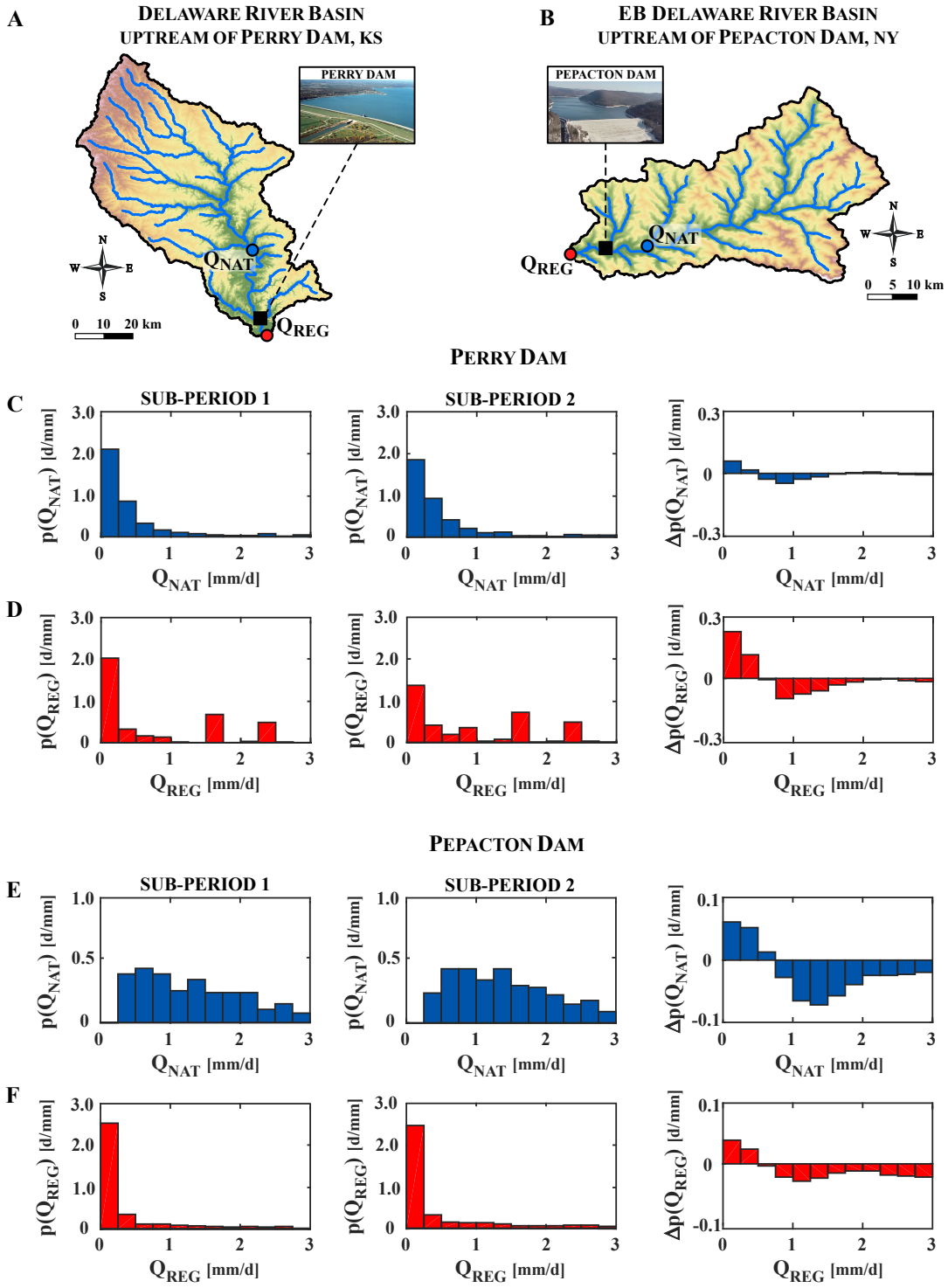

FIGURE 3.15: Typical behaviour of the inter-period differences in streamflow probability. (A and B) Selected study sites. (C and D) Changes in the spring flow regime of the Delaware river upstream (C) and downstream (D) of Perry dam, a high regulation capacity structure (R_C = 328d) primarily used for flood control. (E and F) Changes in the spring flow regime of the East Branch Delaware river upstream (E) and downstream (F) of Pepacton dam, a structure only used for water supply.

3.5 Discussion

Natural river flows upstream of reservoirs exhibit a remarkable spatial and temporal heterogeneity. Eastern catchments are characterized by abundant and weakly variable streamflows, particularly during winter and spring seasons, when many intermediate regimes ($CV_Q \approx 1$) are observed (see figure 3.7). Moving towards the Central US, water availability is reduced and hydrological variability is enhanced. Most catchments exhibit modest and highly variable river flows, and the highest variability is recorded in north-eastern Great Plains, especially during the summer and autumn seasons (see figure 3.7). These features of natural flow regimes turns out to result from the different climatic conditions observed throughout the Central-Eastern United States, here described by mean of four indexes: aridity index, ϕ, rainfall frequency, λ_P, precipitation timing, δ_P^*, and snowiness, f_S. Interestingly, climate signatures are still visible also in regulated flow regimes downstream of flood control and multipurpose structures, though catchments differences in daily streamflow variability are smoothed thanks to the ability of reservoirs to store water through time (i.e., R_C). Only strongly exploited water supply structures are able to partially conceal climate signatures in downstream reaches.

Nowadays, the identification of climatic controls on streamflows is an issue of great relevance as global climate change is affecting the hydrologic cycle, seriously endangering river ecosystems as well as anthropogenic water uses [Lettenmaier et al., 1994; Groisman et al., 2001; Milly et al., 2005]. In this context, the analysis of low flow stability and resilient streamflows offers important clues for an environmentally sustainable exploitation of running water downstream of dams. Low flows selectively influence anthropogenic water uses and ecological instream processes by triggering water withdrawals alongside rivers, and promoting the development of habitats and food availability in riverine ecosystems [Resh et al., 1988; Lazzaro et al., 2013; Vezza et al., 2014; Fabris et al., 2017, 2018]. Resilient flows buffer long-term landscape and climate changes, thus providing a basis to preserve the functioning of hydraulic infrastructures by accommodating inter-annual and long-term hydrological variability. The analysis points out that the inter-annual variability of climatic and hydrologic features controls the long-term

fluctuations of LS and Q_R (figures 3.11 and 3.12), and that, more generally, it modulates the changes in the frequencies of the entire spectrum of discharges experienced by a river. In fact, inter-period differences of the streamflow PDF, $\Delta p(Q)$, display a very similar behaviour upstream and downstream of each dam, in spite of the major changes of $p(Q)$ implied by river regulation. These findings strengthen the idea that dams are unlikely to mitigate the sensitivity of flow regimes to hydroclimatic fluctuations in the entire spectrum of streamflows, due to the lack of self-adapting operating schemes.

River flow regimes are becoming increasingly unsteady in the long-term, and the likelihood of floods and droughts is raising in many region of the world [Easterling et al., 2000; Groisman et al., 2004; IPCC, 2014; NCA, 2014; Mallakpour and Villarini, 2015]. Dams offer the possibility to mitigate the risk induced by hydroclimatic fluctuations, providing a storage that promotes the anthropogenic exploitation of running water [Watts et al., 2011; Ehsani et al., 2017]. Nevertheless, reservoirs as they are currently operated prove to be unlikely to enhance the long-term temporal stability of flow regimes in downstream reaches, as patterns of regulated flow regimes are eventually controlled by the upstream variability of unregulated streamflows. In this context, to improve the reliability of climate models appears as a powerful tool for water resources management [Finger et al., 2012; Majone et al., 2012, 2016], allowing for the implementation of dynamic regulation strategies, in which inter-annual operating schemes are re-adjust according to the observed patterns of majors hydroclimatic forcings. The coarse spatial resolution typical of climate models might be overcome through a similarity framework of the type presented in this chapter (e.g., identifying spatial patterns in the relation between climate and river flow regimes). Since climate signatures are visible in unregulated reaches as well as in a large number of regulated ones, this would be possible for both isolated structures and reservoir systems (i.e., structures built in cascade), though particular attention should be paid to the reservoir main function and regulation capacity. Reservoir release deriving by a dynamic regulation of inflows should support the future sustainability of anthropogenic water uses, as well as ecosystem processes, both impacted by patterns of temporal variations in river flows [Milly et al., 2008; Richter et al., 1996; Poff et al., 1997; Lytle and Poff, 2004]. Note that maintaining key ecological functions while regulating river flows is now possible as the natural flow regime paradigm is making

way for the designer flow concept, a multi-objective strategy that aims at defining the hydrologic condition (which may be different from that observed in natural reaches) able to reduce the trade-off between freshwater conservation and human needs [Poff et al., 2015; Chen and Olden, 2017]. This would represent a remarkable step forward for future water resources management.

Chapter 4

Conclusions

This thesis has analyzed the impact of dams on river flow regimes. On account of the growing pressure on freshwater resources, originated by the current increase of global water demand and climate change, this work was built around two main goals. The first aim is to disclose the hidden connection between reservoir functions and the features of downstream flow regimes modifications by dams. The second is to provide a clear understanding on whether climate signatures are still visible downstream of dams and whether this is dependent on water uses. In doing that, particular emphasis is placed on the characterization of the impact of reservoirs on the response of regulated regimes to inter-annual fluctuations of climate and hydrologic properties. The following conclusions are worth emphasizing:

- Reservoirs devoted to flood control and water supply produce distinctive impacts on flow regimes. Dams for flood control produce a negligible impact on mean water availability, but reduce the intra-seasonal variability of river flows during all seasons and, thus, lower regional-scale differences typical of unregulated regimes. The extent of such effect is modulated by the ability of reservoirs to store water through time, termed regulation capacity: the higher the regulation capacity, the more enhanced the reduction of CV_Q. On the other hand, water supply reservoirs reduce the mean seasonal discharge proportionally to the relative amount of water withdrawn and, concurrently, increase the downstream relative streamflow variability, promoting the differentiation of regulated flow regimes at the regional scale. This effect is particularly enhanced in cases where the amount of water withdrawn is significant and during winter and spring seasons, when the lower variability of

natural flows conceals the unavoidable effect of flood lamination through dams. Accordingly, the reduction of streamflow variability induced by flood control decreases by 30% when reservoirs are used for multiple purposes, including supply freshwater. This is due to the distinctive, compensatory effect of water supply, that partly counterbalance the decrease of flow variability typical of flood control dams;

- A remarkable correlation exists between natural flow regimes and climatic conditions. Clustering of catchments based on climatic indexes shows important hydrological similarities also in terms of regulated river flows. Accordingly, climatic signatures appear to be largely visible also in regulated reaches, despite the significant alterations of flow regimes due to river regulation. This is especially true downstream of flood control and multipurpose structures, though inter-catchment differences in streamflow variability are smoothed due to the homogenization of regional flow dynamics promoted by flood control operations. Conversely, strongly exploited water supply dams slightly alter the climate-dependent nature of flows in downstream reaches;

- The identification of climatic controls on river flows is noteworthy as global climate change is affecting the hydrologic cycle, producing increasing streamflow fluctuations and seriously endangering the anthropogenic exploitation of running water. Reservoirs are unlikely to alter streamflow stability and the magnitude of resilient flows, and temporal patterns of regulated flow regimes are eventually governed by the inter-annual variability of unregulated streamflows upstream of dams. Accordingly, reservoirs appear to obey to fixed time-invariant operating schemes, only driven by the specific water use of each structure.

The findings here presented have major consequences. First, the current increase of water demand might generate a possible shift in the cumulative effect of dams at regional and global scales. On one hand, enhancing the water supply function of multipurpose dams might potentially compensate the impact of flood control, thereby leading to smoothed alterations of streamflow variability. On the other hand, the massive construction of new dams operated mainly for water supply might generate more heterogeneous

and variable flow regimes in the future. Second, the current increase of streamflow fluctuations might be smoothed downstream of dams by implementing dynamic regulation strategies, in which inter-annual operating schemes comply with the observed patterns of majors hydroclimatic forcings. This could be done by improving the reliability of climate models, in case of isolated structures as well as for reservoir systems.
These findings represent a critical step forward for scientist and water managers, and may offer important clues for the sustainable exploitation of water infrastructures in a context of changing climate and increasing freshwater exploitation. This is particularly true in regions where signs of water scarcity have already appeared, as well as in tropical regions, where rainfall is unevenly distributed in space and time, and massive infrastructures are needed to guarantee human exploitation of water resources.

Future research should be devoted to extend the presented study to Central-Western United States, a region which is not yet included due to the low reliability of the physically-based model for $p(Q)$ in arid and snow-dominated regions. In this way, it would be possible to include the analysis of the downstream impact of dams used for irrigation withdrawals, which are mainly located in Central-Western US. Moreover, the variety of hydro-climatic settings found in this region would significantly enforce the analysis on the interaction of climate variability and dam operations in controlling the inter-annual variability in regulated reaches.

Bibliography

Abatzoglou, J., Barbero, R., and Wolf, J. W. Tracking Interannual Streamflow Variability with Drought Indices in the U.S. Pacific Northwest. *J Hydrometeorol*, 15: 1900–1912, 2014.

Allan, D. W. Statistics of atomic frequency standards. *Proceedings of the IEEE*, 54(2): 221–230, 1966.

Ashley, R. and Cashman, A. Infrastructure to 2030: telecom, land transport, water and electricity. Technical report, Organization for Economic Cooperation and Development, Paris, 2006.

Asnar, A., Flyvbjerg, B., Budzier, A., and Lunn, D. Should we build more large dams? The actual costs of hydropower megaproject development. *Energy Polic*, 69:43–56, 2014.

Baldingo, B. P. and Schuler, K., G. E. Riva-Murray. Mussel community composition in relation to macrohabitat, water quality, and impoundments in the Neversink river, New York. Technical report, United States Geological Survey (USGS), 2002.

Barnett, T. P., Pierce, D. W., Hidalgo, H. G., Bonfils, C., Santer, B. D., Das, T., Bala, G., Wood, A. W., Nozawa, T., Mirin, A. A., Cayan, D. R., and Dettinger, M. D. Human-induced changes in the hydrology of the western United States. *Science*, 319 (5866):1080–1083, 2008.

Berghuijs, W. R., Sivapalan, M., Woods, R. A., and Savenjie, H. H. G. Patterns of similarity of seasonal water balances: a window into streamflow variability over a range of time scales. *Water Resour Res*, 50(7):5638–5661, 2014.

Biswal, B. and Marani, M. Geomorphological origin of recession curves. *Geophys Res Lett*, 37(24):L24403, 2010.

Biswal, B. and Marani, M. Universal recession curves and their geomorphological interpretation. *Adv Water Res*, 65:34–42, 2014.

Biswal, B. and Nagesh Kumar, D. A general geomorphological recession flow model for river basins. *Water Resour Res*, 49(8):4900–4906, 2013.

Botter, G. Flow regime shifts in the Little Piney creek. *Adv Water Resour*, 71:44–54, 2014.

Botter, G., Porporato, A., Rodriguez-Iturbe, I., and Rinaldo, A. Basin-scale soil moisture dynamics and the probabilistic characterization of carrier hydrologic flows: slow leaching-prone components and of the hydrologic response. *Water Resour Res*, 43(2): W02417, 2007.

Botter, G., Porporato, A., Rodriguez-Iturbe, I., and Rinaldo, A. Non-linear storage discharge relations and catchment streamflow regimes. *Water Resour Res*, 45(10): W10427, 2009.

Botter, G., Basso, S., Porporato, A., Rodriguez-Iturbe, I., and Rinaldo, A. Natural streamflow regime alterations: damming of the Piave river basin (Italy). *Water Resour Res*, 46(6):W06522, 2010.

Botter, G., Basso, S., Rodriguez-Iturbe, I., and Rinaldo, A. Resilience of river flow regimes. *Proc Natl Acad Sci USA*, 110(32):12925–12930, 2013.

Budiko, M. I. *Climate and life*. Academic Press, 1974.

Carey, S. K., Tetzlaff, D., Seibert, J., Soulsby, C., Buttle, J., Laudon, H., McDonnell, J., McGuire, K., Caissie, D., Shanley, J., Kennedy, M., Devito, K., and Pomeroy, J. W. Inter-comparison of hydro-climatic regimes across northern catchments: synchronicity, resistance and resilience. *Hydrol Process*, 24:3591–3602, 2010.

Carmona, A. M., Sivapalan, M., Yaeger, M. A., and G., P. Regional patterns of interannual variability of catchment water balances across the continental U.S.: A Budyko framework. *Water Resour Res*, 50(12):9177–9193, 2014.

Chen, W. and Olden, J. D. Designing flows to resolve human and environmental water needs in a dam-regulated river. *Nat Commun*, 8:2158, 2017.

Chezik, K. A., Anderson, S. C., and Moore, J. W. River networks dampen long-term hydrological signals of climate change. *Geophys Res Lett*, 44:7256–7264, 2010.

Coopersmith, E., Yaeger, M. A., Ye, S., Cheng, L., and Sivapalan, M. Exploring the physical controls of regional patterns of flow duration curves - Part 3: a catchment classification system based on regime curves indicators. *Hydrol Earth Syst Sci*, 16(11): 4467–4482, 2012.

Cowell, C. M. and Stoudt, R. T. Dam induced modifications to upper Allegheny river streamflow patterns and their biodiversity implications. *JAWRA*, 38(1):87–96, 2002.

Dai, A. Increasing drought under global warming in observations and models. *Nat Clim Change*, 3:52–58, 2013.

Destouni, G., Jaramillo, F., and Prieto, C. Hydroclimatic shifts driven by human water use for food and energy production. *Nat Clim Change*, 3(3):213–217, 2013.

Dewson, Z. S., James, A. B. W., and Death, R. G. Stream ecosystems functioning under reduced flow conditions. *Ecological Applications*, 17(6):1797–1808, 2007.

D'Odorico, P., Ridolfi, L., Porporato, A., and Rodriguez-Iturbe, I. Preferential states of seasonal soil moisture: the impact of climate fluctuations. *Water Resour Res*, 36: 2209–2219, 2000.

Döll, P., Fiedler, K., and Zhang, J. Global-scale analysis of river flow alterations due to water withdrawals and reservoirs. *Hydrol Earth Syst Sci*, 13(12):2413–2432, 2009.

Dooge, J. C. I. Hydrologic models and climate change. *J Geophys Res*, 97(D3):2677–2686, 1992.

Doulatyari, B., Betterle, A., Basso, S., Biswal, B., Shirmer, M., and Botter, G. Predicting streamflow distributions and flow duration curves from landscape and climate. *Adv Water Res*, 83:285–298, 2015.

Doulatyari, B., Betterle, A., Radny, D., Celegon, E. A., Fanton, P., Schirmer, M., and Botter, G. Patterns of streamflow regimes along the river network: the case of the Thur river. *Environmental Modeling & Software*, 93:42–58, 2017.

Doyle, M. W., Stanley, E. H., Straier, D. L., Jacobson, R. B., and Schmidt, J. C. Effective discharge analysis of ecological processes in streams. *Water Resour Res*, 41 (11):W11411, 2005.

Dunne, T. and Leopold, L. B. *Water in environmental planning*. W.H.Freeman and Co Ltd, 1978.

Easterling, D. R., Meehl, G. A., Parmesan, C., Changnon, S. A., Karl, T. R., and Mearns, L. O. Climate extremes: observations, modeling, and impacts. *Science*, 288: 2068–2074, 2000.

Ehsani, N., Vörösmarty, C. J., Fekete, B. M., and Stakhiv, E. Z. Reservoirs operation under climate change: storage capacity options to mitigate risk. *Journal of Hydrology*, 555:435–446, 2017.

Fabris, L., Malcolm, I. A., Buddendorf, W. B., Millidine, K. J., Tetzlaff, D., and Soulsby, C. Hydraulic modelling of the spatial and temporal variability in Atlantic salmon parr habitat availability in an upland stream. *Sci Total Environ*, 601:1046–1059, 2017.

Fabris, L., Lazzaro, G., Buddendorf, W. B., Botter, G., and Soulsby, C. A general analytical approach for assessing the effects of hydroclimatic variability on fish habitat. *Journal of Hydrology*, 566:520–530, 2018.

Ficklin, D. L., Robeson, S. M., and Knouft, J. H. Impacts of recent climate change on trends in baseflow and stormflow in United States watersheds. *Geophys Res Lett*, 43 (10):5079–5088, 2016.

Ficklin, D. L., Abatzoglou, J. T., Robeson, S. M., Null, S. E., and Knouft, J. H. Natural and managed watersheds show similar responses to recent climate change. *Proc Natl Acad Sci USA*, 115(34):8553–8557, 2018.

Field, C., Barros, V., Dokken, D., Mach, K., Mastrandrea, M., Bilir, T., Chatterjee, M., Ebi, K., Estrada, Y., Genova, R., Girma, B., Kissel, E., Levy, A., MacCracken, S., Mastrandrea, P., and White, L. e. *Climate change 2014: impacts, adaptation, and vulnerability*. Cambridge University Press, 2014.

Finger, D., Heinrich, G., Gobiet, A., and Bauder, A. Projections of future water resources and their uncertainty in a glacierized catchment in the Swiss Alps and the subsequent effects on hydropower production during the 21st century. *Water Resour Res*, 48(2):W02521, 2012.

Fitzhugh, T. W. and Richter, B. D. Quenching urban thirst: growing cities and their impacts on freshwater ecosystems. *BioScience*, 54(8):741–754, 2004.

Gleick, P. H. The changing water paradigm: a look at twenty-first century water resources development. *Water International*, 25(1):127–138, 2000.

Graff, W. L. Dam nation: a geographic census of American dams and their large-scale hydrologic impacts. *Water Resour Res*, 35(4):1305–1311, 1999.

Graff, W. L. Downstream hydrologic and geomorphologic effects of large dams on American rivers. *Geomorphology*, 79(3–4):336–360, 2006.

Groisman, P. Y., Knight, R. W., and Karl, T. R. Heavy precipitation and high streamflow in the contiguous United States: trend in the twentieth century. *Bull Am Meteorol Soc*, 82:219–246, 2001.

Groisman, P. Y., Knight, R. W., Karl, T. R., Easterling, D. R., Sun, B., and Lawrimore, J. H. Contemporary changes of the hydrological cycle over the contiguous United States: trends derived from in situ observations. *J. Hydrometeorol.*, 5:64–85, 2004.

Harman, W. N. the effect of reservoirs construction and canalization on the mollusks of the upper Delaware watershed. *Bulletin Am Malac Union*, 39:12–14, 1974.

ICOLD. Annual Meeting of International Commission on Large Dams: final bulletin. Technical report, International Commission on Large Dams, 2014.

IPCC. *Climate Change 2014: Synthesis Report. Contribution of Working Groups I, II and III to the Fifth Assessment Report of the Intergovernmental Panel on Climate Change [Core Writing Team, R.K. Pachauri and L.A. Meyer (eds.)].* IPCC, Geneva, Switzerland, 2014.

Jaramillo, F. and Destouni, G. Local flow regulation and irrigation raise global human water consumption and footprint. *Science*, 350(6265):1248–1251, 2015.

Katul, G. G. and Parlange, M. B. Analysis of land surface heat fluxes using the orthonormal wavelet approach. *Water Resour Res*, 31(11):2743–2749, 1995.

Kirchner, J. W. Catchments as simple dynamical systems: Catchment characterization, rainfall-runoff modeling, and doing hydrology backward. *Water Resour Res*, 45(2): W02429, 2009.

Kirchner, J. W. and Neal, C. Universal fractal scaling in stream chemistry and its implications for solute transport and water quality trend detection. *Proc Natl Acad Sci USA*, 110(30):12213–12218, 2013.

Kundzewicz, Z. W., Mata, L. J., Arnell, N. W., Döll, P., Jimenez, B., Miller, K., Oki, T., ŞEN, Z., and Shiklomanov, I. The implications of projected climate change for freshwater resources and their management. *Hydrological Sciences Journal*, 53:3–10, 2008.

Laio, F., Porporato, A., Ridolfi, L., and Rodriguez-Iturbe, I. Plants in water-controlled ecosystems: active role in hydrologic processes and response to water stress. ii probabilistic soil moisture dynamics. *Adv Water Res*, 24(7):703–723, 2001.

Lazzaro, G., Basso, S., Schirmer, M., and Botter, G. Water management strategies for run-of-river power plant: profitability and hydrologic impact between the intake and the outflow. *Water Resour Res*, 49(12):WR014210, 2013.

Lebel, L., Garden, P., and Imamura, M. The politics of scale, position, and place in the governance of water resources in the Mekong region. *Ecology and Society*, 10(2):18, 2005.

Lehener, B., Liermann, C. R., Revenga, C., Vörösmarty, C., Fekete, B., Crouzet, P., Döll, P., Endejan, M., Frenken, K., Magome, J., Nillson, C., Robertson, J. C., Rodel, R., Sindorf, N., and Wisser, D. High-resolution mapping of the world's reservoirs and dams for sustainable river-flow management. *Front Ecol Environ*, 9(9):494–502, 2011.

Lettenmaier, D. P., Wood, E. F., and Wallis, J. R. Hydro-climatological trends in the continenetal United States, 1948-88. *Journal of Climate*, 7:586–607, 1994.

Lytle, D. H. and Poff, N. L. Adaptation to natural flow regimes. *Trends in Ecology and Evolution*, 19:94–100, 2004.

MacDonald, G. M. Water, climate change and sustainability in the southwest. *Proc Natl Acad Sci USA*, 107:21256–21262, 2010.

Magilligan, F. J. and Nislow, K. H. Changes in hydrologic regimes by dams. *Geomorphology*, 71(1–2):61–78, 2005.

Magilligan, F. J., Nislow, K. H., and Graber, B. E. Scale-indipendent assessment of discharge reduction and riparian disconnectivity following flow regulation by dams. *Geology*, 31(7):569–572, 2003.

Majone, B., Bovolo, C. I., Bellin, A., Blenkinsop, S., and Fowler, H. J. Modeling the impacts of future climate change on water resources for the Gállego river basin (Spain). *Water Resour Res*, 48(1):WR0120985, 2012.

Majone, B., Villa, F., Deidda, R., and Bellin, A. Impact of climate change and water use policies on hydropower potential in the south-eastern Alpine region. *Science of Total Environment*, 543:965–980, 2016.

Mallakpour, I. and Villarini, G. The changing nature of flooding across the central United States. *Nat Clim Change*, 5:250–254, 2015.

Milly, P. C. D. An analytic solution of the stochastic storage problem applicable to soil water. *Water Resour Res*, 29(11):3755–3758, 1993.

Milly, P. C. D. Climate, soil water storage, and the average annula water balance. *Water Resour Res*, 30(7):2143–2156, 1994.

Milly, P. C. D. and Dunne, K. A. Macroscale water fluxes 2. Water and energy supply control of their inter-annual variability. *Water Resour Res*, 38(10):WR000760, 2002.

Milly, P. C. D., Dunne, K. A., and Vecchia, A. V. Global pattern of trends in streamflow and water availability in a changing climate. *Nature*, 438(7066):347–350, 2005.

Milly, P. C. D., Betancourt, J., Fankelmark, M., Hirsch, R. M., Kundzewicz, Z. W., Lettenmaier, D. P., and Stouffer, R. J. Stationarity is dead: whither water management? *Science*, 319:573–574, 2008.

Moriasi, D. N., Arnold, J. G., Van Liew, M. W., Bingner, L. R., Harmel, R. D., and Veith, T. L. Model evaluation guidelines for systematic quantification of accuracy in watershed simulations. *Trans ASABE*, 50(3):885–900, 2007.

Moyle, P. B. and Mount, J. F. Homogenous rivers, homogenous faunas. *Proc Natl Acad Sci*, 104(14):5711–5712, 2007.

Müller, M. F. and Levy, M. C. Complementary vantage points: integrating hydrology and economics for sociohydrologic knowledge generation. *Water Resour Res*, Submitted.

Müller, M. F., Dralle, D. N., and Thompson, S. E. Analytical model for flow duration curves in seasonallydry climates. *Water Resour Res*, 50(7):5510–5531, 2014.

NCA. *Climate change impact in the United States: the third national climate assessment.* U.S. Global Change Research Program, 2014.

NRC. *Global change and extreme hydrology: testing conventional wisdom.* The National Academies Press, Washington, D.C., 2011.

Olden, J. D. and Poff, N. L. Redundancy and the choice of hydrologic indices for characterizing streamflow regimes. *River Res Applic*, 19(2):101–121, 2003.

O'Neill, P. L., Nicolaides, D., Honnery, D., and Soria, J. Autocorrelation functions and the determination of integral length with reference to experimental and numerical data. In *Proceedings of the Fifteenth Australasian Fluid Mechanics Conference*, volume 1, pages CD–ROM. University of Sydney, 2004.

Patterson, L. A., Lutz, B., and Doyle, M. W. Streamflow changes in the South Atlantic United States during the mid and late 20th centur. *J Am Water Resour Assoc*, 8: 1126–1138, 2012.

Patterson, L. A., Lutz, B., and Doyle, M. W. Climate and direct human contributions to changes in mean annual streamflow in the South Atlantic, USA. *Water Resour Res*, 49:7278–7291, 2013.

Petchey, O. L., Gonzalez, A., and Wilson, H. B. Effects on population persistence: the interaction between environmental noise colour, intraspecific competition and space. *Proc R Soc Lond B*, 264(1389):1841–1847, 1997.

Petts, G. E. Complex response of river channel morphology subsequent to reservoir construction. *Progress in Physical Geography*, 3(3):329–362, 1979.

Petts, G. E. *Impounded rivers: perspectives for ecological management.* Chichester, John Wiley, 1994.

Pike, J. G. The estimation of annual runoff from metereological data in a tropical climate. *J Hydrol*, 2(2):116–123, 1964.

Poff, N. L., Allan, J. D., Bain, M. B., Karr, J. R., Prestegaard, K. L., Richter, B. D., Sparks, R. E., and Stromberg, J. C. The natural flow regime: a paradigm for river conservation and restoration. *BioScience*, 47(11):769–784, 1997.

Poff, N. L., Olden, J. D., Merritt, D. M., and Pepin, D. M. Homogenization of regional river dynamics by dams and global biodiversity implications. *Proc Natl Acad Sci USA*, 104(14):5732–5737, 2007.

Poff, N. L., Brown, C. M., Grantham, T. E., Matthews, J. H., Palmer, M. A., Spence, C. M., Wilby, R. L., Haasnoot, M., Mendoza, G. F., Dominique, K. C., and Baeza, A. Sustainable water management under future uncertainties with eco-engineering decision scaling. *Nat Clim Change*, 6:25–34, 2015.

Porporato, A. and Ridolfi, L. Detecting determinism and non-linearity in river flow time series. *Hydrological Sciences Journal*, 48(5):763–780, 2003.

Porporato, A., Daly, E., and Rodriguez-Iturbe, I. Soil water balance and ecosystem response to climate change. *Am Nat*, 164(5):625–632, 2004.

Porporato, A., Vico, G., and Fay, A. Superstatistics of hydroclimatic fluctuations and interannual ecosystems productivity. *Geophys Res Lett*, 33:L15402, 2006.

Potter, N. J., Zhang, L., Milly, P. C. D., McMahon, T. A., and Jakeman, A. J. Effects of rainfall seasonality and soil moisture capacity on mean annual water balance for Australian catchments. *Water Resour Res*, 41(6):W06007, 2005.

Resh, V. H., Brown, A. V., Covich, A. P., Gurtz, M. E., Li, H. W., Minshall, G. W., Reice, S. R., Sheldon, A. L., Wallace, J. B., and Wissnar, R. C. The role of disturbance in stream ecology. *Journal of the North American Benthological Society*, 7:433–455, 1988.

Richter, B. D., Baumgartner, J. V., Powell, J., and Braun, D. P. A method for assessing hydrological alterations within ecosystems. *Conservation Biology*, 10:1–12, 1996.

Riley, W. J. *Handbook of frequency stability analysis.* NIST Special Publication, 2008.

Sabo, J. L. and Post, D. M. Quantifying periodic, stochastic, and catastrophic environmental variation. *Ecological Monographs*, 78(1):19–40, 2008.

Sankarasubramanian, A., Sabo, J., Larson, K., Seo, S., Sinha, T., Bhowmik, R., Ruhi Vidal, A., Kunkel, K., Mahinthakumar, G., Berglund, E., and Kominoski, J. Synthesis of public water supply use in the United States: spatio-temporal patterns and socioeconomic controls. *Earth's Future*, 5(7):771–788, 2017.

Sawicz, K., Wagener, T., Sivapalan, M., Troch, P. A., and Carrillo, G. Catchment classification: empirical analysis of hydrologic similarity based on catchment function in the eastern USA. *Hydrol Earth Syst Sci*, 15:2895–2911, 2011.

Schaefli, B., Rinaldo, A., and Botter, G. Analytic probability distributions for snow-dominated streamflow. *Water Resour Res*, 49(5):2701–2713, 2013.

Schwager, M., Johst, K., and Jeltsch, F. Does red noise increase or decrease extinction risk? Single extreme events versus series of unfavorable conditions. *Am Nat*, 167(6): 879–888, 2006.

Settin, T., Botter, G., Rodriguez-Iturbe, I., and Rinaldo, A. Numerical studies on soil moisture distributions in heterogeneous catchments. *Water Resour Res*, 43(5): WR005737, 2007.

Stoer, J. and Bulirsch, R. *Introduction to numerical analysis*. Springer Verlag, 1993.

Trewartha, G. T. *An introduction to climate*. Kogakusha Company Ltd, 1954.

USACE. Annual report of the secretary of the army on civil works activities. Technical report, U.S. Army Corps of Engineers, 1980–2010.

USGS. Estimated use of water in the United States. Technical report, United States Geological Survey (USGS), 1950–2010.

Van Vliet, M. T. H., Jarsley, J. R., Ludwig, F., Vogele, S., Lettenmaier, D. P., and Kabat, P. Vulnerability of US and European electricity supply to climate change. *Nat Clim Change*, 2:676–681, 2012.

Vezza, P., Parasiewicz, P., Spairani, M., and Comoglio, C. Habitat modeling in high-gradient streams: the mesoscale approach and application. *Ecological Applications*, 24(4):844–861, 2014.

Watts, R. J., Richter, B. D., Opperman, J. J., and Bowmer, K. H. Dam reoperation in an era of climate change. *Marine and Freshwater Research*, 62:321–327, 2011.

WCD. Dams and Development: a new framework for decision making. Technical report, Earthscan Publications Ltd, London and Sterling, VA, 2000.

Wilks, D. S. *Statistical Methods in the Atmospheric Science*. Elsevier, 2011.

Woods, R. A. Analytical model of seasonal climate impacts on snow hydrology: continuous snowpacks. *Adv Water Resour*, 32(10):1465–1481, 2009.

Ye, S., Yaeger, M. A., Coopersmith, E., Cheng, L., and Sivapalan, M. Exploring the physical controls of regional patterns of flow duration curves - Part 2: role of seasonality, the regime curve, and the associated process controls. *Hydrol Earth Syst Sci*, 16 (11):4447–4465, 2012.

Zarfl, C., Lumsdon, A., Berlekamp, J., Tydecks, J., and Tockner, K. A global boom in hydropower dam construction. *Aquat Sci*, 77:161–170, 2014.

Ziv, G., Baran, E., Nam, S., Rodriguez-Iturbe, I., and Levin, S. A. Trading-off fish biodiversity, food security, and hydropower in the Mekong River Basin. *Proc Natl Acad Sci USA*, 109(15):5609–5614, 2012.

Zolezzi, G., Bellin, A., Bruno, M. C., B., M., and Siviglia, A. Assessing hydrological alterations at multiple temporal scales: Adige River, Italy. *Water Resour Res*, 45(12): W12421, 2009.